Hydrologic sensitivities of western U.S. rivers to climate change

Julie A. Vano

A dissertation

submitted in partial fulfillment of the

requirements for the degree of

Doctor of Philosophy

University of Washington

2013

Reading Committee:

Dennis P. Lettenmaier, Chair

Alan F. Hamlet

Erkan Istanbulluoglu

Program Authorized to Offer Degree:

Civil and Environmental Engineering

University of Washington

Abstract

Hydrologic sensitivities of western U.S. rivers to climate change

Julie A. Vano

Chair of the Supervisory Committee:

Professor Dennis P. Lettenmaier

Civil and Environmental Engineering

As the climate continues to change, increasing temperatures and changes in precipitation will lead to fundamental changes in the seasonal distribution of streamflow, especially in the western United States where snowmelt plays a key role. These changes will inevitably lead to challenges for water resource managers. There is, however, considerable uncertainty as to the character of these hydrologic changes, especially at local and regional scales ($10^2 – 10^5$ km^2). My research aims to better understand how climate influences hydrologic processes, with a particular focus on variations in runoff sensitivities to changes in precipitation and temperature, and the use of this information in water management. Using land surface model simulations, I explore the sensitivity of runoff to changes in precipitation (defined as precipitation elasticities, ε, the fractional

change in runoff divided by the fractional change in precipitation), changes in temperature (defined as temperature sensitivities, S, percent change in runoff per degree change in temperature) and to the combined effect of temperature and precipitation changes. The character of these sensitivities varies considerably depending on how the land surface is simulated (e.g., type of land surface model), the particulars of the location (e.g., elevation, vegetation, soil types), and the season in which changes in temperature and precipitation occur.

I explore these variations through hydrologic model experiments in the Colorado and Columbia River basins - two basins which can be considered end points of hydroclimatic variability in the West, and which also have diverse management concerns as existing reservoir storage in these systems varies strongly. The total storage relative to annual inflow ratio of over four in the Colorado River, results in a management focus on total (annual) magnitudes in streamflow, whereas this ratio is about 0.3 in the Columbia River and hence changes in the seasonal distribution of streamflow is the primary driver there.

Within this body of work, I use the nature of these hydrologic sensitivities (e.g., spatial and temporal variability, superposition, and the linearity of their underlying functions) to develop two complementary methodologies that can be applied to generate viable first-order estimates of future change for long-term (e.g., 30-year) annual change (applied in the Colorado River basin) and seasonal change (applied in the Pacific Northwest). My results show that these sensitivity-based estimation approaches to future change compare well with the more common, computationally intensive full-simulation approaches that force a hydrologic model with downscaled future climate scenarios.

These methods can be applied to newly released climate information to easily assess underlying drivers of change and to bound, at least approximately, the range of future streamflow uncertainties for water resource planners.

DEDICATION

For my family.

ACKNOWLEDGEMENTS

I would like to thank Dennis Lettenmaier, my academic advisor, for his guidance, insights, and trust. I feel incredibly fortunate to have participated in a variety of interesting, meaningful research projects while in his research group. Thank you to my committee members Alan Hamlet, Erkan Istanbulluoglu, Joseph Cook, David Pierce, and Brad Udall for their valuable feedback and encouragement. I have also benefited greatly from the mentorship of Steve Burges, Jessica Lundquist, and Bart Nijssen. My research has been enhanced through my interactions with others in the Land surface hydrology group, and I have enjoyed sharing the graduate school experience with fellow students in Civil and Environmental Engineering and the Program on Climate Change. It has been an honor to work with each of you, and I hope our research collaborations and friendships continue to grow.

I am extremely grateful for my family and their support and encouragement of my academic pursuits – with a special thank you to Brian for his unceasing enthusiasm, patients, and good humor.

My graduate research has been funded by the Steve and Sylvia Burges Endowed Presidential Fellowship in Civil and Environmental Engineering, House Bill 1303 of the 2007 Washington State Legislature which funded the Washington Climate Change Impacts Assessment report, the NOAA Regional Integrated Scientific Assessment (RISA) program, and the Climate Impacts Research Consortium (CIRC).

TABLE OF CONTENTS

LIST OF FIGURES

LIST OF TABLES

I. INTRODUCTION

As the climate continues to change (Fig. 1.1), increasing temperatures and changes in precipitation will lead to fundamental changes in the seasonal distribution of streamflow, especially in the western United States. These changes will inevitably lead to challenges for water resource managers, although the character of the changes at regional and local scales remains uncertain. Future precipitation and temperature changes, as simulated by Global Climate Models (GCMs), vary considerably (IPCC 2007), and there is considerable uncertainty as to how changes in climate (e.g., in precipitation and temperature) will translate to changes in streamflow (Vano et al. 2013). My research aims to better understand how climate influences hydrologic processes and explores how this information can be integrated into water management decision-making.

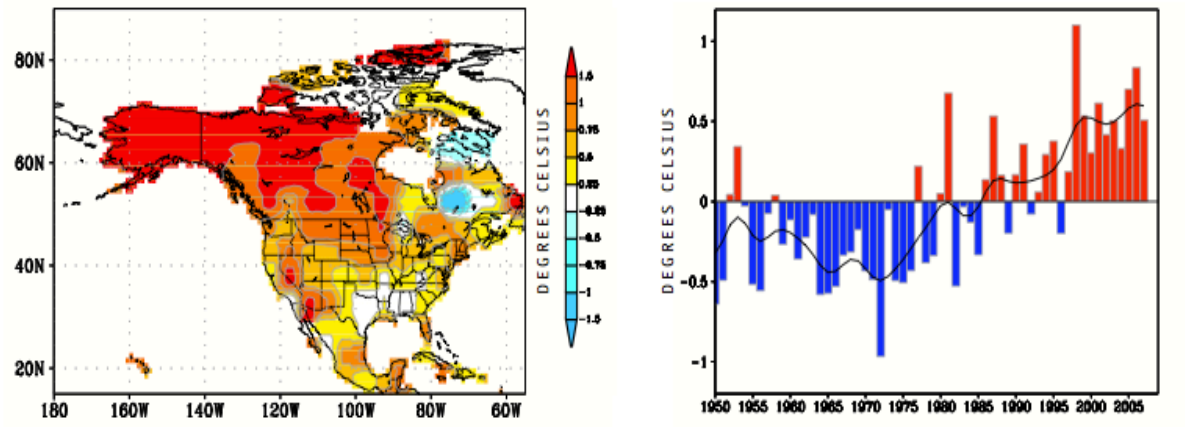

FIG 1.1 The 1950-2007 trend in observed annual North American surface temperature (°C, *left*) and the time series of the annual values of surface temperature averaged over the whole of North America (*right*). Annual anomalies are with respect to 1971-2000 reference. The smoothed curve (*black line*) highlights low frequency variations. (Data source: UK Hadley Center's CRUv3 global monthly gridded temperatures).

SOURCE: Figure and caption from Fig. 4-1 of WWA (2008).

In 2007, The Intergovernmental Panel on Climate Change (IPCC) Fourth Assessment reported unequivocal evidence that climate change was occurring and that an ensemble of GCMs showed general agreement that temperature will continue to increase and runoff will decrease across the western U.S. (IPCC 2007). The GCMs, however, operate at coarse spatial scales (e.g. ~200 km x 200 km) relative to the river basin scale at which management decisions are made. To generate information for management applications, there have been numerous approaches used to translate this global scale information to more local scales, although the extent to which these methods capture basin-specific hydrologic characteristics differs considerably. For example, the Colorado River has been the focus of several recent studies that have attempted to estimate future flows. These efforts produced future flow projections that range from less than 10% to almost 50% flow declines over the next century (WWA 2008; Hoerling et al. 2009; Vano et al. 2013). These differences could be attributed to various uncertainties, including a wide range of climate model projections, different methods of downscaling the climate projections to the scales required by hydrologic models, and differences in hydrologic model structure and hence sensitivity to changes in forcings. This dissertation focuses on the latter, specifically how changes in hydrologic model precipitation and temperature forcings propagate to changes in predicted streamflows. I apply concepts of hydrologic sensitivity similar to those introduced by Schaake (1990) and Dooge (1992) to evaluate the behavior of more computationally intense land surface models.

Previous studies that have attempted to quantify hydrologic sensitivities define them in various ways, mostly from observations (e.g. Schaake 1990; Dooge 1992; Dooge et al. 1999; Sankarasubramanian et al. 2001; Fu et al. 2007; Gardner 2009; and Zheng et al. 2009; among others). For example, Schaake (1990) defined precipitation elasticity as the change in

precipitation that will produce a unit fractional change in streamflow. He demonstrated how variable this sensitivity (or elasticity, as defined in economics) was in different regions of the U.S., with a range from less than one in very humid areas to as high as ten in some arid areas. Sensitivities to temperature changes are not as straightforward to estimate as those to precipitation changes. Dooge (1992) suggested formulation of an elasticity of streamflow with respect to potential evapotranspiration (PET). However, unlike precipitation, which is a common forcing for all models, PET is a computed quantity, which varies by land surface model, and can be difficult to extract. Additionally, surface air temperature is the best-understood and widely archived variable simulated by climate models, so I have chosen to formulate a temperature sensitivity rather than a PET elasticity.

Throughout my work, precipitation elasticity of runoff (ε) is defined as the percent change in annual model runoff (Q) divided by percent change in annual precipitation (Δ %) (Eq. 1.1) and temperature sensitivity of runoff (S) as percent change in annual runoff (Q) for an imposed incremental increase in annual temperature (Δ) (Eq. 1.2). ε and S of both runoff and streamflow are both considered, where runoff is defined as the sum of surface runoff and baseflow at the grid cell level and streamflow is defined as runoff routed to a gauge.

$$\varepsilon = \frac{\frac{Q_{ref+\Delta\%} - Q_{ref}}{Q_{ref}}}{\Delta\%} \qquad (1.1)$$

$$S = \frac{\frac{Q_{ref+\Delta} - Q_{ref}}{Q_{ref}}}{\Delta} \qquad (1.2)$$

Measures of ε and S can be useful at many levels. They can provide a way to compare hydrologic model performance relative to other models and observations. Spatial ε and S maps can help to identify locations where there is more uncertainty as well as areas with greater and lesser sensitivity to future change, suggesting key locations for targeted investment in *in situ* observations and further research. And ultimately, understanding ε and S can help to understand the likely range of future runoff projections prior to embarking on the somewhat-laborious process of downscaling climate model projections and running them through a hydrologic model.

1.1. Study Area

My work focuses on the western United States, and the Colorado River basin (**Chapter II and III**) and extended Columbia River basin (**Chapter IV**) in particular (Fig. 1.2). I define the extended Columbia River basin as the Basin and its adjacent coastal drainages, and I also referred to it as the Pacific Northwest (PNW) as it comprises that hydrologic region. These two basins can be considered end points of hydroclimatic

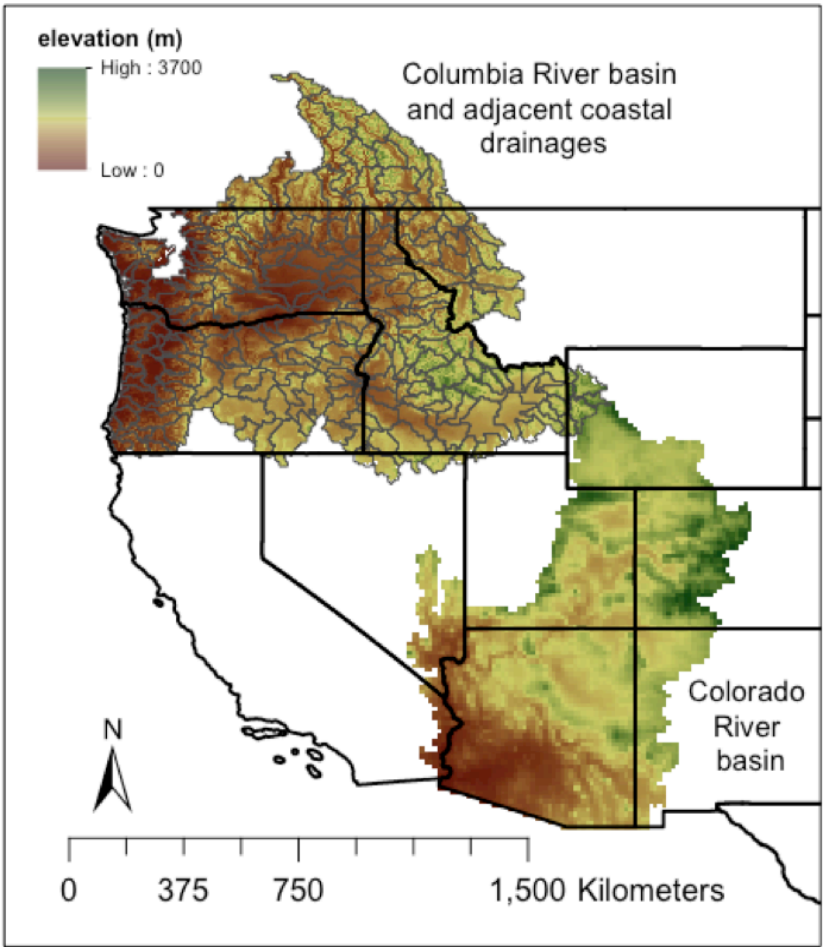

FIG 1.1. Study area

variability in the West. These locations also have diverse management concerns as their existing reservoir storage relative to mean annual discharge, varies considerably (even though their total storage capacity is roughly equivalent). The Colorado River basin has a total storage relative to annual inflow ratio of over four, which results in management decisions that focus on total (annual) magnitudes in streamflow. In contrast, the Columbia River basin has a ratio of about 0.3, and consequently, seasonality is the critical streamflow characteristic that drives water management decisions in the PNW region.

1.2. Research Questions and Approach

This dissertation seeks to understand the extent to which land-surface hydrology modulates or exacerbates regional scale sensitivities to future (global) change by addressing the following research questions:

(1) How sensitive is runoff to changes in precipitation, temperature, and to combined changes in both precipitation and temperature?

(2) How do hydrologic sensitivities vary spatially across the western United States?

(3) How can runoff sensitivities to precipitation and temperature changes be defined on a seasonal basis?

(4) How can hydrologic sensitivities be used to construct future streamflow projections for use in water management applications?

These questions are addressed in three core chapters. **Chapter II** (published as Vano et al. 2012) investigates annual precipitation elasticities (ε) and temperature sensitivities (S) in the Colorado River basin in a multiple (land surface model) context, using five commonly used land surface models [Catchment (Koster et al. 2000), Community Land Model (Oleson et al. 2007), Noah (Lohmann et al. 2004), Sacramento Soil Moisture Accounting model (Burnash et al. 1973), and the Variable Infiltration Capacity model (Liang et al. 1994)]. Chapter II quantifies how different representations of the land surface respond similarly (or differently), how responses vary spatially, and the extent to which changes in temperature and precipitation are additive (*questions 1 and 2*). **Chapter III** (in review as Vano and Lettenmaier 2013a) evaluates how understandings of variations in ε and S, developed in the previous chapter, estimated for different seasons and at different change increments, can be used in water management planning and decision making. It outlines a methodology that uses hydrologic sensitivities to approximate cumulative distribution functions of long-term annual streamflow change (*question 4*). **Chapter IV** (to be submitted to *Water Resources Research* as Vano and Lettenmaier 2013b) explores seasonal variations in ε and S throughout watersheds of the PNW. The region's hydroclimatology provides a diversity of watershed responses that can be leveraged to quantify and classify the effects of seasonally applied changes to annual and seasonal streamflow. The seasonal hydrologic sensitivities can then be used to estimate future seasonal hydrographs. This study uses a method similar in concept to the sensitivity-based method of Chapter III, but focuses on the long-term seasonal responses, which are of most interest to water resource planners in the PNW (*questions 2, 3, and 4*).

References

Burnash, R. J. C., R. L. Ferral, and R. A. McGuire, 1973: A generalized streamflow simulation system: Conceptual models for digital computers, technical report, Joint Fed.-State River Forecast Cent., U.S. Natl. Weather Serv. and Calif. Dep. of Water Resour., Sacramento, Calif.

Dooge, J.C.I., 1992: Sensitivity of Runoff to Climate Change: A Hortonian Approach. *Bull. Amer. Meteor. Soc.*, **73**, 2013–2024.

Dooge, J. C. I., Bruen, M. and B. Parmentier, 1999: A simple model for estimating the sensitivity of runoff to long-term changes in precipitation without a change in vegetation, *Advances in Water Resources*, **23**:2, 153-163, ISSN 0309-1708, DOI: 10.1016/S0309-1708(99)00019-6.

Fu, G., S. P. Charles, and F. H. S. Chiew, 2007: A two-parameter climate elasticity of streamflow index to assess climate change effects on annual streamflow, *Water Resour. Res*., **43**, W11419, doi:10.1029/2007WR005890.

Gardner, L.R., 2009: Assessing the effect of climate change on mean annual runoff, *Journal of Hydrology*, **379**, 351-359, ISSN 0022-1694, DOI:10.1016/j.jhydrol.2009.10.021.

Hoerling, M., Lettenmaier, D.P., Cayan D., and B. Udall, 2009: Reconciling projections of Colorado River streamflow. *Southwest Hydrology* **8**(3): 20-21, 31.

Intergovernmental Panel on Climate Change, 2007: The physical science basis, *in* Solomon, S., Qin, D., Manning, M., Chen, Z., Marquis, M., Averyt, K.B., Tignor, M., and Miller, H.L., eds., Contribution of Working Group I to the Fourth Assessment Report of the Intergovernmental Panel on Climate Change: Cambridge, United Kingdom, Cambridge University Press. (Also available online at *http://www.ipcc.ch/ipccreports/ar4-wg1.htm*).

Koster, R.D., M.J. Suarez, A. Ducharne, M. Stieglitz, and P. Kumar, 2000: A catchment-based approach to modeling land surface processes in a general circulation model. 1. Model structure. *J. of Geophysical Research*, 105:D20, 24809-22.

Liang, X., D. P. Lettenmaier, E. F. Wood, and S. J. Burges, 1994: A simple hydrologically based model of land surface water and energy fluxes for General Circulation Models. *J. Geophys. Res.,* 99, 14 415– 14 428.

Lohmann D., K.E. Mitchell, P.R. Houser, E.F. Wood, J.C. Schaake, A. Robock, B.A. Cosgrove, J. Sheffield, Q. Duan, L. Luo, R.W. Higgins, R.T. Pinker, and J. D. Tarpley, 2004: Streamflow and water balance intercomparisons of four land surface models in the North American Land Data Assimilation System project, J. Geophys. Res., 109, D07S91, doi:10.1029/2003JD003517.

Mitchell, K. E., et al., 2004: The multi-institution North American Land Data Assimilation System (NLDAS): Utilizing multiple GCIP products and partners in a continental distributed hydrological modeling system, *J. Geophys. Res*., **109**, D07S90, doi:10.1029/2003JD003823.

Oleson, K.W., and Coauthors, 2007: CLM 3.5 Documentation, on line available: *http://www.cgd.ucar.edu/tss/clm/distribution/clm3.5/CLM3_5_documentation.pdf* 34 pp.

Sankarasubramanian A., R.M. Vogel, and J. F. Limbrunner, 2001: Climate elasticity of streamflow in the United States, *Water Resour. Res*., **37**, 1771-1781.

Schaake, J. C., 1990: From climate to flow, in *Climate Change and U.S. Water Resources*, edited by Waggoner, p. 177-206, John Wiley, New York.

Vano, J.A., T. Das, and D.P. Lettenmaier, 2012: Hydrologic sensitivities of Colorado River runoff to changes in precipitation and temperature, *J. of Hydrometeorology*, **13**, 932-949,

doi:10.1175/JHM-D-11-069.1.

Vano, J.A., B. Udall, D.R. Cayan, J.T. Overpeck, L.D. Brekke, T. Das, H.C. Hartmann, H.G. Hidalgo, M. Hoerling, G.J. McCabe, K. Morino, R.S. Webb, K. Werner, and D.P. Lettenmaier, 2013: Understanding Uncertainties in Future Colorado River Streamflow, *Bull. Amer. Meteor. Soc*., (in press).

Vano, J.A. and D.P. Lettenmaier, 2013a, A sensitivity-based approach to evaluating future changes in Colorado River Discharge, *Climatic Change* (in review).

Vano, J.A. and D.P. Lettenmaier, 2013b: Mapping the diversity of seasonal hydrologic responses to climate change in the Pacific Northwest, *Water Resources Research* (in preparation)

Wang A., T.J. Bohn, S.P. Mahanama, R.D. Koster, and D.P. Lettenmaier, 2009: Multimodel ensemble reconstruction of drought over the continental United States, *J. Climate*, **22**, 2694–2712, doi:10.1175/2008JCLI2586.1.

Western Water Assessment (WWA), Colorado Climate Change: A Synthesis to Support Water Resource Management and Adaptation. Oct 2008 (available online at: *http://cwcb.state.co.us/public-information/publications/Documents/ReportsStudies/ClimateChangeReportFull.pdf*).

Zheng, H., L. Zhang, R. Zhu, C. Liu, Y. Sato, and Y. Fukushima, 2009: Responses of streamflow to climate and land surface change in the headwaters of the Yellow River Basin, *Water Resour. Res*., **45**, W00A19, doi:10.1029/2007WR006665.

II. HYDROLOGIC SENSITIVITIES OF COLORADO RIVER RUNOFF TO CHANGES IN PRECIPITATION AND TEMPERATURE

This chapter has been published in its current form in the Journal of Hydrometeorology:

Vano, J.A., T. Das, and D.P. Lettenmaier, 2012: Hydrologic sensitivities of Colorado River runoff to changes in precipitation and temperature, *J. of Hydrometeorology*, **13**, 932-949, doi:10.1175/JHM-D-11-069.1.

Abstract

The Colorado River is the primary water source for much of the rapidly growing southwestern United States. Recent studies have projected reductions in Colorado River flows from less than 10% to almost 50% by midcentury because of climate change—a range that has clouded potential management responses. These differences in projections are attributable to variations in climate model projections but also to differing land surface model (LSM) sensitivities. This second contribution to uncertainty—specifically, variations in LSM runoff change with respect to precipitation (elasticities) and temperature (sensitivities)—are evaluated here through comparisons of multi-decadal simulations from five commonly used LSMs (Catchment, Community Land Model, Noah, Sacramento Soil Moisture Accounting model, and Variable Infiltration Capacity model) all applied over the Colorado River basin at 1/8° latitude by longitude spatial resolution. The annual elasticity of modeled runoff (fractional change in annual runoff divided by fractional change in annual precipitation) at Lees Ferry ranges from two to six for the different LSMs. Elasticities generally are higher in lower precipitation and/or runoff

regimes; hence, the highest values are for models biased low in runoff production, and the range of elasticities is reduced to two to three when adjusted to current runoff climatology. Annual temperature sensitivities (percent change in annual runoff per degree change in annual temperature) range from declines of 2% to as much as 9% per degree Celsius increase at Lees Ferry. For some LSMs, small areas, primarily at mid-elevation, have increasing runoff with increasing temperature; however, on a spatial basis, most sensitivities are negative.

2.1. Introduction

The Colorado River is the major water source for much of the southwestern U.S. The river's discharge is regulated by numerous dams on tributaries and two major main stem dams, Glen Canyon and Hoover, which form impoundments (Lakes Powell and Mead, respectively) that store about four times the mean annual natural flow of the river (observed discharge adjusted for effects of upstream diversions and storage) at its mouth. In a relative sense, the storage provided by these reservoirs is large (in contrast, the storage in the Columbia River basin is only about one-third of the river's mean naturalized - absent water management effects - flow). Therefore, the Colorado River reservoir system is operated to carry over water from wet years to dry years, notwithstanding that it also reshapes the seasonal pattern of discharge. Because of the large storage, the reliability of the Colorado River reservoir system for water supply is relatively insensitive to changes in the seasonal pattern of discharge (see e.g. Christensen et al. (2004) and Christensen and Lettenmaier (2007)). However, the system is vulnerable to long-term changes in climate, such as the general drying projected for the southwestern U.S. by many climate models (Christensen and Lettenmaier 2007; IPCC 2007; Seager et al. 2007). The multi-year drought experienced over the last decade highlights the potential impacts of long-term changes in

Colorado River discharge (Barnett and Pierce 2009; Cayan et al. 2010; Overpeck and Udall 2010).

Because of the Colorado River's water supply importance, it has been evaluated in several studies that have projected future flows (e.g. Milly et al. 2005; Hoerling and Eischeid 2006; Christensen and Lettenmaier 2007; Seager et al. 2007; WWA 2008). The methods used in these studies differ, and methodological differences explain some of the wide range of projected future changes in Colorado River discharge, which vary from reductions in mean annual discharge of less than 10% to almost 50% by the mid-2000s (Hoerling et al. 2009). Part of this range is attributable to differences in the forcing data used, both in resolution and in the variation of climate models included in the different studies. Differences also reflect biases in the runoff projections (as shown below, hydrologic sensitivities are highly nonlinear, and hence depend on the models' estimates of current climate runoff) and reflect variations in hydrologic model sensitivities to changes in precipitation and temperature. In this paper, we evaluate the LSM contribution to the overall uncertainty, specifically, how runoff change differs depending on model responses to changes in precipitation and temperature.

Many LSMs have been developed with varying levels of complexity and philosophies with respect to their representations of the land surface hydrologic cycle. We focus on five LSMs that have been widely applied at regional to global scales. Included are three that were developed for use in global climate models [Catchment, Community Land Model (CLM), and Noah] and two that have been used primarily in uncoupled hydrologic applications [Sacramento Soil Moisture Accounting (Sac) and Variable Infiltration Capacity (VIC)]. LSMs used in global and regional climate models have the primary purpose of partitioning net radiation into turbulent and ground heat fluxes, and hence the lower boundary conditions for the atmosphere.

Hydrologic models, in contrast, have the primary purpose of partitioning precipitation into evapotranspiration and runoff. The two LSMs with hydrologic heritage were developed primarily for hydrologic prediction purposes, albeit at large scales. They generally have more detailed representations of runoff production dynamics than do the LSMs intended for coupled applications. Nonetheless, with one exception discussed below, all models predict the full energy and water balances at the land surface, typically at time steps of one day or shorter.

Many studies have compared the performance of different LSMs in different hydroclimatic settings (e.g. Henderson-Sellers et al. 1995; Pitman et al. 1999; Boone et al. 2004; Mitchell et al. 2004; Wang et al. 2009). The Project for Intercomparison of Land surface Parameterization Schemes (PILPS), for example, had four phases of controlled experiments that were intended to better understand the implications of parameterizations of water, energy, and momentum between the atmosphere and land surface (Henderson-Sellers et al. 1995; Pitman et al. 1999). As many as 30 LSMs participated in the various phases of PILPS. The North American Land Data Assimilation System (NLDAS) project compared the performance of four LSMs across the continental U.S. domain with respect to their capabilities in the context of land data assimilation (Mitchell et al. 2004; Lohmann et al. 2004). These and other studies have improved LSM performance by comparing models to one another and observations to highlight their strengths and weaknesses. The studies have also illustrated the implications of differences in LSM parameterizations and complexity (Koster and Milly 1997; Mitchell et al. 2004). These differences, compounded by potential issues of numerical processes (e.g., Kavetski and Clark 2010) and diverse philosophies that underlie LSM development (e.g., focusing on the largely vertical processes that control land-atmosphere fluxes, as contrasted with the largely horizontal

processes that control runoff generation) make understanding differences and uncertainties in LSM formulations exceedingly difficult.

Little previous work has been done to compare LSMs with respect to their hydrologic sensitivities to changes in long-term precipitation and temperature. Many previous studies have, however, investigated how changes in climate influence streamflow, and in so doing have attempted to quantify hydrologic sensitivities (e.g., Schaake 1990; Dooge 1992; Dooge et al. 1999; Sankarasubramanian et al. 2001; Fu et al. 2007; Gardner 2009; and Zheng et al. 2009; among others), mostly from observations. These studies define hydrologic sensitivities in various ways. For example, Schaake (1990) first defined precipitation elasticity as the change in precipitation that will produce a unit fractional change in runoff. He demonstrated how variable this sensitivity (or elasticity, as defined in economics) was in different regions of the U.S., with a range from less than one in very humid areas to as high as ten in some arid areas. Dooge (1992) calculated sensitivity factors (similar in nature to Schaake's runoff elasticities) using empirical expressions that related (annual) evaporation normalized by potential evaporation to different humidity indexes, where the higher the humidity index, the lower the elasticity. He cautioned that the usefulness of the annual analysis was limited in some ways, and that inclusion of seasonality – which he later addressed (Dooge et al. 1999) - could change the interpretation. Sankarasubramanian et al. (2001) estimated streamflow elasticity across the continental U.S. through use of both parametric and non-parametric estimators applied to time series of annual streamflow and precipitation. They found elasticity values for tributaries and main stem locations in the Colorado River Basin (CRB) that ranged from a little less than two to a little more than four.

These two bodies of research - the LSM comparison studies and hydrological sensitivities studies – provide important foundations for understanding hydrologic sensitivities to changes in precipitation and temperature. LSMs play an important role in global and regional climate models, which in turn are the basis – directly or indirectly – for most projections of hydrologic impacts of climate change. We argue that better understanding of the relative sensitivities of these models to climate forcings is essential to understanding uncertainties in hydrologic projections. In this paper, we take a straightforward approach to evaluating the hydrologic sensitivities of five commonly used LSMs to precipitation and temperature changes, with the intent of better understanding: (1) to what extent does land-surface hydrology modulate or exacerbate regional scale sensitivities to global climate change? (2) how much of the range of results of these hydrologic sensitivities is attributable to model bias? and (3) how do these

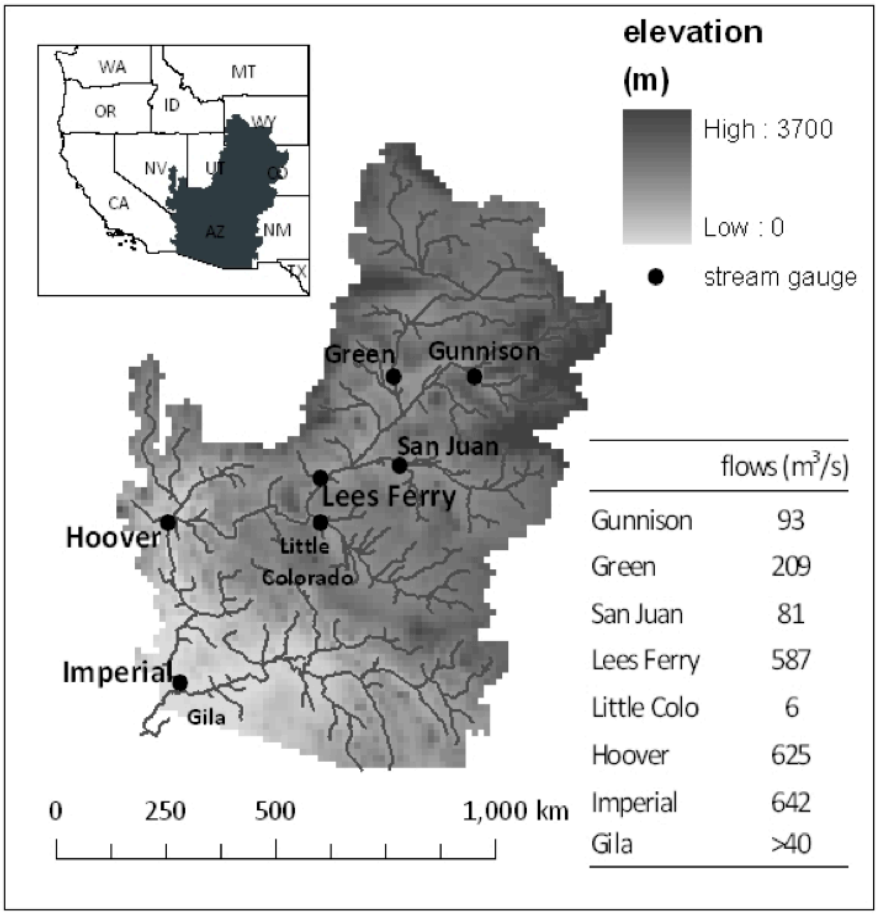

FIG 2.1 Colorado River topography and sub-basin flows. Flows in the table, except for Gila, are naturalized flow averages from USBR (2010) from 1975-2005 and correspond to the dots in the figure. USBR did not report flows for the Gila, so we report a predevelopment estimate from Blinn and Poff (2005).

sensitivities vary spatially across the CRB?

2.2. Study area

The Colorado River (Fig. 2.1) drains parts of seven U.S. states and Mexico (642,000 km^2) and ranges in elevation from over 4000 m in its northeastern headwaters to sea level at its mouth at the head of the Sea of Cortez 2250 km downstream. For purposes of water allocation, the Colorado River Compact of 1922 divided the CRB into the Upper Basin (above Lees Ferry, including Lake Powell, and the Lower Basin (below Lees Ferry, including Lake Mead). On basin average, about half of the CRB's precipitation comes in winter (although more so in the north than the south) and summer, however from a hydrological standpoint, runoff is dominated by winter precipitation which occurs mostly as snow in the Upper Basin, and is the source of the spring freshet that accounts for most of the river's annual streamflow (Fig 2.2).

The CRB has large temperature and precipitation gradients, as well as diverse

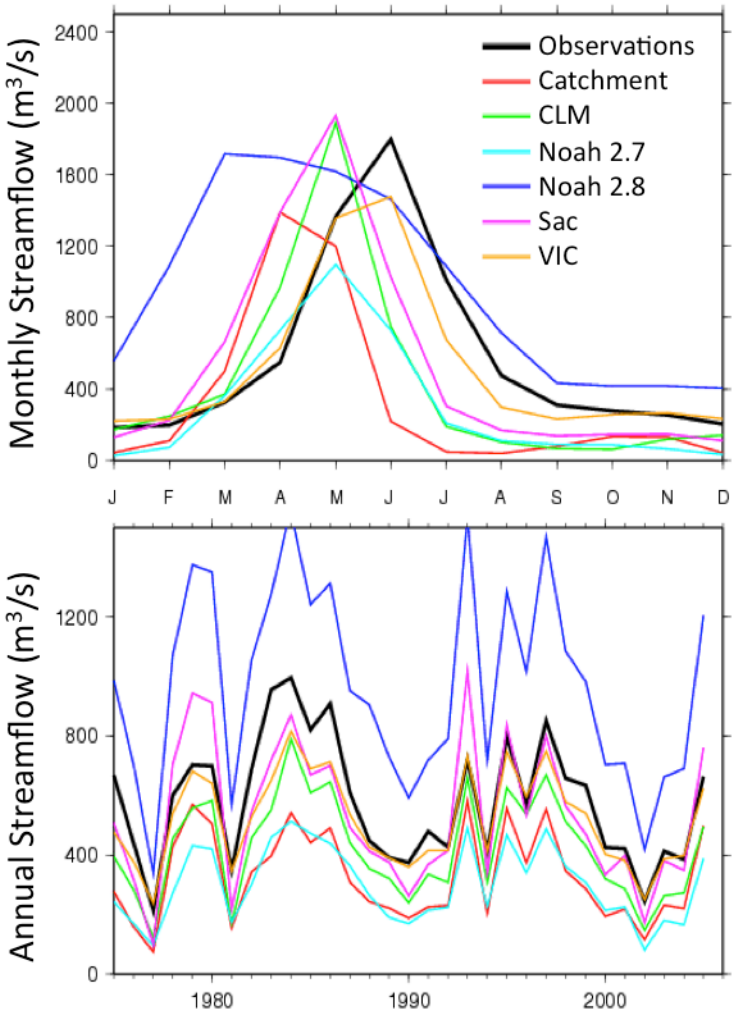

FIG 2.2 Comparison of LSM streamflow with naturalized USBR flow at Lees Ferry from 1975 to 2005, seasonal (top) and annual (bottom).

vegetation and soil types, all of which combine with variability in precipitation to produce one of the most variable hydrologic regimes in the continental U.S. The coefficient of variation (standard deviation/mean) of annual flow volume at Lees Ferry as calculated by McMahon (1982) is 0.37, which is higher than most (median 0.25) of the 126 rivers included in the UNESCO study of world rivers (for comparison, the coefficient of variation of annual discharge of other large global rivers are: Columbia (0.18), Mississippi (0.28), Amazon (0.06), and Mekong (0.12)). In addition to spatial variations in surface and subsurface properties, hydrologic variability in the basin is strongly affected by elevation. Hence relatively high spatial resolution is required for adequate representation of the basin's water balance. Water balance variations are strongly driven by evapotranspiration, which accounts for over 85% of precipitation on average (however, runoff ratios are much higher than the ~15% basin average in the high elevation headwaters).

2.3. Approach

We focus on LSM water balance calculations, and the sensitivity of these calculations to changes in precipitation and temperature. To do so, we forced all five models with the same surface meteorological data and implemented all models at the same (one-eighth degree latitude-longitude) spatial resolution, over the same domain. For each model, we compared both grid cell runoff (the sum of the model's surface runoff and drainage) and streamflow (runoff routed through a simplified representation of the channel network) at selected stream gauge locations (Fig. 2.1). In the context of LSMs, runoff is a quantity that is generated instantaneously at each grid cell. We applied the routing model of Lohmann et al. (1996; 1998) to all five LSMs. The routing model accounts, in a simplified manner using a unit hydrograph, for the effect of the

channel system in transforming spatially distributed (grid cell) runoff to streamflow, and accounts both for lags within a grid cell that affect the timing of runoff exiting a grid cell, and within the channel system, which represents lagged effects from grid cell outlets to a (stream gauge) location on the channel network. A spatial average of runoff is slightly different than streamflow (primarily due to travel time considerations), but the long-term average is nearly the same.

2.3.1 Meteorological forcing data set

We used methods described in Maurer et al. (2002) as modified by Wood and Lettenmaier (2006) to generate daily historical gridded forcings of temperature minima and maxima, precipitation, and wind speed at one-eighth degree latitude-longitude resolution from observed station data. The modification of the approach by Wood and Lettenmaier (2006) uses a smaller set of index stations, which reliably report over many years, and avoids the problem of ephemeral stations, which can bias the long-term variability of the data set. To meet requirements for models that run on a sub-daily time step, daily values of precipitation and temperature were disaggregated into 3-hourly time steps according to methods outlined in Nijssen et al. (2001) and Wang et al. (2009). Similar to Maurer (2002), other meteorological and radiation variables are calculated from established relationships, for example downward solar and longwave radiation and dew point were derived from the daily temperature and temperature range using methods described in Nijssen et al. (2001). Surface air temperature, precipitation, wind speed, specific humidity, air pressure, and surface incident shortwave and longwave radiation forcings were identical for all LSMs. Because we focus on relative differences, we distributed precipitation uniformly throughout the day in all LSMs even though the Catchment

model is more sensitive to diurnal precipitation variations than are the other four models (Wang et al. 2009). We selected 1975 to 2005 as our period of analysis because it includes the drought years in the early 2000s.

2.3.2. Land-surface models

The five LSMs we used have diverse heritages, however all of them have been used in either or both of the past multi-LSM studies of Mitchell et al. (2004) and Wang et al. (2009) and are structured to run off-line in a semi-distributed manner (Table 2.1). We included two versions of the Noah LSM, as recent changes to Noah model parameterization processes to improve warm season simulations (see Wei et al. 2012 for modification details) have resulted in much different model performance (see Fig. 2.2). Each LSM was initialized by running it from 1970-2005, then cycling with 1970 forcings ten times before beginning the simulation in 1970. The simulation was then continued through water years 1975-2005, which was our period of analysis.

We used LSM versions – including parameters – used in previous studies, with modifications only in spatial resolution and extent and forcing data. VIC was implemented as in Christensen and Lettenmaier (2007), which was calibrated at one-eighth degree spatial resolution. We used Noah 2.7 and 2.8, Sac, and CLM as used within the University of Washington's real-time national Surface Water Monitor multi-model system (see http://www.hydro.washington.edu/forecast/monitor), which required an increase in the resolution from half a degree to one-eighth degree. Sac does not generate potential evapotranspiration (PET), and instead uses PET generated by Noah 2.7 similar to Mitchell et al. (2004) multiplied by monthly vegetation adjustment factors. In this study we focus on results of the semi-distributed version of Sac as used in Wang et al. (2009), although we have found in limited

TABLE 2.1 Overview of land-surface models, table modified from Wang et al. 2009

	version	heritage	soil hydrology scheme	soil/vegetation parameters	Potential Evapo-transpiration (PET) formulation	references
Catchment		developed at NASA Goddard as the land scheme within their CEOS-5 global data assimilation system	TOPMODEL-based	soil and veg parameters consistent with Global Soil Wetness Project (GSWP)-2 global parameters	Penman-Monteith equivalence	Koster et al. 2000; Ducharne et al. 2000
Community Land Model (CLM)	3.5	developed as the land surface component of CCSM3	TOPMODEL-based (surface); groundwater scheme	Vegetation from MODIS (Moderate Resolution Imagining Spectoradiometer) and soil from International Geosphere-Biosphere Programme (IGBP)	Monin-Obukhov similarity theory	Oleson et al. 2004; 2007; 2008; Wang et al. 2009
Noah	2.7 and 2.8	developed as the LSM for the NCEP mesoscale Eta model	Exponential distribution of infiltration capacity (surface); base flow proportional to storage; drainage driven by gravity	2.7 from NLDAS, see Mitchell et al. 2004, 2.8 uses updated STATSGO soil and UMD vegetation with seasonally and spatially varying leaf area index	Penman type approach	2.7 as described in Lohmann et al. 2004; 2.8 as described in Livneh et al. 2010 and Wei et al. 2012
Sacramento soil moisture accounting model (Sac)	NLDAS version of the coupled Sac/Snow 17 model	developed as a generalized streamflow simulation system for use by NWS River Forecast Centers for operational streamflow predictions	Runoff from impervious and saturated soils; base flow and percolation between reserviors based on current storage	No vegetation, soil from NLDAS, see Mitchell et al. 2004	uses Noah 2.7 PET multiplied by a vegetation adjustment factor	Anderson 1973; Burnash et al. 1973; Mitchell et al. 2004
Variable Infiltration Capacity (VIC)	4.0.6, water balance mode	developed as a hydrologic model suitable to incorporate variable infiltration capacity into GCMs	Variable infiltration capacity curve (surface), ARNO model for base flow, and drainage driven by gravity	from Christensen et al. 2004	Penman-Monteith	Liang et al. 1994; Christensen et al. 2004; Christensen and Lettenmaier 2007

comparisons that results are comparable to the operational version (which is well-calibrated, using only catchment-level characteristics) used by the CRB River Forecast Center, e.g., for historical values at Lees Ferry, the elasticity was 2.4 (vs. 2.6 with the distributed version) and the temperature sensitivity was 4% (vs. 5%). We increased the spatial resolution of Catchment as used by Wang et al. (2009) from one-half degree to one-eighth degree, and used Catchment parameters provided by S. Mahanama (NASA Goddard Space Flight Center) that were produced specifically for a one-eighth degree implementation of the model.

As their diverse heritage indicates (Table 2.1), the various LSMs were constructed for different purposes and thus also differ in the extent to which they have been calibrated and compared with observed streamflow (Mitchell et al. 2004). VIC and Sac were developed specifically for streamflow simulation purposes. VIC was calibrated to a number of stream

gauges within the Colorado basin (Christensen et al. 2004; Christensen and Lettenmaier 2007) however its implementation here uses slightly different forcing data, and the model version is slightly different than the one for which calibrations were performed. The Sac version we used has not been calibrated, nor did we attempt to transfer parameters from the operational version, which has been implemented for somewhat different sub-basins than the ones we used. No previous attempts had been made to calibrate Catchment, CLM, or either version of Noah. As a result, in general we do not expect simulated streamflows to match observations closely, and this is not our goal. However, in section 2.4, we do evaluate the nature of variations across models in their sensitivities, and assess how the model sensitivities are affected by biases in the LSM simulations.

LSM formulation and validation is particularly challenging in the CRB because there are limited in situ observations that capture the basin's highly variable (in space and time) snow and soil moisture, especially at high elevations. Also, because such a large fraction of the basin's precipitation either evaporates or is transpired, the accuracy of runoff predictions is highly susceptible to evapotranspiration (ET) prediction errors. For example, a 5% error in annual ET prediction (assuming ET is 85% of the total mass balance) translates to 25% errors in annual runoff.

2.3.3. Precipitation elasticity and temperature sensitivity formulation

We perturbed both precipitation (P) and temperature (T) by uniform amounts each day of the year throughout the period of record. We created reference climates by using multiplicative perturbations in P (70%, 80%, 90%, 100%, and 110%) and additive perturbations in T (0°, 1°, 2°, and 3°C). For both precipitation elasticity (ε) and temperature sensitivity (S) computations, we

calculated the model response to an incremental change (1% and 0.1 °C change respectively) relative to each reference climate. We selected these increments of change (1% and 0.1 °C) to be as small as possible so as to approximate the tangent (vs. the secant) while limiting computational artifacts. As an example, for historical ε we compared the historical simulation (0°C T change, 100% of historical P) to a simulation where P was multiplied by 1.01; whereas for a 110% reference climate, we compared historical climate P multiplied by 1.10 with historical climate multiplied by 1.11. We estimated ε as the fractional change in annual average runoff (Q) divided by the imposed fractional change in P. In this study we use $\Delta = 1\%$.

$$\varepsilon = \frac{\frac{Q_{ref+\Delta\%} - Q_{ref}}{Q_{ref}}}{\Delta\%} \qquad (2.1)$$

Sensitivities to T changes are not as straightforward to estimate as those to P changes. Dooge (1992) suggests formulation of an elasticity of runoff with respect to potential evapotranspiration (PET), however, unlike P, which is a common forcing for all models, PET is not a measurable quantity but a function of measurable quantities, which is computed differently depending on LSM, and can be difficult to extract from the various models. While net radiation, rather than T, is the primary variable that defines PET, net radiation is T dependent, especially because downward solar radiation depends on daily T range as described below. Additionally, surface air T is the best-understood and widely archived variable simulated by climate models, so it makes some sense to formulate a T sensitivity rather than a PET elasticity. Furthermore, surface air T is the variable that is most often perturbed in hydrologic simulations of climate change (e.g. Christensen and Lettenmaier 2007; Elsner et al. 2010; and others). T affects and/or is affected by downward solar and net longwave radiation, sensible and latent heat fluxes, ground heat flux, and snow processes, which change evaporative demand and thus runoff. It is also

notable that net radiation, vapor pressure deficit, and wind speed (along with air T) all affect evapotranspiration rates. All of these variables have been changing in the last few decades, and as Donohue et al. (2010) found by investigating these variables in Australia, non-temperature attributes can have an influence greater than T. For this reason, we perturb T in two ways as described below.

We defined temperature sensitivity (S) as the percent change in annual average runoff (Q) per 1°C T change (Eq. 2.2).

$$S = \frac{\frac{Q_{ref+\Delta} - Q_{ref}}{Q_{ref}}}{\Delta} \qquad (2.2)$$

Because the model forcing data include daily temperature maxima (T_{max}) and minima (T_{min}), we used two methods to perturb T. Both increase the daily average T by the same amount, Δ – either increasing both T_{min} and T_{max} by Δ (referred to as $S_{Tmin\&max}$) or by fixing T_{min} and increasing T_{max} by 2Δ (referred to as S_{Tmin_fixed}). We used $\Delta = 0.1^{o}C$, where in $S_{Tmin\&max}$ calculations T_{min} and T_{max} are both increased by $0.1^{o}C$ and in S_{Tmin_fixed} calculations T_{min} remains the same and T_{max} is increased by $0.2^{o}C$. In the model forcing data set, downward solar radiation is indexed to the daily temperature range, $T_{max} - T_{min}$, using the method of Thornton and Running (1999). In this algorithm, if T_{min} and T_{max} are both changed by the same increment (for $S_{Tmin\&max}$), the daily T range, and hence downward solar radiation is unchanged (however downward longwave radiation and humidity, both of which are forcings to the evapotranspiration algorithms used by the various LSMs, do change). On the other hand, when only T_{max} is increased (for S_{Tmin_fixed}), it has the effect of changing downward solar radiation, as well as downward longwave radiation, and humidity, hence in general resulting in larger changes in net radiation and vapor pressure deficit.

Our approach allows us to investigate changes in ε and S spatially both within and across models. We also evaluate ε and S of streamflow at Lees Ferry, where this spatially averaged value avoids having ε and S dominated by areas of the basin that produce little runoff but have large ε or S.

2.3.4. Precipitation and temperature interactions

As the climate changes, both T and P are projected to change simultaneously, however in our LSM simulations in section 2.3.2 and 2.3.3, we altered the reference climate's P or T, but not both. To determine the extent to which changes in P and changes in T interact we compared four simulations for each LSM: (1) historical runoff, Q_{his} (ΔT=0°C, P=100%), (2) perturbed T, $Q_{\Delta T}$ (1°C, 100%), (3) perturbed P, $Q_{\Delta P}$ (0°C, 101%), and (4) both perturbed T and P, $Q_{\Delta T \Delta P}$ (1°C, 101%). We compared $Q_{\Delta T \Delta P}$ and $Q_{\Delta T \Delta Pest}$, where $Q_{\Delta T \Delta P}$ is the model simulation with both T and P perturbed simultaneously, and $Q_{\Delta T \Delta Pest}$ is estimated by Eq. 2.3.

$$Q_{\Delta T \Delta Pest} = Q_{his} + (Q_{\Delta P} - Q_{his}) + (Q_{\Delta T} - Q_{his}) \qquad (2.3)$$

For these simulations, unlike the ones outlined in section 2.3.3, we use ΔT=1°C (instead of 0.1°C) changes in T so that differences in runoff resulting from T and P changes are more similar in magnitude. We also select opposing responses (ΔT=1°C will decrease runoff whereas ΔP=1% will increase runoff) to better distinguish the effects of each perturbation. Our analysis of P and T interactions includes all 4518 grid cells, effectively representing a wide range of reference conditions.

2.4. Results and Discussion

We examine the influence of changes in forcing data sets by evaluating LSM performance with historical forcing data (section 2.4.1), through perturbations in precipitation (P) (2.4.2), temperature (T) (2.4.3), and both P and T (2.4.4). Because Lees Ferry is the key gauge in the Colorado basin for water management purposes, we report naturalized flows at this gauge. Flows at Lees Ferry are generally representative of basin-wide runoff as average annual naturalized streamflow at Lees Ferry is greater than 90% of the flow at Imperial Dam (USBR 2010), the most downstream location for which naturalized streamflows are reported. The spatial patterns within each model also reveal meaningful differences between LSMs; therefore, we provide both gauge information and values at each one-eighth-degree grid. Although we focus on water years 1975 to 2005, results changed little when different multi-decadal periods of analysis were used.

2.4.1 Historical water balance

We compared LSM routed streamflow to naturalized flows at Lees Ferry as estimated by the U.S. Bureau of Reclamation (USBR); we refer to USBR values as observed (USBR 2010) (Fig. 2.2). In the observations, flows generally peak in spring (usually June), and vary in total average annual flow from 220 to 1010 m^3/s in individual years between 1975-2005, with an average of 590 m^3/s. The seasonality and magnitude of streamflows differed among models, although trends in wet and dry years generally coincided with observations (Fig. 2.2). When compared to naturalized streamflow, baseline historical simulations for each LSM run had a range of biases. VIC simulated the peak in seasonal flow in the same month as observed, but had a dry bias averaging 12% for 1975-2005. Sac simulated peak flows a month earlier than observations on

average and had a negative bias of 9% for 1975-2005. The two versions of Noah were the two extreme LSMs. Noah 2.8 was extremely wet relative to observations (64% wet bias in annual flows) and peaked three months earlier, whereas Noah 2.7 was dry (49% dry bias in annual flows) and peaked a month earlier. CLM also consistently underestimated (28%) annual flow and had a much a narrower peak in monthly flow relative to observations and other models. Catchment peaked two months earlier and had a dry bias (44% in annual flows).

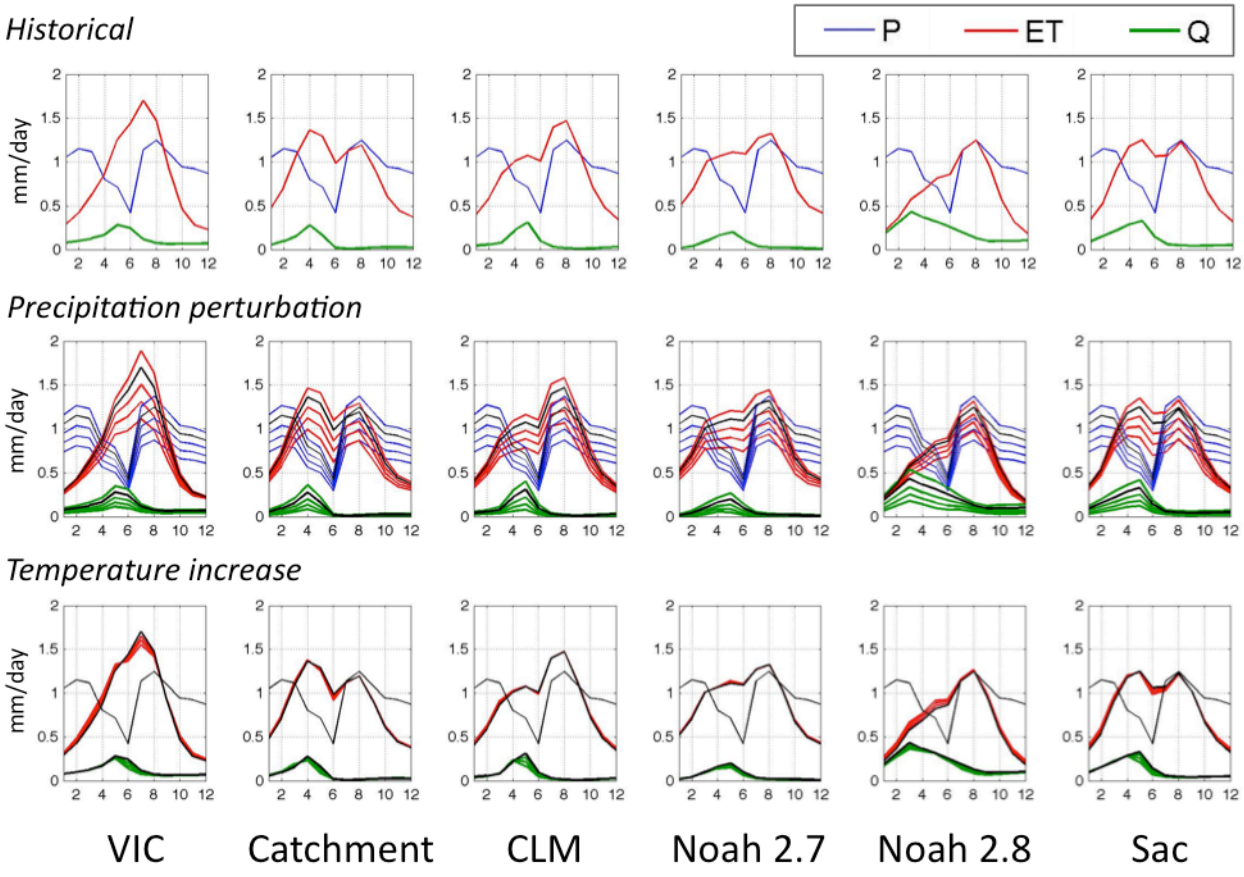

FIG 2.3 Multi-model basin-wide water balance. Averages from 1975-2005 for months from January to December. Values are averages across all basin grid cells (not routed flows). Values in the lower two rows represent change from precipitation perturbations of 70%, 80%, 90% and 110% (second row) and temperature increases of 1, 2, and 3 °C (bottom row), where black lines reflect the historical values in each water balance component and lines further from historical are more extreme changes.

TABLE 2.2 Multi-model basin-wide water balance, 1975-2005. Observations are basin-wide estimates that assume zero storage, see text for more detail, n/a=not available.

	Precipitation (mm/day)	Runoff (mm/day)	Evapotran-spiration (mm/day)	Storage (mm/day)	Storage/ Precipitation	Evapotran-spiration/ Precipitation	Snow Water Equivalents (mm)	Surface Runoff/Total Runoff
observations	*0.96*	*0.09*	*0.87*	*0*	*0%*	*91%*	*n/a*	*n/a*
Catchment	0.96	0.07	0.88	0.00	0.1%	92%	5.9	73%
CLM	0.96	0.08	0.88	0.00	0.5%	91%	7.3	34%
Noah 2.7	0.96	0.06	0.90	0.00	-0.1%	94%	7.8	60%
Noah 2.8	0.96	0.22	0.66	0.08	8.3%	69%	4.2	38%
Sac	0.96	0.13	0.84	-0.01	-1.1%	88%	9.9	50%
VIC	0.96	0.12	0.83	0.00	0.2%	87%	9.4	30%

In LSM simulations, runoff (Q) by construct should equal the residual of P minus evapotranspiration (ET) in long-term mean, assuming no long-term change in storage. When averaged over the entire basin (Fig. 2.3 top panels; Table 2.2), most LSMs had long-term storage changes that were less than one percent of P over the period of simulation (Table 2.2). Noah 2.8 was an exception, with 8% of P per year on average not accounted for in either Q or ET. Basin-wide averages of water balance in Table 2.2 differ from those at Lees Ferry (e.g., P=1.0 mm/day at Lees Ferry vs. 0.96 mm/day across the entire basin) primarily because the entire basin includes the drier lower basin- that is similar values of runoff are averaged over larger areas.

Averaged over the entire basin, ET varied from 69% of P in Noah 2.8 to 94% of P in Noah 2.7 (Table 2.2). Basin-wide P from the forcing data set minus an estimate of observed streamflow averaged for 1975-2005 was approximately 0.87 mm/day, or 90% of P. In this estimate we add 40 m^3/s, the lower bound, to naturalized flow values at Imperial to include the Gila basin, as USBR does not report values for the Gila. In the LSMs, ET was influenced by both T and P – higher in the summer with a slight decline in June when P was lowest, which resulted in a bimodal peak. All LSMs simulated this phenomenon to some extent (Fig. 2.3). Catchment and Sac had ET peaks that occurred early (in April and May respectively) at the same time Q peaked and again in August, while Noah (both versions) and CLM peaked in August with

a smaller increase occurring in May. VIC ET had one well-defined peak in July, although when temperatures were increased, a bi-modal peak began to appear.

The springtime peak in runoff coincided with the ET peak in all LSMs except VIC and Noah 2.8. In VIC snow melted later than in the other LSMs, which might be associated with lower ET, as the growing season is shorter. In Noah 2.8, this is likely because the runoff peak occurred much earlier – before net radiation, which drives ET, was high enough to support a peak in ET.

Spatially, all LSMs had somewhat similar patterns in ET, Q, and snow water equivalents (SWEs) with most Q produced at the highest elevations (Fig. 2.4). Noah 2.8 had low SWE throughout the winter and ET values were much lower than for the other models, resulting in more Q. The relative fraction of Q generated in the lower basin varied considerably across

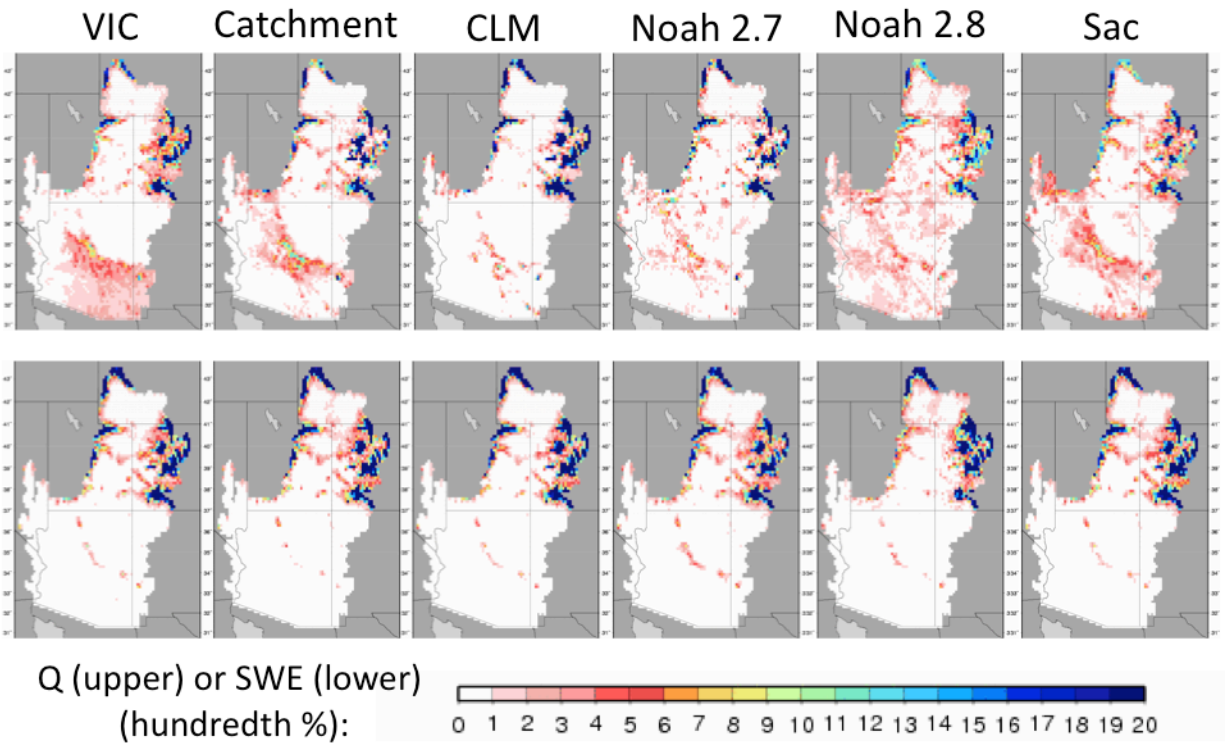

FIG 2.4. Spatial variations in historical simulations of total runoff (Q, surface runoff + drainage) (upper) and average snow water equivalents (SWE) (lower) as a percentage of basin totals.

models - VIC, Sac, Noah 2.8, and Catchment generated 36 to 32% of total basin Q from the lower basin (below Lees Ferry), whereas CLM and Noah 2.7 generated much smaller amounts – 12% for CLM and 23% for Noah 2.7 with most of the runoff coming from elevations greater than 1500 m. The lower basin is heavily managed (e.g., according to Blinn and Poff (2005), the Gila River's virgin flows were greater than 40 m^3/s, whereas now they are less than 6 m^3/s). If however we conservatively assume naturalized flows below Imperial are 40 m^3/s, lower basin flows are approximately 15% of the total basin. Similarities in model performance were somewhat surprising given that the partitioning of water between surface runoff and drainage differs considerably among models (e.g. about 30% of total runoff is surface water in VIC versus 73% in Catchment, Table 2.2).

The data set we used (Wood and Lettenmaier 2006) may have a slight dry annual bias. When VIC streamflow generated with this forcing data set is compared to other VIC simulations run with forcing data sets of Maurer et al. (2002) and Hamlet and Lettenmaier (2005) from 1950-1999, streamflow values at Lees Ferry were lower when using Wood and Lettenmaier (2006) by about 9 and 12% respectively. Therefore some dry bias in streamflow is not unexpected – the extent to which Noah 2.7, Catchment, and CLM streamflows were dry, however, resulted in biases that go beyond the effects of modest P differences. In particular, the wetness of Noah 2.8 relative to Noah 2.7 likely has to do with model physics parameterizations of turbulent fluxes (see Wei et al. 2012 for details on version differences) that result in low ET in the early spring and an apparent imbalance in the Noah 2.8's water budget.

2.4.2 Precipitation changes

Precipitation (P) perturbations of +10%, -10%, -20%, and -30% relative to historical (1975-2005) resulted in large but relatively consistent changes in ET and Q across the LSMs (Fig. 2.3,

second row). The applied percentage changes in P were uniform over the year, but because P had a strong seasonality the magnitude of change in P (e.g., in mm) was not uniform. For instance, the *smallest* absolute changes in P averaged over the basin were in summer. Other water balance terms, however, did not have the same seasonal fluctuations. In fact, the *largest* absolute change in ET occurred for all models in the summer. The largest absolute Q change occurred when Q peaked, which varied among LSMs but was typically in the spring or early summer.

Precipitation elasticities (ε) – the percent change in Q for a 1% change in P – varied depending on reference climate (Fig. 2.5) and location within the basin (Fig. 2.6, top row). ε calculated with historical values (see reference P=100% on Fig. 2.5 left panel) ranged from 2.2 to

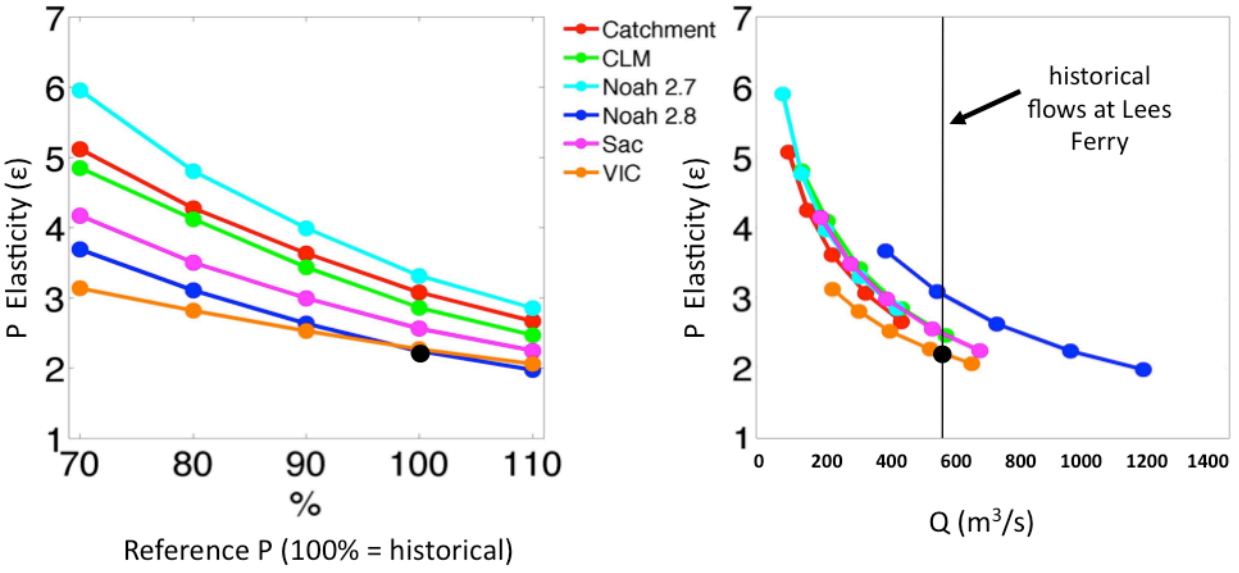

FIG 2.5 Precipitation elasticities (ε) at Lees Ferry. Values on y-axis are ε. For example, if ε is 3, a 10% decrease in precipitation would result in a 30% decrease in streamflow. The same values are plotted in two different ways. Left panel, delta perturbations and resulting change in ε where percentages relate to differences in reference climate from historical. Right panel, same ε but plotted relative to average runoff, lowest to highest runoff values of each LSM relate to 70%, 80%, 90%, historical, and 110% precipitation perturbation simulations respectively. The black dot is the value calculated using the non-parametric estimator in Sankarasubramanian et al. 2001 and the black line represents historical flows at Lees Ferry (587 m^3/s) for the period of analysis 1975-2005.

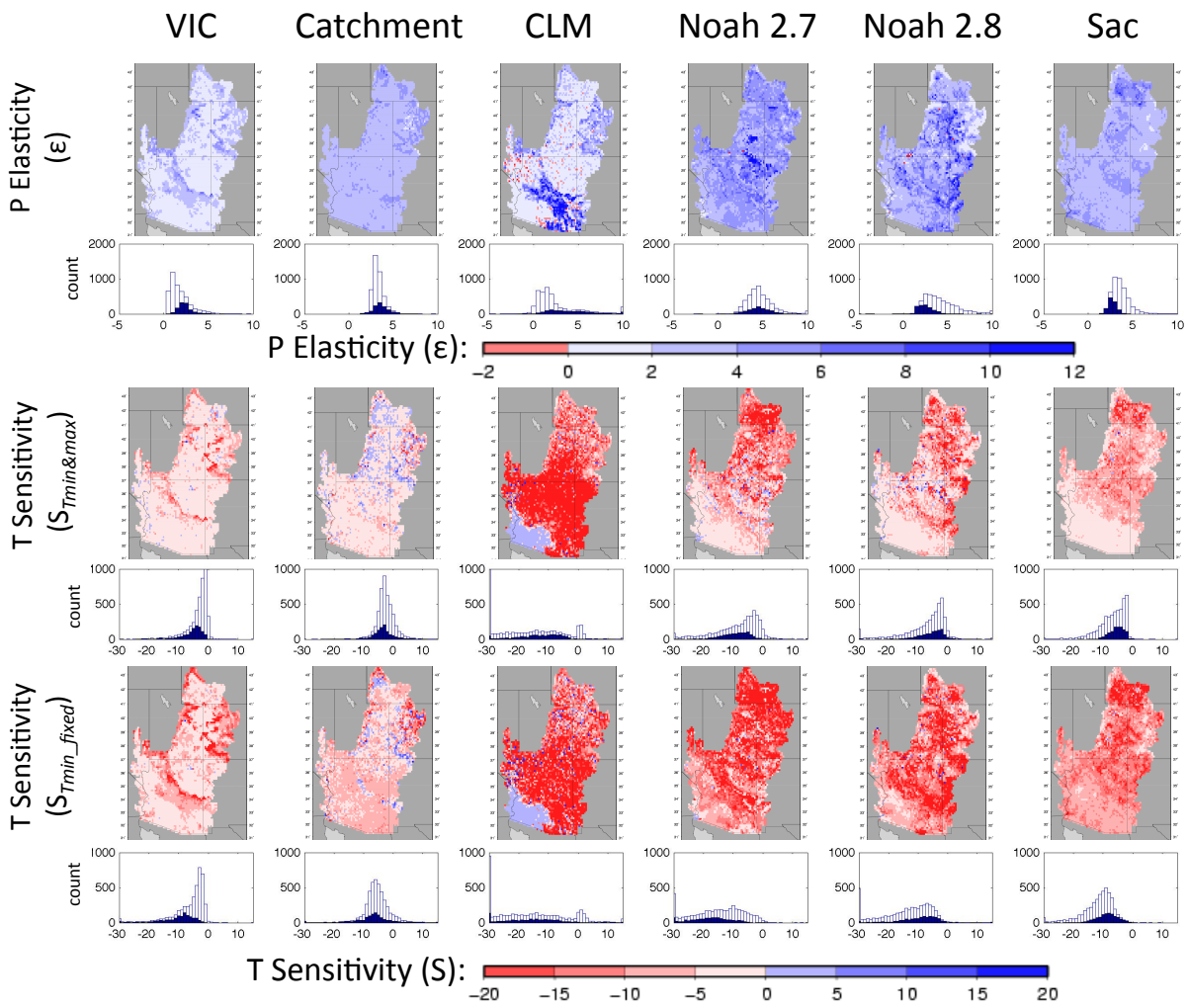

FIG 2.6 Historical precipitation elasticities (ε) and temperature sensitivities (S). In the histogram, dark blue values are grid cells that have the highest 25% of runoff values in the basin.

3.3 at Lees Ferry for different LSMs. In other words, a decrease in P of 1% relative to the climatology resulted in a decrease in Q from between 2.2-3.3%. This compares with an observed elasticity of 2.2 calculated at Lees Ferry from 1975-2005 using the non-parametric median estimator described in Sankarasubramanian et al. (2001).

Values of ε varied within LSMs depending on the reference climate and basin location. Drier (-30% to -10%) and wetter (+10%) simulations relative to climatology had ε values that

ranged from 2.0 to 6.0. Values of ε for all LSMs decreased with increasing P. Declines in ε with increasing P had relatively similar slopes between LSMs with a slight concave curve that is more pronounced in LSMs and at locations that have lower flows (i.e., if the current climate flow was anomalously low for a given LSM, its ε value tended to be high relative to the others). Elasticity values greater than one, and strong increases in elasticity with declining precipitation, denote water limitations (Dooge 1992). These limitations become increasingly severe as precipitation declines. This is consistent with the Budyko hypothesis and analysis of climate sensitivities by Dooge (1992). It is therefore not surprising that the rank of the models from most to least elastic closely aligns with the magnitude of their historical flows. Specifically, Noah 2.7 (0.11 mm/day), Catchment (0.12 mm/day), and CLM (0.15 mm/day) have the lowest average current climate flows at Lees Ferry, and the highest ε values (3.3, 3.0, and 2.9 respectively). This trend continues across different reference P values. If ε is plotted as a function of total flow rather than percent change, Noah 2.7, Catchment, CLM, and Sac tend to align on a single curve (Fig. 2.5, right panel), while VIC is slightly lower and Noah 2.8 higher. This highlights the importance of computing ε using simulations that reproduce historical streamflow. This result suggests that Noah 2.7, CLM, Catchment, and Sac would have similar ε values if their parameters were adjusted so that the simulated (reference climatology) streamflows were similar, whereas VIC would be less elastic and Noah 2.8 more elastic (if Noah 2.8 were not biased wet, it would have considerably higher ε values than shown in Fig. 2.5, right panel).

LSMs differ considerably as to where within the basin they are most elastic (Fig. 2.6). For example, VIC has its highest ε values at high elevations that contribute the most to runoff, whereas, these same areas have the lowest ε values in Sac (see the histogram below each map in Fig. 2.6). Most VIC grid cells have ε values that range from 0.3 to 5.0, whereas for Sac the

range is from about 2 to 8, yet overall basin ε values are nearly identical between these two models because the area that contributes most of the runoff has similar ε values – even though these values are at opposite ends of their entire-basin histograms. In other words, the highest 25% of runoff comes from the parts of the basin where ε values are most similar between models (see dark blue areas of histograms in Fig. 2.6). For parts of the basin that generate less flow, the model ε values are much more divergent (Fig. 2.7). Notably, the basin's runoff is strongly controlled by the relatively small headwaters area. Therefore, it clearly is most important for models to simulate the headwaters accurately since it is such a large contributor to the entire basin's flows.

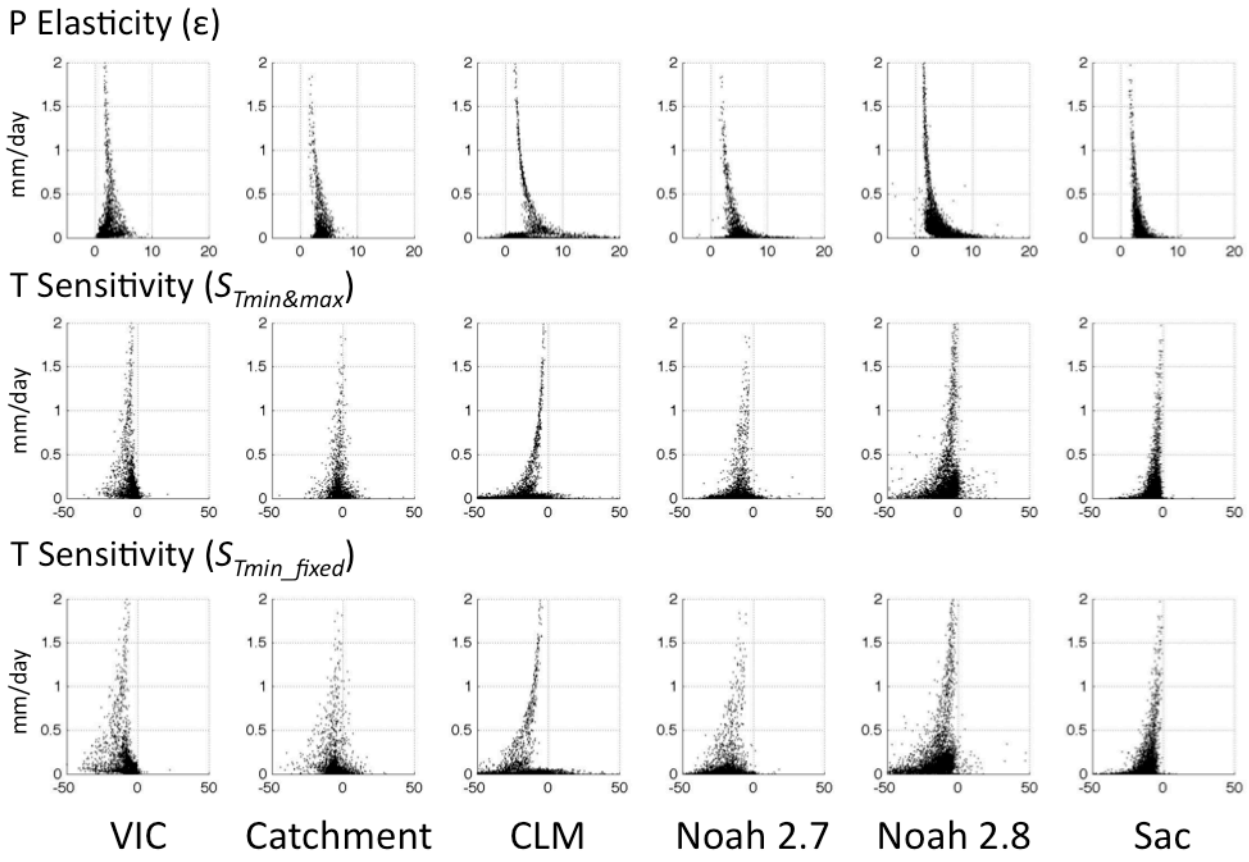

FIG 2.7 Hydrologic sensitivity and average runoff. Average runoff for each grid cell (y-axis) plotted verses historical hydrologic sensitivities. As runoff increases, values between LSMs become more similar.

Negative ε values were rare, but occurred in all models except for Sac. These values appear to be computational artifacts, as the few values disappeared when perturbation values were increased from 1 to 10% and only continued to occur with any frequency in CLM at locations where runoff values were smaller than any other model (values of 0.001 mm/day and less). CLM also had some very high ε values in the lower basin (Fig. 2.6). This appears to occur because CLM generated exceptionally low runoff in the arid parts of the lower basin (Fig. 2.4), hence even small increases can imply high ε values.

2.4.3 Temperature changes

Essentially all climate projections indicated that air temperature (T) will increase in the CRB as over most of the globe (IPCC, 2007). To explore how the basin will respond to increases in T, we increased reference T by 1°C, 2°C, and 3°C by increasing daily T minimum and maximum (Fig. 2.3, bottom row). Generally, as T increased, ET seasonal peaks became wider, and Q declined in all LSMs. Changes in water balance resulting from T increases had a stronger seasonal signal than P changes and the magnitude of the annual Q change varied considerably among LSMs. Most notably, the results of T increases were declines in Q primarily in the spring and summer, and a shift in peak Q to earlier in the year.

As noted above, the daily T range is used to infer downward solar radiation. Therefore, keeping the daily T range the same implies no change in downward solar radiation, which suppresses changes in net radiation. If, however, the T perturbation increases T_{max} without changing T_{min}, the increase in T range results in increased net radiation. We calculated temperature sensitivities (S) by perturbing T in the two ways described in section 2.3.3 (Fig. 2.6, middle ($S_{Tmin\&max}$) and lower row (S_{Tmin_fixed}). We first focus on $S_{Tmin\&max}$ results and then discuss the differences between the two T perturbation approaches.

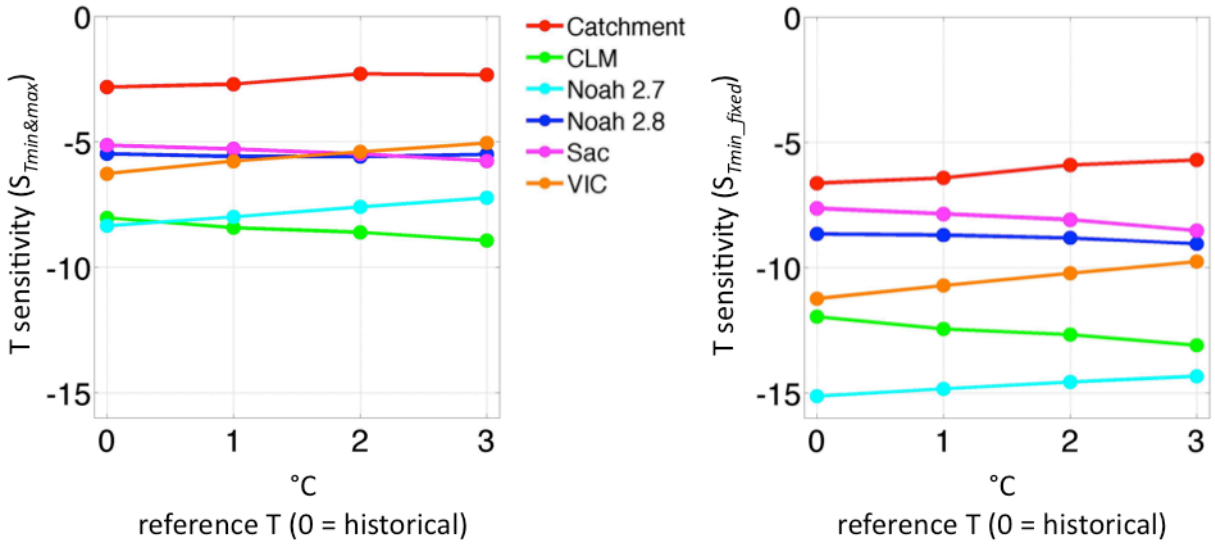

FIG 2.8 Temperature sensitivities (S) at Lees Ferry. Values on y-axis are S from Eq. 2.2 by increasing both T_{min} and T_{max} by Δ (left panel) and by fixing T_{min} and increasing T_{max} by 2Δ (right panel) at historical 1°C, 2°C, and 3°C reference climates, Δ=0.1°C.

Values of S were largely negative and differed only slightly between reference conditions, but varied considerably among the different LSMs (Fig. 2.8) and spatially (Fig. 2.6; Fig. 2.7). CLM and Noah 2.7 had the highest aggregate S, whereas Catchment tended to be the least sensitive. When T_{min} and T_{max} were both increased, $S_{Tmin\&max}$ ranged from a -2.8% change in Q per °C for Catchment to -8.4% in Noah 2.7 (Fig. 2.8, left panel) at Lees Ferry. Although $S_{Tmin\&max}$ remained relatively constant with reference T (range for all reference T was -2.3% to -8.9%), VIC and Noah 2.7 had S that became slightly less negative as the reference T increased, whereas CLM and Sac had slight decreasing trends (became more negative)(Fig. 2.8). Aggregate S for different sub-basins (not shown) had generally similar trends.

The spatial distributions of $S_{Tmin\&max}$ (Fig. 2.6, middle row) varied considerably, although most values were negative reflecting an increase in ET and subsequent decline in runoff. The greatest difference in S among LSMs were at locations with the lowest runoff values (Fig. 2.7).

There were grid cells in all LSMs that had positive S, although the number and magnitudes of these values differed considerably among LSMs. Positive S appears to occur in three types of conditions. Two are essentially computational artifacts, while the third relates to physical processes. One condition has to do with outliers in S (dark blue or dark red cells in Fig. 2.6, middle panel) that are related to small, imposed T changes. These positive S values disappeared when larger T increments were used. A second condition occurs only in CLM (manifested as a large, light blue area in the lower basin in Fig. 2.6 middle panel, which constitutes about 10% of the basin area. This coincides with very small CLM total runoff (less than 0.005 mm/day) and more specifically with the sandiest soil in the basin. These values appear to reflect internal computational issues within the model.

The third category of positive S is values that appear consistently when the T references change and is relatively insensitive to the T increment. These conditions were most noticeable in Catchment (9% of grid cells), but also occurred in Noah 2.7 (3%), Noah 2.8 (0.7%), VIC (0.6%) and CLM (0.02%). LSMs higher surface runoff ratios tended to have the largest fraction of positive S (especially Catchment, where surface runoff was almost always greater than 50% of total runoff). Many of these positive S values occurred around 2000 m (over 60% of positive values occurred between elevations of 2000 to 2500 m).

The magnitude and direction of S demonstrates how land-surface hydrology can both exacerbate, and more rarely modulate, regional scale sensitivities to global climate change. Generally, as T increases, ET increases and runoff decreases (resulting in negative S). There are, however some locations (the third category of positive S noted above) where there is a plausible mechanism for T increases to result in runoff increases because of land-surface processes. This mechanism for positive S is the so-called Dettinger Hypothesis, the details of which are

described by Jeton et al. (1996). The hypothesis is that warmer T advances spring snowmelt, and provides greater availability of moisture for runoff at a time of year when the energy available for ET is small. Hence, snowmelt is more efficiently transformed to runoff than later in the year, when evaporative demand is higher. Arguably this mechanism should be most prevalent in locations where there is transitional snow (i.e., modest T increase results in large decreases in snowpack). It also stands to reason that this phenomenon would be more prevalent when there is more surface runoff relative to drainage, meaning that moisture available for runoff leaves the system sooner. There were, however, few locations where these positive values exert much change in runoff. The San Juan sub-basin (near Bluff, UT) in Catchment appears to be one location where both positive and negative S contributed to the lower overall negative S, but in other basins and especially in other LSMs, the aggregate flow changes were always negative and influenced little by areas with positive S.

The effect of increasing reference T on S was modest, however changing the method of perturbing daily T ($S_{Tmin\&max}$ vs. S_{Tmin_fixed}) resulted in large changes -- roughly double for most of the LSMs (Fig. 2.8). When T_{min} was fixed and T_{max} was increased by 0.2 °C for an average increase of 0.1°C (S_{Tmin_fixed}, see Eq. 2.2 discussion above), S became more pronounced in all LSMs (Fig. 2.8, right panel) although spatial patterns remained similar (Fig. 2.6, bottom row). The historical climate had S_{Tmin_fixed} that ranged from -7% to -15% for Catchment and Noah 2.7 respectively. S_{Tmin_fixed} was about a factor of two larger $S_{Tmin\&max}$ averaged over all models for aggregate streamflow at Lees Ferry. The ratio was largest for Catchment (about 2.4) and least for CLM and Sac (about 1.5). Noah 2.8, VIC, and Noah 2.7 were intermediate, with (factors of 1.6, 1.9, and 1.9 respectively). Notably, changes in net radiation and vapor pressure deficit from changing the range in our T formulations changed S and thus indicate an important consideration

in understanding the uncertainty of future climate impacts to water resources - highlighting considerations of climate variables beyond T and P. Donohue et al. (2010) found there are other climate variables that matter to potential ET calculations (e.g. net radiation, vapor pressure deficit, and wind speed).

In the larger context, T minima and maxima have been shown to not be changing uniformly over recent decades. Easterling et al. (1997) found that T records globally indicated a decline in the diurnal T range primarily from T minima increasing more than T maxima. They attributed changes to increases in cloudiness, surface evaporative cooling from precipitation, greenhouse gases, and tropospheric aerosols that may be the result of urbanization, irrigation, desertification and variations in local land use. Within the Colorado basin, their collection of non-urban stations showed that T minima values in the past 100 years increased while T maxima decreased, resulting in an overall decrease in the diurnal T range. Although extensive investigation into the implication of observed changes in CRB T ranges is beyond the scope of this study, our results do suggest that changes in the diurnal T range can have strong implications for S, which vary among LSMs, and thus is important to consider when constructing and evaluating climate change scenarios.

2.4.4. Precipitation and temperature

Understanding P and T impacts on runoff independently provides a foundation from which to understand future changes. In reality, however, climate change most likely will be manifested by a combination of changes (e.g. both P and T). To test the extent to which the two effects can be superimposed (i.e., the combined effect estimated as the sum of P and T effects), we compared a simulation where both P and T were changed with the predicted sum of the individual effects for each variable (Fig. 2.9; Fig. 2.10), see Eq. 2.3. For all of the LSMs, the combined effects were

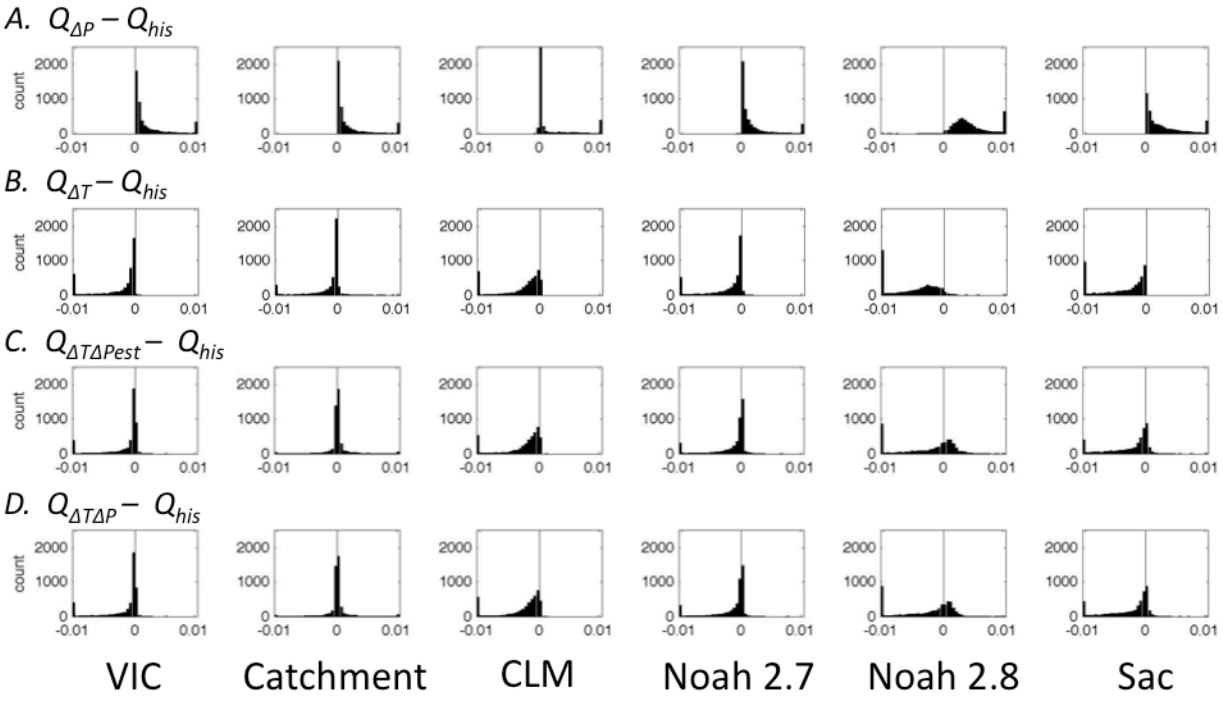

FIG 2.9 Precipitation and temperature superposition. Histograms show response for 4518 grids cells of (A) difference from 1% P change, (B) difference from 1°C T change, (C) estimated difference (additive) from both 1% P and 1°C T change, and (D) simulated difference from both 1% P and 1°C T. Differences estimated by superposition (C) are similar to D indicating interaction effects were quite small.

quite close to those estimated by superposition, indicating that interaction effects were quite small, e.g. differences between $Q_{\Delta T \Delta Pest}$ and $Q_{\Delta T \Delta P}$, assuming no interaction, were within 1.5% of $Q_{\Delta T \Delta P}$ for over 90% of all grid cells in all LSMs except for CLM (which 90% of grid cells were within 2.5%, and 77% of grid cells were within 1.5%). $Q_{\Delta T \Delta P}$ tended to be minutely smaller than $Q_{\Delta T \Delta Pest}$, which would be expected since the combined run ($Q_{\Delta T \Delta P}$) has more P, and therefore runoff, for simultaneously occurring T increases to diminish.

We also examined the spatial patterns of the inferred interaction effect (Fig. 2.10). The percent difference of $Q_{\Delta T \Delta Pest}$ from $Q_{\Delta T \Delta P}$ had spatial patterns that coincided with areas where runoff is more sensitive to changes in T and P. VIC had the greatest correlation ($r_{\%diff,elast}$=0.72) with ε values and $r_{\%diff,sens}$=0.68 with S values. Sac had the second highest correlations:

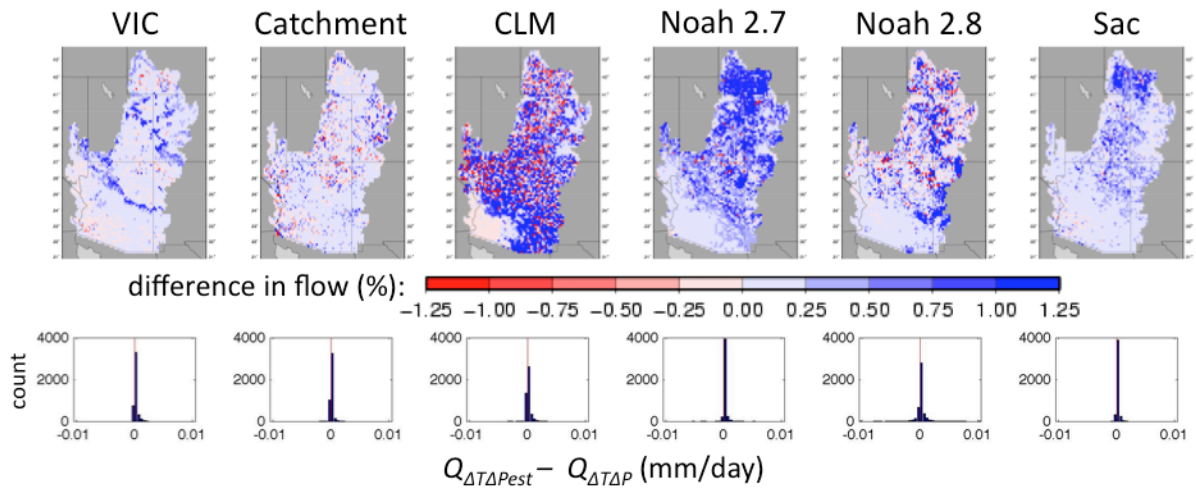

FIG 2.10 Combined precipitation and temperature changes. Maps show the percent difference in $Q_{\Delta T \Delta Pest}$ from $Q_{\Delta T \Delta P}$, note that the scale is considerably small relative to previous figures (e.g. total range of 2.5% vs. the temperature sensitivity range of 40%). Histograms show total difference in flow with the majority of differences in all LSMs being within ±0.0005 mm/day of zero.

$r_{\%diff,elast}$=0.61 and $r_{\%diff,sens}$=0.58. Correlations with ε values were greater than with S values, except for Noah 2.7 (which had small correlations for both $r_{\%diff,elast}$=0.20 and $r_{\%diff,sens}$=0.26).

More broadly, areas that were more sensitive to changes in P were also, generally, more sensitive to changes in T as evident in similar, yet opposite, spatial patterns and histograms of ε and S (Fig. 2.6; Fig. 2.7). Correlation coefficients between ε and S for all individual grid locations (n=4518) were, however, small for most models with VIC having the greatest correlation (r=0.81), Sac the second largest (r=0.48) and all others less than 0.3.

It is unclear why models converge in ε and S in the headwaters and diverge elsewhere. This divergence in lower flow regions is of somewhat diminished importance for understanding overall Colorado River flow, but arguably is important for understanding changes in water demand (which is beyond the scope of this study). For example, Sac and Noah 2.8 simulations have hydrologic sensitivities that indicate considerably more water stress as T increase and P decreases in the lower basin (i.e., a need for more water to compensate for climate change) than in VIC and Catchment simulations.

2.5. Conclusions

We investigated the hydrologic sensitivities of five commonly used land surface models (LSMs) to precipitation and temperature changes. We found the magnitude of predicted runoff changes resulting from these changes differs considerably among models as evidenced by large variations in precipitation elasticities and temperature sensitivities among the LSMs. Identifying the nature of these differences helps to better understand how land-surface hydrology exacerbates or, in the Colorado River Basin (CRB) more rarely, modulates regional scale sensitivities to global climate change, how the range of hydrologic sensitivities is attributable to model bias, and how hydrologic sensitivities vary spatially across the CRB. More specifically, we found:

(1) The direction of runoff change among LSMs is similar, with declines in annual streamflow at Lees Ferry when either precipitation decreased or temperature increased in all models. However, in most LSMs, there are some areas where temperature sensitivities are positive – mostly in the transient snow zone. In these areas, land surface processes modulate change, although the fraction of the CRB affected is quite small (and accounts for at most 7% of total runoff).

(2) Model biases have an overt effect on the range of precipitation elasticity values, and an equivalent effect is not apparent in temperature sensitivity values. Most models have larger elasticities with respect to precipitation than are inferred from observations. This results in part because most of the models are biased downward in their reproduction of current runoff. Differences in LSM elasticities are amplified by these dry biases, which highlights the importance of simulating historical runoff magnitudes reasonably before performing climate perturbations. However, even with runoff bias accounted for, with elasticities interpolated to observed flows at Lees Ferry, there remains a range from about 2.2 to 3.1 in the elasticity of

aggregate flows. Temperature sensitivities vary by at least a factor of two among LSMs, but are not influenced much by biases in the models' runoff simulations (an analogous interpolation for temperature to adjust for dry biases would not be appropriate).

(3) The elasticities and temperature sensitivities are more consistent among models in headwater regions that produce most of the CRB's runoff, relative to other locations in the basin. Convergence in the headwaters tends to mask larger differences in parts of the basin that produce less runoff.

(4) Superposition of precipitation and temperature changes largely holds with respect to annual runoff in the CRB in all LSMs across 4518 grid locations that represent a range of reference conditions; i.e. the combined effect of precipitation and temperature changes are essentially equivalent to the sum of the precipitation and temperature contributions computed separately.

These findings for the CRB highlight a way to evaluate LSM performance that relates directly to their use in climate change studies. Similar investigations in other major river basins would be advantageous to further compare LSM performance. Notably, the CRB is more extreme than most river basins, especially considering that differences in LSM responses reflect differences in the models' evapotranspiration parameterizations, meaning the CRB is particularly sensitive because evapotranspiration in the basin comprises more than 85% of the basin's water balance.

Acknowledgements

The authors thank Ted Bohn and Ben Livneh for assistance with model set up; Randy Koster for use of the Catchment model and feedback on earlier versions of the paper; Brad Udall, Robin

Webb, Dan Cayan, Levi Brekke, and Kevin Werner for early feedback on research direction; and two anonymous reviewers for suggestions on manuscript revisions. This publication was funded by the NOAA Regional Integrated Sciences and Assessments program and the NOAA Climate Dynamics and Experimental Prediction/Applied Research Centers program under NOAA Cooperative Agreement NA17RJ1232 and NA10OAR4320148 to the Joint Institute for the Study of the Atmosphere and Ocean (JISAO), and by U.S. Department of Energy Grant DE-FG02-08ER64589 to the University of Washington. This is JISAO Contribution 1871.

References

Anderson, E. A., 1973: National Weather Service River Forecast System: Snow Accumulation and Ablation Model, NOAA Tech. Memo. NWS Hydro-17, Natl. Weather Serv., Silver Spring, Md.

Barnett and Pierce, 2009: Sustainable water deliveries from the Colorado River in a changing climate, *Proc. Natl. Acad. Sci*., **106**(18), 7334-7338. doi: 10.1073/pnas.0812762106

Blinn, D.W. and N.L. Poff, 2005, Chapter 11. Colorado River Basin. *In:* A. Benke and C.E. Cushing (eds.). *Rivers of North America*. Academic Press. Pp. 483-538.

Boone, A., F. Habets, J. Noilhan, D. Clark, P. Dirmeyer, S. Fox, Y. Gusev, I. Haddeland, R. Koster, D. Lohmann, S. Mahanama, K. Mitchell, O. Nasonova, G.-Y. Niu, A. Pitman, J. Polcher, A. B. Shmakin, K. Tanaka, B. van den Hurk, S. Vérant, D. Verseghy, P. Viterbo, and Z.-L. Yang,2004: The Rhone-aggregation land surface scheme inter- comparison project: An overview, *J. Clim*., **17**(1), 187–208.

Burnash, R. J. C., R. L. Ferral, and R. A. McGuire, 1973: A generalized streamflow simulation system: Conceptual models for digital computers, technical report, Joint Fed.-State River Forecast Cent., U.S. Natl. Weather Serv. and Calif. Dep. of Water Resour., Sacramento, Calif.

Cayan D.R., Das T., Pierce D.W., Barnett T.P., Tyree M. and Gershunov A. 2010. Future dryness in the southwest US and the hydrology of the early 21st century drought. Proceedings of the National Academy of Sciences, 107(50), 21271-21276, doi: 10.1073/pnas.0912391107.

Christensen, N.S., A.W. Wood, N. Voisin, D.P. Lettenmaier, and R.N. Palmer, 2004: Effects of climate change on the hydrology and water resources of the Colorado River Basin. *Climatic Change*, **62**, 337–363.

Christensen, N., and D. P. Lettenmaier, 2007: A multimodel ensemble approach to assessment of climate change impacts on the hydrology and water resources of the Colorado River basin. *Hydrology and Earth System Sciences,* **3**, 1–44.

Dooge, J.C.I., 1992: Sensitivity of Runoff to Climate Change: A Hortonian Approach. *Bull. Amer. Meteor. Soc.*, **73**, 2013–2024.

Dooge, J. C. I. , Bruen, M. and B. Parmentier, 1999: A simple model for estimating the sensitivity of runoff to long-term changes in precipitation without a change in vegetation, *Advances in Water Resources*, **23**:2, 153-163, ISSN 0309-1708, DOI: 10.1016/S0309-1708(99)00019-6.

Donohue, R.J., T.R. McVicar, and M.L. Roderick, 2010: Assessing the ability of potential evaporation formulations to capture the dynamics in evaporative demand within a changing climate, *J. of Hydrology*, **386**(1-4),186-197, DOI:10.1016/j.jhydrol.2010.03.020.

Ducharne, A., R. D. Koster, M. J. Suarez, M. Stieglitz, and P. Kumar, 2000: A catchment-based approach to modeling land surface processes in a general circulation model 2. Parameter estimation and model demonstration, *J. Geophys. Res*., **105**(D20), 24,823–24,838, doi:10.1029/2000JD900328.

Easterling et al, 1997: Maximum and Minimum Temperature Trends for the Globe, *Science*, **227**, 364-367.

Elsner, M.M., L. Cuo, N. Voisin, J.S. Deems, A.F. Hamlet, J.A. Vano, K.E.B. Mickelson, S.Y. Lee, and D.P. Lettenmaier, 2010: Implications of 21st Century climate change for the hydrology of Washington State, *Climatic Change*, **102**(1-2), 225-260, doi:10.1007/s10584-010-9855-0

Fu, G., S. P. Charles, and F. H. S. Chiew, 2007: A two-parameter climate elasticity of streamflow index to assess climate change effects on annual streamflow, *Water Resour. Res*., **43**, W11419, doi:10.1029/2007WR005890.

Gardner, L.R., 2009: Assessing the effect of climate change on mean annual runoff, *Journal of Hydrology*, **379**, 351-359, ISSN 0022-1694, DOI:10.1016/j.jhydrol.2009.10.021.

Hamlet, A. F., and D. P. Lettenmaier, 2005: Production of temporally consistent gridded precipitation and temperature fields for the continental United States, *J. Hydrometeorol*., **6**, 330–336.

Henderson-Sellers et al, 1995: The project for Intercomparison of land surface parameterisation schemes PILPS) Phases 2 and 3, *Bull. Amer. Meteorol. Soc*., **76**, 489-503.

Hoerling, M., and J. K. Eischeid, 2006: Past peak water in the southwest. *Southwest Hydrology*, **35**, 18–19.

Hoerling, M., Lettenmaier, D.P., Cayan D., and B. Udall, 2009: Reconciling projections of Colorado River streamflow. *Southwest Hydrology* **8**(3): 20-21, 31.

Intergovernmental Panel on Climate Change, 2007, The physical science basis, *in* Solomon, S., Qin, D., Manning, M., Chen, Z., Marquis, M., Averyt, K.B., Tignor, M., and Miller, H.L., eds., Contribution of Working Group I to the Fourth Assessment Report of the Intergovernmental Panel on Climate Change: Cambridge, United Kingdom, Cambridge University Press. (Also available online at *http://www.ipcc.ch/ipccreports/ar4-wg1.htm*.)

Jeton, A.E., Dettinger, M.D., and J.L. Smith, 1996: Potential effects of climate change on streamflow, eastern and western slopes of the Sierra Nevada, California and Nevada: U.S. Geological Survey Water Resources Investigations Report 95-4260, 44 p.

Kavetski D. and M.P. Clark, 2010: Numerical troubles in conceptual hydrology: Approximations, absurdities and impact on hypothesis testing. *Hydrol. Process*. **25**:4, 1099-1085 DOI: 10.1002/hyp.7899

Koster, R.D., M.J. Suarez, A. Ducharne, M. Stieglitz, and P. Kumar, 2000: A catchment-based approach to modeling land surface processes in a general circulation model. 1. Model structure. *J. of Geophysical Research*, **105**:D20, 24809-22.

Koster, R. D. and P. C. D. Milly, 1997: The interplay between transpiration and runoff formulations in land surface schemes used with atmospheric models. *J. Climate*, **10**, 1578–1591.

Liang, X., D. P. Lettenmaier, E. F. Wood, and S. J. Burges, 1994: A simple hydrologically based model of land surface water and energy fluxes for General Circulation Models. *J. Geophys. Res.,* **99**, 14 415– 14 428.

Lohmann D., K.E. Mitchell, P.R. Houser, E.F. Wood, J.C. Schaake, A. Robock, B.A. Cosgrove, J. Sheffield, Q. Duan, L. Luo, R.W. Higgins, R.T. Pinker, and J. D. Tarpley, 2004: Streamflow and water balance intercomparisons of four land surface models in the North American Land Data Assimilation System project, *J. Geophys. Res*., **109**, D07S91, doi:10.1029/2003JD003517.

Lohmann, D., R. Nolte-Holube, and E. Raschke, 1996: A large-scale horizontal routing model to be coupled to land surface parameterization schemes. *Tellus,* **48:** 708-721

Lohmann, D., E. Raschke, B. Nijssen, and D. P. Lettenmaier, 1998: Regional Scale Hydrology: I. Formulation of the VIC-2L Model Coupled to a Routing Model. *Hydrological Sciences Journal,* **43,** 131-141.

Livneh, B., Y. Xia, K.E. Mitchell, M.B. Ek, and D.P. Lettenmaier, 2010: Noah LSM Snow Model Diagnostics and Enhancements, *J. Hydrometeorol*., **11**(3),721-738

Maurer, E.P., A.W. Wood, J.C. Adam, D.P. Lettenmaier, and B. Nijssen, 2002: A long-term hydrologically-based data set of land surface fluxes and states for the conterminous United States, *J. Climate*. **15**, 3237-3251.

McMahon, T.A., 1982: *Hydrological Characteristics of Selected Rivers of the World Technical Documents in Hydrology*, Unesco, Paris.

Milly, P. C. D., K. A. Dunne, and A. V. Vecchia, 2005: Global pattern of trends in streamflow and water availability in a changing climate. *Nature*, **438**, 347–350.

Mitchell, K. E., D. Lohmann, P.R. Houser, E.F. Wood, J.C. Schaake, A. Robock, B.A. Cosgrove, J. Sheffield, Q. Duan, L. Luo, R.W. Higgins, R.T. Pinker, J.D. Tarpley, D.P. Lettenmaier, C.H. Marshall, J.K. Entin, M. Pan, W. Shi, V. Koren, J. Meng, B. H. Ramsay, and A.A. Bailey , 2004: The multi-institution North American Land Data Assimilation System (NLDAS): Utilizing multiple GCIP products and partners in a continental distributed hydrological modeling system, *J. Geophys. Res*., **109**, D07S90, doi:10.1029/2003JD003823.

Nijssen, B., D. P. Lettenmaier, X. Liang, S. W. Wetzel, and E. F. Wood, 1997: Streamflow simulation for continental-scale river basins. *Water Resour. Res*., **33**, 711-724.

Nijssen, B., R. Schnur, and D. P. Lettenmaier, 2001: Global retrospective estimation of soil moisture using the Variable Infiltration Capacity land surface model, 1980-1993. *J. Climate*, **14**, 1790-1808.

Oleson, K.W., Y. Dai et al., 2004: Technical description of the Community Land Model (CLM), *NCAR Technical Note NCAR/TN-461+STR*, 173 pp., National Center for Atmospheric Research, Boulder, CO. available online at: *http://www.cgd.ucar.edu/tss/clm/distribution/clm3.0/TechNote/CLM_Tech_Note.pdf*

Oleson, K.W., G.Y. Niu, Z.L. Yang, D.M. Lawrence, P.E. Thornton, P.J. Lawrence, R. Stockli, R.E. Dickinson, G.B. Bonan, and S. Levis, 2007: CLM 3.5 Documentation, available online: *http://www.cgd.ucar.edu/tss/clm/distribution/clm3.5/CLM3_5_documentation.pdf* 34 pp.

Oleson, K. W., G Y Niu, Z L Yang, D M Lawrence, P E Thornton, P J Lawrence, R Stöckli, R E Dickinson, G B Bonan, S Levis, A Dai, T Qian, 2008: Improvements to the Community Land Model and their impact on the hydrological cycle*, J. Geophys. Res*., **113**, G01021, doi:10.1029/2007JG000563.

Overpeck and Udall, 2010: Dry times ahead, *Science* **328**(5986): 1642-1643. DOI: 10.1126/science.1186591

Pitman, A. J., A. Henderson-Sellers, F. Abramopolous, A. Boone, C. E. Desborough, R. E. Dickinson, J. R. Garratt, N. Gedney, R. Koster, E. A. Kowalczyk, D. Lettenmaier, X. Liang, J.-F. Mahfouf, J. Noilhan, J. Polcher, W. Qu, A. Robock, C. Rosenzweig, C. A. Schlosser, A. B. Shmakin, J. Smith, M. Suarez, D. L. Verseghy, P. Wetzel, E. F. Wood, Y. Xue, and Z.-L. Yang,, 1999: Key results and implications from Phase 1(c) of the

Project for Intercomparison of Land-surface Parameterization Schemes. *Climate Dyn.,* **15**, 673–684.

Sankarasubramanian A., R.M. Vogel, and J. F. Limbrunner, 2001: Climate elasticity of streamflow in the United States, *Water Resour. Res*., **37**, 1771-1781.

Schaake, J. C., 1990: From climate to flow, in *Climate Change and U.S. Water Resources*, edited by Waggoner, p. 177-206, John Wiley, New York.

Seager, R., M. Ting, I. Held, Y. Kushnir, J. Lu, G. Vecchi, H.-P. Huang *et al*., 2007: Model projections of an imminent transition to a more arid climate in southwestern North America. *Science* **316**: 1181–1184

Thornton, P. E. and Running, S. W, 1999: An Improved Algorithm for Estimating Incident Daily Solar Radiation from Measurements of Temperature, Humidity, and Precipitation, *Agric. For. Meteorol.* **93**, 211–228.

U.S. Bureau of Reclamation (USBR), 2010: "CURRENT natural flow data 1906-2007," downloaded at http://www.usbr.gov/lc/region/g4000/NaturalFlow/current.html on January 14, 2010

Wang A., T.J. Bohn, S.P. Mahanama, R.D. Koster, and D.P. Lettenmaier, 2009: Multimodel ensemble reconstruction of drought over the continental United States, *J. Climate*, **22**, 2694–2712, doi:10.1175/2008JCLI2586.1.

Wei H., Y. Xia, M.B. Ek, and K.E. Mitchell, 2012: Improvement of the Noah Land Surface Model for Warm Season Processes: Evaluation of Water and Energy Flux Simulation, accepted to *Hydrological Processes*

Western Water Assessment (WWA), Colorado Climate Change: A Synthesis to Support Water Resource Management and Adaptation. Oct 2008 (available online at:

http://cwcb.state.co.us/public-information/publications/Documents/ReportsStudies/ClimateChangeReportFull.pdf)

Wood, A.W. and D.P. Lettenmaier, 2006: A testbed for new seasonal hydrologic forecasting approaches in the western U.S., *Bull. Amer. Meteorol. Soc.*, **87**(12), 1699-1712, doi:10.1175/BAMS-87-12-1699.

Zheng, H., L. Zhang, R. Zhu, C. Liu, Y. Sato, and Y. Fukushima, 2009: Responses of streamflow to climate and land surface change in the headwaters of the Yellow River Basin, *Water Resour. Res*., **45**, W00A19, doi:10.1029/2007WR006665.

Zhu, C.M., L.R. Leung, D. Gochis, Y. Qian and D.P. Lettenmaier, 2009: Evaluating the influence of antecedent soil moisture on variability of the North American Monsoon precipitation in the coupled MM5/VIC modeling system, *The Journal of Advances in Modeling Earth Systems* (JAMES) **1**, 22, doi:10.3894/JAMES.2009.1.13.

III. A sensitivity-based approach to evaluating future changes in Colorado River Discharge

This chapter has been submitted in its current form and currently in review in the journal *Climatic Change:* Vano, J.A. and D.P. Lettenmaier, 2013, A sensitivity-based approach to evaluating future changes in Colorado River Discharge, *Climatic Change* (in review).

Abstract

Projections of a drier, warmer climate in the U.S. Southwest would complicate management of the Colorado River system – yet these projections, often based on coarse resolution global climate models, are quite uncertain. Water managers frequently make decisions under uncertain conditions. It is therefore not the concept of climate uncertainty, but not having a good basis for characterizing the uncertainty in terms of a range of hydrologic futures that makes integrating climate information into planning difficult. We present an approach to understanding future uncertainties based on land surface characterizations that maps the region's hydrologic sensitivities (e.g., changes in streamflow magnitude) to annual and seasonal changes in temperature and precipitation. The approach uses a macroscale land surface model (LSM; in this case, the Variable Infiltration Capacity hydrologic model, although methods are applicable to any LSM) to develop sensitivity maps, and then uses these maps to evaluate long-term annual streamflow responses to future precipitation and temperature change. We show that global climate model projections combined with estimates of hydrologic sensitivities, estimated for different seasons and at different change increments, can provide a basis for

approximating cumulative distribution functions of streamflow changes similar to those that result from more common, computationally intensive full-simulation approaches that force the hydrologic model with downscaled future climate scenarios. For purposes of assessing risk, we argue that the sensitivity-based approach produces viable first-order estimates that can be easily applied to newly released climate information to assess underlying drivers of change and to bound, at least approximately, the range of future streamflow uncertainties for water resource planners.

3.1. Introduction

The Intergovernmental Panel on Climate Change (IPCC) Fourth Assessment reported unequivocal evidence that climate change was occurring and global climate models (GCMs) showed general agreement that temperature will increase and runoff will decrease across the western U.S. in the coming century (IPCC 2007; Bates et al. 2008). These changes will make managing water supplies for human consumption and healthy ecosystems more challenging, yet notwithstanding the IPCC statement, there remains much uncertainty as to the nature of regional and local impacts. A major challenge is that GCMs operate at coarse spatial scales (mostly around ~200 km x 200 km, although the resolution has been increasing over time) relative to the river basin scale where management decisions are made. To respond to this scale mismatch, various approaches have been developed which translate global scale information to more local scales (Barnett et al. 2004; Wood et al. 2004; and others), although the extent to which these methods capture basin-specific hydrologic characteristics differs considerably (WWA 2008; Vano et al. 2013).

In recent years, a common "end-to-end" approach to integrating climate information into management has been to use an ensemble of downscaled GCM output using the methods such as those outlined in Wood et al. (2004), run through a hydrology model to generate streamflow sequences which are then used to explore future changes in reservoir operations (e.g., Payne et al. 2004; Christensen and Lettenmaier 2007; USBR 2011; and others) (Fig. 3.1, schematic on left). This approach, which we refer to as the "full-simulation approach", is widely used and is generally the preferred approach for inferring local effects of climate change. It is also useful to water managers because it provides sequences of future streamflows that are similar with respect to temporal aggregation and record length as the historical streamflow sequences that they often use in planning studies. It does, however, require considerable computing and data management, as each scenario is its own realization, which might be viewed as only one ensemble member of many that provide a representation of possible future conditions. Furthermore, each time new climate model runs are released the entire process has to be repeated (e.g., at the approximately five-year interval of the IPCC reports – the fourth

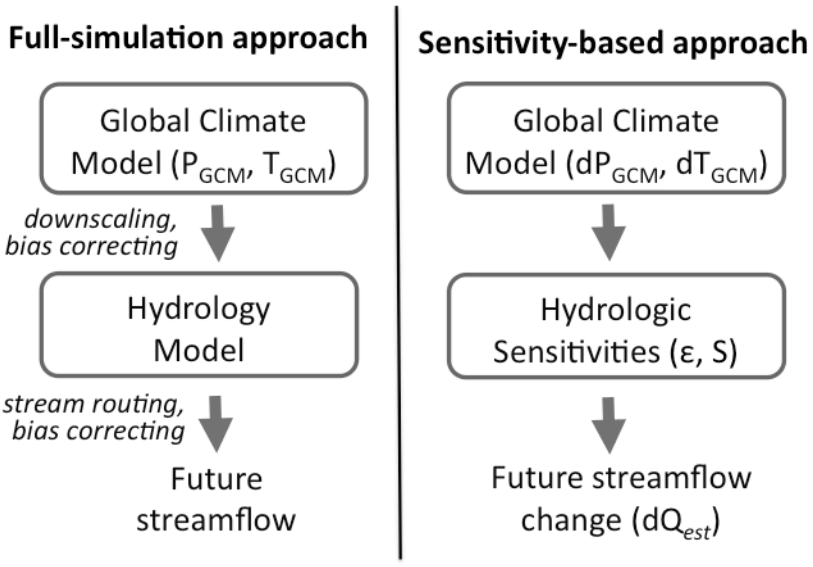

FIG 3.1 Schematic of two approaches. The full-simulation approach provides a daily time series of future streamflow, whereas the sensitivity-based approach provides only a change in mean streamflow.

Assessment Report (AR4) GCMs, generated through the Coupled Model Intercomparison Project (CMIP) results were made available around 2005 and AR5 models are becoming available as this paper is written). In most past studies, the end-to-end approach has used a single land surface model to simulate the land surface response, but this ignores the uncertainty in the simulated land-surface response simulated by a range of land surface models, which can be considerable (see Vano et al. 2012).

Although the linking of models is arguably an approach that encompasses best-available science, it often focuses more on data processing than the underlying mechanisms that control hydrologic change. Models are imperfect representations of land surface hydrologic processes, and thus each step of the modeling cascade requires decisions as to how best to span space and time. Too often, there are so many modeling steps between the climate change projections and their potential impacts (each with unquantified uncertainties), that it is difficult to assess aggregate uncertainties at the end of the modeling cascade, and it is hard to judge which approaches are appropriate for which questions (Hamlet et al. 2010; Abatzoglou and Brown 2012). These unquantified uncertainties result from various decisions including what models (e.g., GCMs, hydrology models) are used, what is the spatial resolution of the analysis, and what is and is not preserved in the downscaling of climate information (Vano et al. 2013). Increased computing capacity has allowed scientists to generate more scenarios, increasing the stream of data from one model to the next, but with this increase in volume, it has become harder to control the quality of the simulations. The implementation of the end-to-end approach also requires bias-correction procedures, which are often viewed with skepticism by the water resource management community.

We present here a sensitivity-based approach to scenario planning (Fig. 3.1, right) that leverages our best understanding of the hydrological processes within the atmosphere-hydrosphere-biosphere continuum. It can produce first-order estimates to help bound the uncertainties in estimated long-term hydrologic response to changes in climate forcings. It can also provide complimentary information to other downscaling approaches to help assess sources of uncertainties (e.g., whether streamflow change is more sensitive to precipitation (P) or temperature (T) change in a particular river basin). The approach uses precipitation elasticity (ε) and temperature sensitivity (S) as defined in Vano et al. (2012) to translate climate forcings into changes in streamflow, which can be used to generate cumulative distribution function (CDFs) of future change. This provides a simplified way of incorporating climate change information into planning by making the process less computationally intensive and more accessible, yet still based on physical processes. That said, it is *extremely* important to match the nature of the management questions to be addressed with the temporal scale of the hydrologic sensitivities. For example, the ε and S we use here are average responses (e.g., they are descriptive of changes in mean streamflow) that do not capture extremes and therefore are not appropriate for management questions related to extremes. This new approach is intended to help understand the range and central tendencies of annual-average landscape-level streamflow responses to long-term annual and seasonal changes in P and T (30-year averages), providing a sense of what expected changes might be prior to conducting more detailed end-to-end simulations.

3.2. Site description

The Colorado River basin (Fig. 3.2) has been, and will continue to be, an area of great interest with respect to projected climate change (Barnett and Pierce 2008; WWA 2008; Brekke et al. 2009). The Colorado River and its tributaries are the primary water supply for much of the Southwest and provide an important source of electricity to the region through operation of numerous hydropower facilities (Fulp 2005). The water resources of the basin are distributed according to water allocations set by the Colorado River Compact of 1922. In retrospect, the allocations were based on a relatively wet period, before much was understood about the Basin's inter-decadal variability, the result of which is that the basin's water resources are overallocated according to the best current estimates of the river's average flows (Woodhouse et al. 2006). Aggregate storage capacity of the Colorado River's reservoirs is large (about four times the river's annual naturalized flow; in contrast, the Columbia River's reservoirs have a capacity of only about one-third of the mean annual flow). The reservoir system does, therefore, allow for carry over from wet to dry years, although multi-year sustained

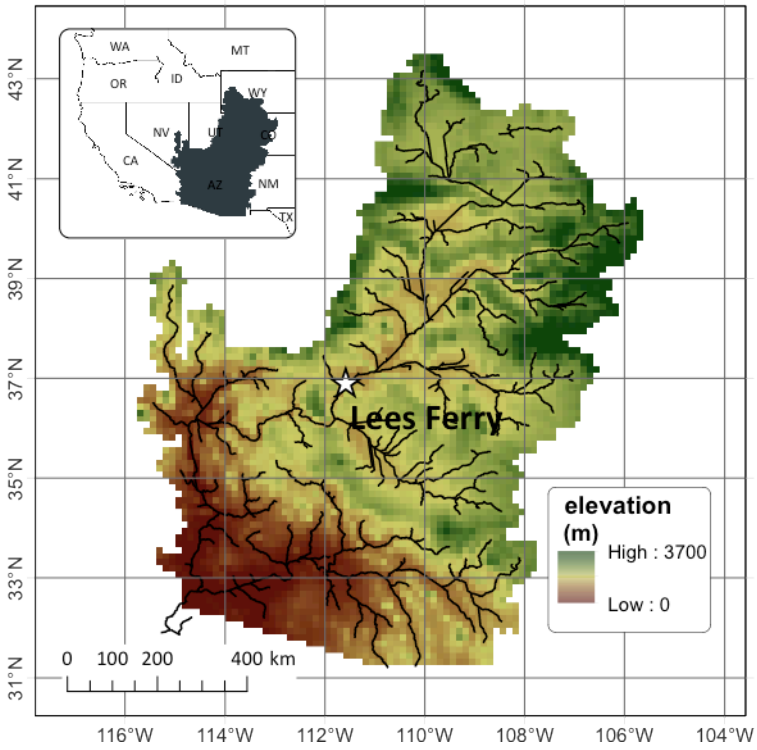

FIG 3.2 Colorado River basin showing elevation for the 1/8° resolution of the hydrology model. The resolution of the GCM output is approximately 2° resolution, which is indicated by the larger grid overlay.

dry periods are nonetheless problematic. Because of the large storage capacity of the reservoir system, climate change implications on management are typically focused on annual (as contrasted with seasonal) responses, and the sensitivity-base approach we describe here is well suited to this characteristic of the basin.

As a result of drought and the resultant low reservoir levels in the 2000s, the Colorado River has been the focus of many studies that have attempted to estimate future streamflows (Vano et al. 2013). The modeling framework we describe here builds on this previous work, including studies by Christensen and Lettenmaier (2007), USBR (2011), and Vano et al. (2012). In particular, the USBR study reflects the interest of the Basin's water managers in understanding the nature of future streamflows. As such, the Basin provides an opportunity to evaluate the sensitivity approach's usefulness, and we use the USBR (end-to-end) results to test our method. We primarily focus on and show results for Lees Ferry, the major control point for water allocation purposes (and which defines the Upper and Lower basins; Fig. 3.2), but our method can also be applied to other locations within the basin.

3.3. Methods

We explore how concepts of precipitation elasticity (ε) and temperature sensitivity (S) can be used to represent the land-surface response to precipitation (P) and temperature (T) change, and how these concepts can then be used to provide first-order estimates of future hydrological changes from GCM output. These sensitivity values serve two important purposes. First, they promote more synthesized understanding of what drives hydrological responses across a landscape (e.g., T, P, vegetation, soil) independent of any

future scenario (see Vano et al. 2012). Second, they create a tool, equivalent to a nomogram, that can be used to bound future runoff change across the Colorado River basin. We demonstrate the latter here.

Values of ε (Eq. 3.1) are a measure of how an incremental (e.g., percentage) change in precipitation (ΔP) results in a percentage change in streamflow (Q). Similarly, values of S (Eq. 3.2) are a measure of how an incremental temperature increase (ΔT) results in a percentage change in Q.

$$\varepsilon = \frac{\frac{Q_{hist+\Delta P} - Q_{hist}}{Q_{hist}}}{\Delta P} \quad (3.1)$$

$$S = \frac{\frac{Q_{hist+\Delta T} - Q_{hist}}{Q_{hist}}}{\Delta T} \quad (3.2)$$

These sensitivities have been explored throughout the Colorado basin by Vano et al. (2012). The values calculated here vary slightly from the values reported there because we use a fixed (historical) reference here for different increments of change. This is roughly equivalent to integrating changes at various reference conditions. Our use here of changes relative to the historical reference streamflow is more amenable to projections of future streamflow and more similar to the full-simulation approach in how T and P changes are applied. We also calculated monthly S in which we incremented the temperature for each month (by 0.1°C).

To estimate streamflow sensitivities, we used the Variable Infiltration Capacity (VIC) macroscale hydrology model (Liang et al. 1994). VIC has been used extensively at regional and global scales in numerous studies, mostly in off-line simulations where

gridded surface P, T, wind speed, downward solar and longwave radiation, and vapor pressure (humidity) are prescribed (e.g., Nijssen et al. 2001; Elsner et al. 2010; and many others). In this study we used VIC, as applied by Christensen and Lettenmaier (2007) and USBR (2011), although this same approach can be used with other land surface models. We used the Maurer et al. (2002) historical gridded data set, as in Christensen and Lettenmaier (2007) and USBR (2011). We ran simulations from 1970-1999 using initialized conditions from Vano et al. (2012) and calculated hydrologic sensitivities for 1975-1999, although as tested in Vano et al. (2013) the period of analysis and dataset have little effect on the hydrologic sensitivity values. Sensitivity results are roughly equivalent if we use another historical dataset (e.g., Wood and Lettenmaier 2006) or another averaging period.

To estimate future streamflow changes with the sensitivity-based approach, we multiplied P and T changes from GCM output (Fig. 3.3) by their related hydrologic sensitivity measures (ε, S) to estimate the long-term average percent change in streamflow (dQ) at a specific location and time period. We first calculated dQ according to Eq. 3.3, where dP is the

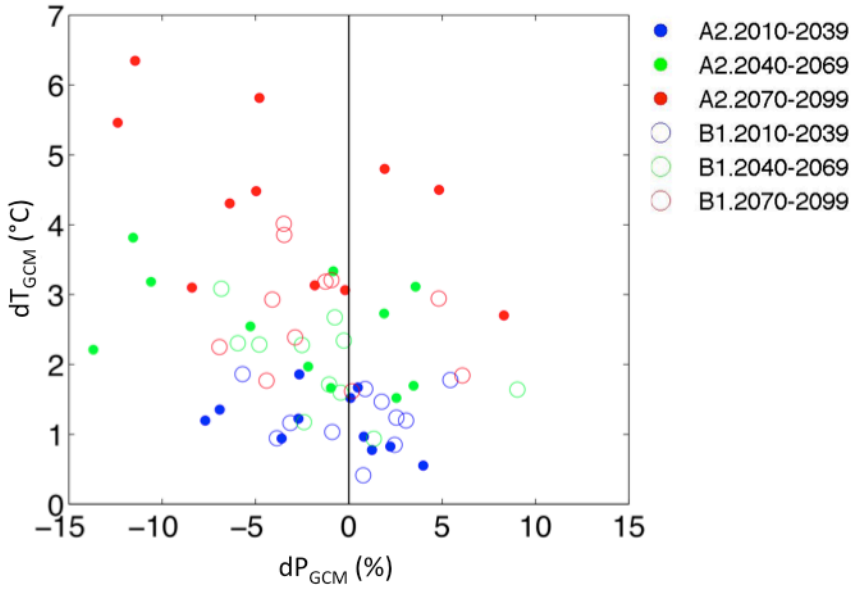

FIG 3.3 Temperature (dT) and Precipitation (dP) changes for GCMs used in Chistensen and Lettenmaier (2007)

long-term average *percent change* in P and dT is the *difference* in long-term average T between the future and historical GCM simulation. $d(P,T)_{int}$ is the interaction between P and T changes which was neglected, due to the additive nature of S and ε in the Colorado River basin reported by Vano et al. (2012).

$$dQ_{est} = dP_{GCM*}\,\varepsilon + dT_{GCM*}\,S + d(P,T)_{\text{int}} \qquad (3.3)$$

where:

$dP_{GCM} = (P_{GCMfut} - P_{GCMhis})/P_{GCMhis}$

$dT_{GCM} = T_{GCMfut} - T_{GCMhis}$

To improve the performance of the sensitivity-based approach, we made three adjustments (Eq. 3.4) which: (1) account for variations in annual ε and S values as a function of dP_{GCM} and dT_{GCM} respectively (Fig. 3.4), (2) account for seasonal T by applying monthly $dT_{GCM.mon}$ and monthly S_{mon} values (Fig. 3.5), and (3) adjust dP_{GCM} to coincide with the bias-corrected change applied in the bias-correction spatial disaggregation (BCSD) downscaling technique used in the full-simulation approach (Fig. 3.6). Section 3.4.1 provides more details on these three adjustments.

$$dQ_{adj\_est} = dP_{GCM_{adj}} * \varepsilon(dP) + \sum_{mon=1}^{12} (dT_{GCM,mon} * (\frac{S_{mon} * S(dT)}{\sum S_{mon}})) + d(P,T)_{\text{int}} \qquad (3.4)$$

Full-simulation approach streamflow changes (dQ_{sim} in Eq. 3.5) were calculated using routed, bias-corrected future streamflows from VIC model simulations (Q_{fut}) and historical naturalized streamflows from USBR (2012) (Q_{obs}).

$$dQ_{sim} = (Q_{fut} - Q_{obs}) / Q_{obs} \quad (3.5)$$

We first compared runoff changes from the sensitivity-based approach (Eq. 3.3) to the full-simulation approach (Eq. 3.5) using bias-corrected streamflow for two global emissions scenarios (A2, B1) of the 11 GCM simulations used by Christensen and Lettenmaier (2007). We calculated future streamflows for three future 30-year average time periods (2010-2039, 2040-2069, 2070-2099) relative to the 1970-1999 historical period. We used these values for comparisons to develop the adjusted estimation method (Eq. 3.4). 95% confidence intervals were estimated for the predicted values. We then used the full-simulation approach of the USBR (2011) to test the adjusted estimation method, using the same 30-year time periods. The USBR study produced 112 monthly (mean) streamflows for three emission scenarios (A2, A1B, B1) at Lees Ferry. These data were generated as part of the USBR Colorado River Basin Water Supply and Demand Study; see USBR (2011) and Harding et al. (2012) for details.

3.4. Results and Discussion

3.4.1. Development and testing of the sensitivity-based approach

Fig. 3.7a (at end of section) is our first estimate of projected runoff change (dQ_{est}, from Eq. 3.4), prior to adjustment. The calculation uses a single ε and S (ε=2.23, S=-6.47% per ºC, values generated from 1% dP and 0.01ºC dT differences applied to historical simulations respectively, see Fig. 3.4 and bold values in Table 3.1) value for Lees Ferry for 30-year annual average GCM estimates of P and T change (n=66, 2 emission scenarios by 3 time periods by 11 GCMs). Each value corresponds to a unique dQ_{sim} (Eq. 3.5) from bias-corrected flows taken from Christensen and Lettenmaier (2007). The proximity of responses to the 1:1 line reflects how well the methods compare for the 66 simulations. The linear relationship between dQ_{est} and dQ_{sim} has a R^2=0.58, which reflects considerable scatter, where dQ_{est} is biased towards overestimating dQ_{sim} (the y-intercept of the regression is -5.6%). An extreme example of this bias is GFDL's A2 scenario in 2070-2099, which simulates a decline in streamflow of -22% whereas the sensitivity-based approach estimates a -63% decline.

TABLE 3.1 Annual ε and S from VIC simulations for a range of dP and dT values

dP from Historical Simulation	Precipitation Elasticity (ε)
-30%	1.78
-20%	1.93
-10%	2.07
1%	**2.23**
10%	2.36
dT from Historical Simulation	**Temperature Sensitivity (S)**
0.01 °C	**-6.47%**
1 °C	-6.18%
3 °C	-5.54%
6 °C	-4.81%

**Bold values are used for single ε and S values prior to adjustments.*

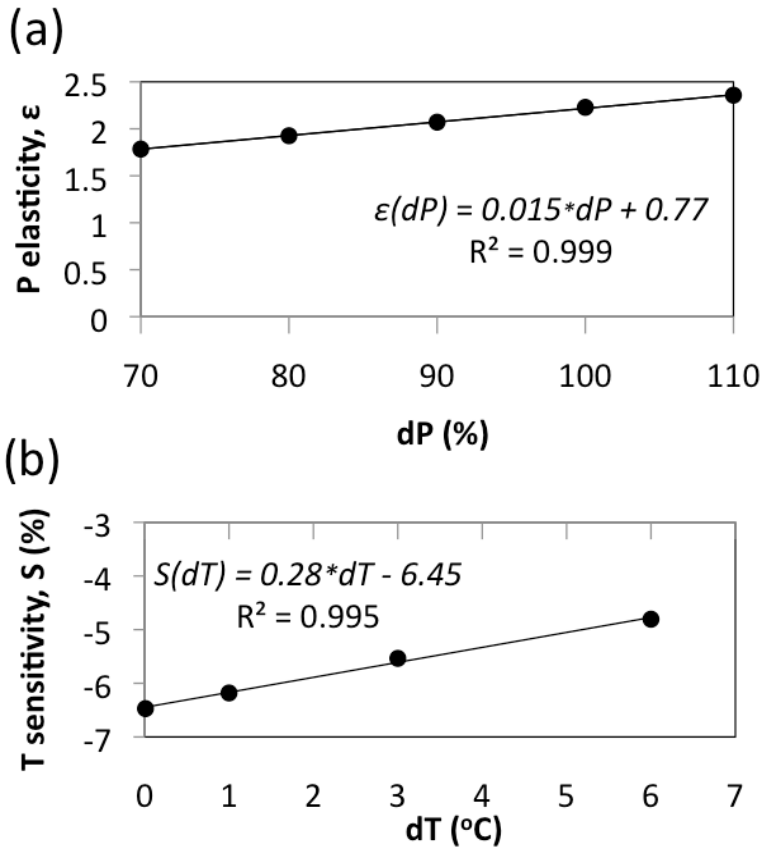

FIG 3.4 Variable long-term annual precipitation elasticities (ε) and temperature sensitivities (S) at Lees Ferry. (a) ε calculated using Eq. 3.1 as a function of changing precipitation at 70%, 80%, 90%, 101% and 110% of historical values. (b) S calculated using Eq. 3.2, using 0.1, 1.0, 3.0, and 6.0 °C increases. See Table 3.1 for actual values.

TABLE 3.2 Sensitivity-based adjustments

	slope	y-intercept	R^2
prior to adjustments	1.08	-5.60	0.58
only adjustment 1[a]	0.98	-4.41	0.63
only adjustment 2[b]	1.13	-5.51	0.61
only adjustment 3[c]	1.01	-3.04	0.60
adjustments 1 and 2	1.02	-4.35	0.66
adjustments 1 and 3	0.93	-1.66	0.63
adjustments 2 and 3	1.07	-2.94	0.65
all three adjustments	**0.98**	**-1.61**	**0.68**

[a]adjustment 1: *ε(dP) and S(dT)*

[b]adjustment 2: S_{mon}

[c]adjustment 3: dP_{GCMadj}

We made three adjustments (below) to the sensitivity-based approach to reduce bias and scatter; the influence of each independently and in combination is noted in Table 3.2.

Adjustment 1, ε(dP) and S(dT): As dP and dT change, their sensitivities also change (Fig. 3.4). Therefore, instead of a single value for ε and S, we varied the long-term annual changes according to dT_{GCM} and dP_{GCM} values based on two regression equations generated using hydrology model simulations at different perturbations (Fig. 3.4). These perturbations were selected to cover the range of climate change projections as shown in Fig. 3.2. At Lees Ferry, both ε(dP) and S(dT), when calculated using a fixed (historical) reference, result in values that can be approximated with a linear equation (Fig. 3.4). As mentioned in section 3.3, these values can also be calculated by integrating changes at various reference conditions (which captures the tangent of the change as reported in Vano et al. (2012)). However, for this application, we calculate ε and S as a function of dP and dT increments from the fixed historical values, similar to how changes are applied in the full-simulation approach (this captures the secant of the change, where changes can be taken directly from the figure without integrating).

Adjustment 2, S_{mon}: Simulation experiments by Das et al. (2011) found that annual streamflow responses at Lees Ferry differ according to seasonal warming patterns, where greater decreases in annual streamflow occur for warming in the warm season, as opposed to warming in the cool season. To capture this in our sensitivity-based approach, we apply temperature changes on a seasonal basis according to the values in Fig. 3.5, which were determined through 12 model simulations where we perturbed a

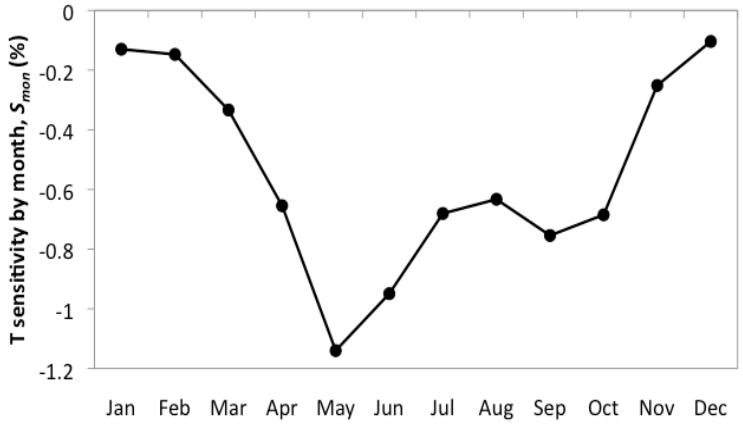

FIG 3.5 Sensitivities of annual streamflow at Lees Ferry to warming increases (% change in annual streamflow per °C of warming) in each month. For example, a 1°C temperature increase in January results in a -0.14% decrease in annual flow.

single month's temperature by 0.1ºC in each simulation and calculated how warming in that month affects annual sensitivity values. These values when added together equal -6.46%, which is very close to -6.47%, the sensitivity for annual T changes of our unadjusted estimate. We weight these values according to the long-term annual S(dT) value as described in the preceding paragraph. Seasonal sensitivities range from -0.10% in December to -1.14% in May, with warm season (April-September) sensitivities about three times higher than cool season (October-March) (Fig. 3.5). With this adjustment, GCMs that have more warming in the summer than the winter will have greater streamflow changes.

Adjustment 3, dP_{GCM}*:* The BCSD statistical downscaling approach adjusts precipitation according to the probability distribution of historical observations (e.g., the Maurer et al (2002) gridded dataset), this adjustment, in essence, projects the percentage change between GCM future and GCM historical precipitation values of each month onto historical observations. We performed a simplified adjustment that mimics this bias-correction step through a simple rescaling. Instead of using the direct percent difference

from long-term annual future and historical GCM precipitation as our dP_{GCM} values (as in the unadjusted estimate), we calculated monthly percent differences of GCM precipitation and apply those (percent) differences to the historical observed dataset to calculate a new estimate for future precipitation. Then, these two values (the historical observations and the new estimate for future precipitation) were used to calculate dP_{GCM_adj}, which was then multiplied by precipitation elasticity as in Eq. 3.4. In most cases, this adjustment had little effect on the dP values. In the 66 adjustments performed, 51 made dP more positive, although most dP values (73%) changed by less than 2%. There were, however, a few cases where the changes were substantial. These occurred mostly when the GCM precipitation did not capture the observed seasonality. For example, in GFDL a2 maximum precipitation occurs in the springtime and not in the fall

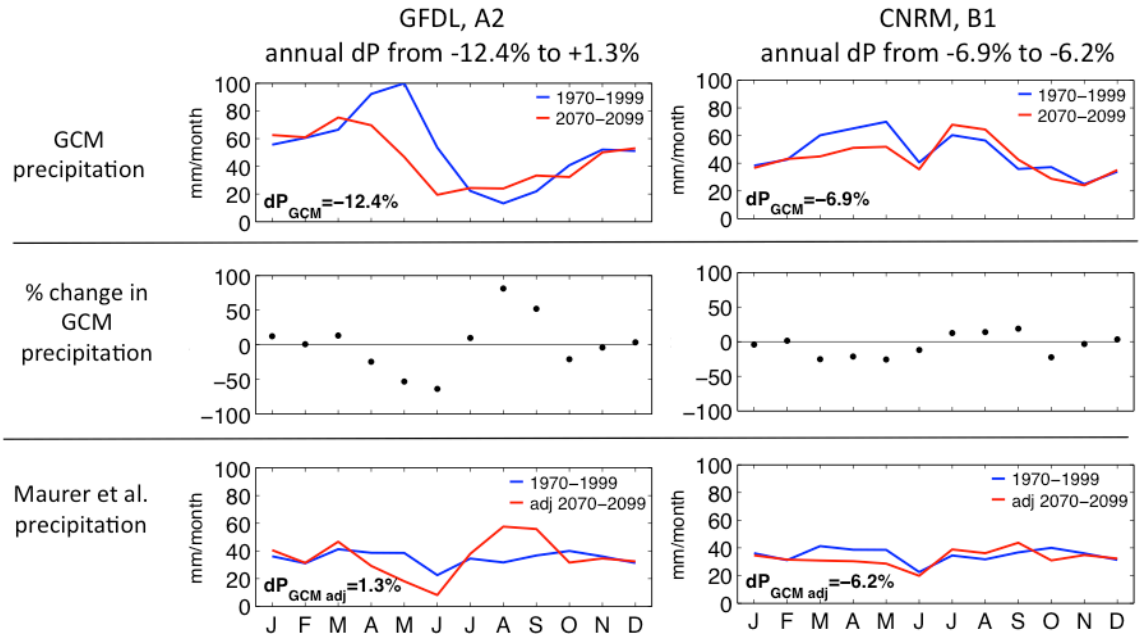

FIG 3.6 Two examples of adjustment 3 ($dP_{GCM\ adj}$). Prior to adjustment (top panels) annual dP_{GCM} is calculated directly from raw GCM output. The adjustment calculates the % change in monthly GCM precipitation (middle panel) and applies this to the historical precipitation dataset (blue line lower panel, from Maurer et al. (2002) over the Colorado River basin), resulting in adjusted monthly values of future precipitation. From this, the annual $dP_{GCM\ adj}$ (inset values in the lower panels) is calculated. This adjustment has a large effect on GFDL a2, but little effect on CRNM b1, which relates to how well each GCM captures observed precipitation seasonality.

(Fig. 3.6, left panels), therefore a relatively small increase in average fall precipitation in 2070-2099 translates to a much larger increase in precipitation when the percent difference is applied to the observed precipitation, changing dP from -12.4% to -1.4%. In contrast, CRNM b1 precipitation has a seasonal cycle that is more similar to the climatology, and therefore the percent differences applied to historical observations does not change dP by much (-6.9% to -6.2%) (Fig. 3.6, right panels). If the BCSD bias correction is not desired, this adjustment should not be applied.

When all three adjustments were applied, the ability to reproduce the end-to-end results increased considerably (Fig. 3.7b). The R^2 in the linear relationship between $dQ_{est,adj}$ and dQ_{sim} improved from 0.58 to 0.68, and, there was considerable improvement in the dQ_{est} bias towards underestimation of dQ_{sim} (y intercept of the regression is -1.61% vs. -5.60%). Also, the slope of the relationship was closer to one (see Table 3.1 for comparisons of each adjustment). The GFDL's A2 scenario in 2070-2099 (highlighted in Fig. 3.6, left panels) is an example of how an individual estimate can improve, from an unadjusted estimate of -63% to an adjusted estimate of -27%, which is considerably closer to the -22% projected using the full-simulation method. The 95% confidence intervals for predicted values are within +14% and -17% of those from the full-simulation method.

We also evaluated the sensitivity-based approach using full-simulation results from USBR (2011), for which a total of 112 simulations from 3 emission scenarios were available, totaling 336 comparisons (36 A2, 39 A1B, and 37 B1 GCMs by 3 time periods each) (Fig. 3.7c). These values, which also incorporate the three adjustments discussed above, also have a negative bias (y-intercept of the regression is -2.69%) and a slope of

1.01. The 95% confidence intervals for predicted values are similar to those from the example with the Christensen and Lettenmaier (2007) full-simulation results; our estimated values were within +15% and -21% of the USBR (2012) full-simulation values.

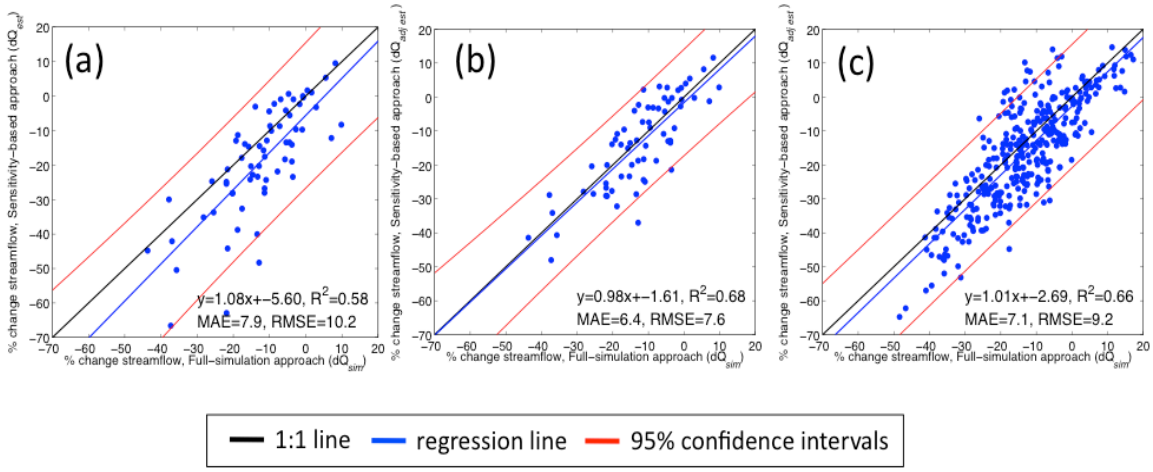

FIG 3.7 Comparisons between the full-simulation and sensitivity-based approaches. (a) using full-simulation results from Christensen and Lettenmaier (2007) and a single value for ε and S for the sensitivity-based approach (Eq. 3.3), (b) using Christensen and Lettenmaier (2007) and the adjusted sensitivity-based approach (Eq. 3.4), (c) using USBR (2011) full-simulation results and the adjusted sensitivity-based approach (Eq. 3.4).

3.4.2. Assessing risk with the sensitivity-based approach

The main interest of future streamflow projections by water managers is to assess risks associated with climate change. To test whether the sensitivity-based results provide similar ensemble distributions to full-simulation results, we compared the cumulative distribution functions (CDFs) of streamflows generated using both approaches. In the development of the sensitivity-based approach (section 3.4.1), we combined time periods and scenarios; this is appropriate for testing how temperature and precipitation change can be used to estimate streamflow change, where each 30-year segment can be treated independently. In practice, however, the particular emission scenario and (especially) the

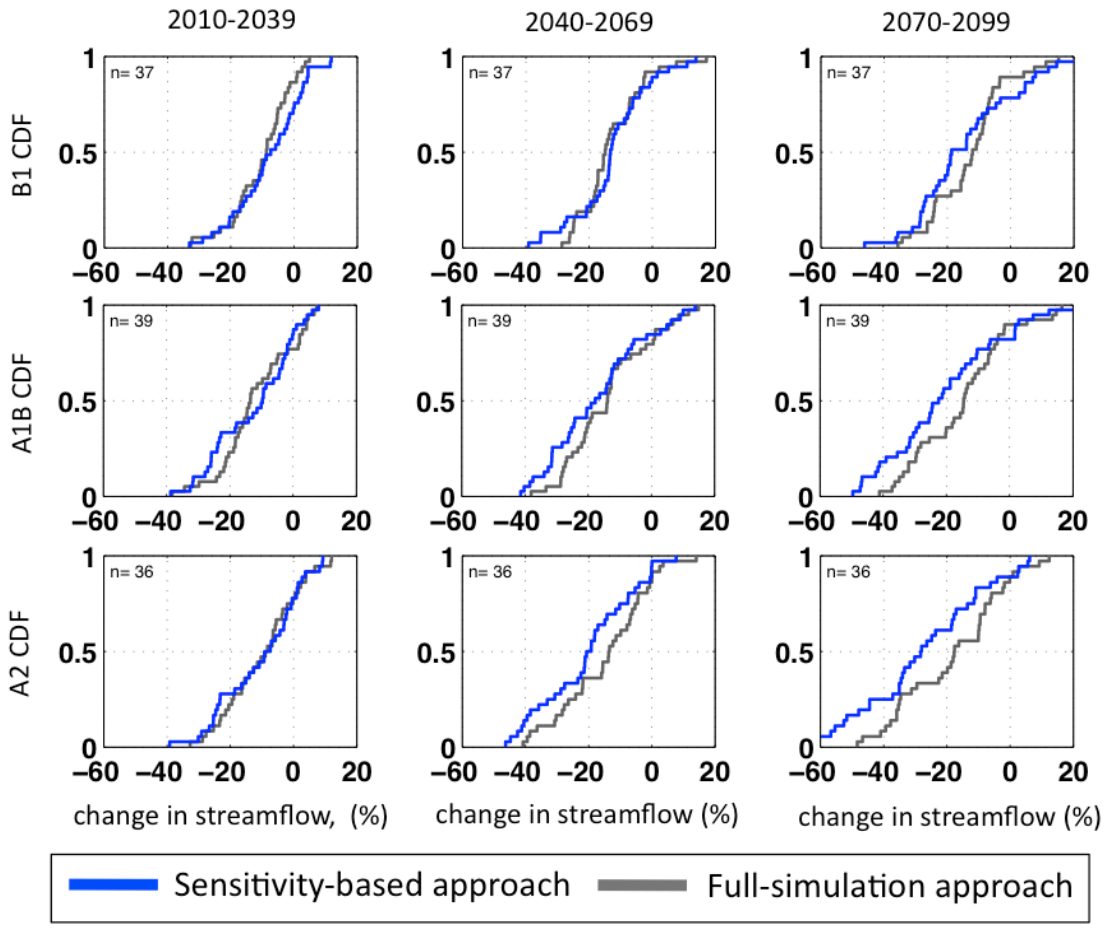

FIG 3.8 Cumulative distribution functions (CDFs) of 112 USBR simulations of streamflow change from sensitivity-based (dQ_{est_adj}) and full-simulation (dQ_{sim}) approaches by future time period and emission scenarios.

future time period are important considerations in planning – especially given that planning horizons typically are several decades (hence the difference between emissions scenarios is usually less than the differences among GCMs). Fig. 3.8 shows the CDFs for the two approaches using the USBR simulations (as in Fig. 3.7c) for three future time periods (columns) and three emission scenarios (rows). Differences between emissions scenarios become greater through time, becoming more pronounced in the mid 21st century (IPCC 2007); therefore in 2010-2039 emissions scenarios have no noticeable influence.

Across emission scenarios and future time periods, the ensemble range is captured well (Fig. 3.8). The magnitudes of changes are similar in earlier periods, however the ensembles that are further in the future and associated with more extreme emissions scenarios show more discrepancies between approaches. The reason for the discrepancies most likely is that at these more extreme values, linearization of the sensitivity-based approach breaks down and the sensitivity-based values, relative to the full-simulation, show greater streamflow declines in the Colorado River basin.

From a climate risk standpoint, the agreement or lack thereof among the cumulative distribution functions is more important than whether the inferred changes associated with any specific GCM agree. In general, the distributions are consistent, especially at modest change levels (first 30-year period in particular), although there is a bias in the sensitivity-based approach towards overestimating streamflow declines for periods farther in the future and/or for scenarios with large (in absolute value) temperature and precipitation changes (Fig. 3.8). The tendency of the sensitivity-based approach to estimate larger flow declines (vs. the full-simulation approach) may be specific to the Colorado River basin and further testing is needed to determine whether this same bias applies elsewhere, particularly in energy-limited regions.

3.4.3. Added value of the sensitivity-based approach

In addition to providing a "shortcut" method for estimating future flows, the sensitivity-based approach allows the influence of temperature and precipitation changes to be segregated, and in so doing encourages better understanding of the factors that will drive changes in the hydrologic system. For instance, maps of ε and S can be used as

evaluation tools. As an example, Fig. 3.9 shows the same results as in Fig 3.7c, where effects from precipitation change (dP_{GCM}) (Fig 3.9a) and temperature change (dT_{GCM}) (Fig 3.9b) are plotted independently. The plots show that both dP_{GCM} and dT_{GCM} are important factors that will affect future streamflow changes at Lees Ferry. On average, dP_{GCM} contributes more to the slope (0.74 of 1.01), while dT_{GCM} has a considerable effect on the total magnitude and some effect on slope (0.27).

The three adjustments outlined in section 3.4.1 highlight key elements that are important for prediction of the effects of climate change on streamflow: a) how streamflow responds to both temperature and precipitation changes at different reference conditions, b) the seasonal effects of temperature change, and c) how precipitation changes are downscaled. These elements suggest ways in which end-to-end prediction methods might be evaluated. For example, do LSMs used in climate change studies accurately capture streamflow responses to changes in precipitation and temperature (ε and S values), and do the values change appropriately as the climate becomes drier and

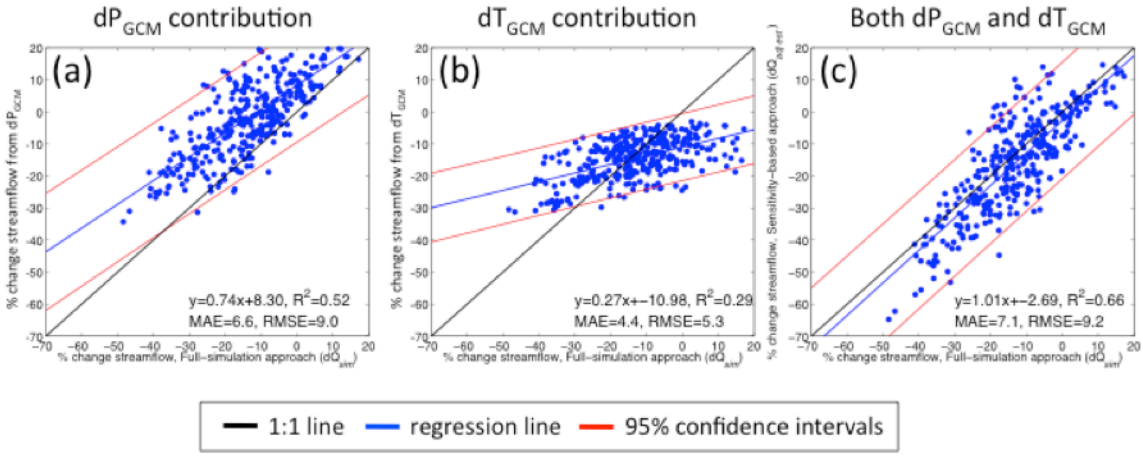

FIG 3.9 Sensitivity-based adjustments (y-axis) for dP_{GCM} (a) and dT_{GCM} (b) in isolation and for the combined adjustment of both dP_{GCM} and dT_{GCM} (c) plotted vs. the predicted changes in Colorado River discharge from the full-simulation approach (which includes both dP_{GCM} and dT_{GCM} changes; x-axis).

warmer? How should downscaling methods capture precipitation changes, especially when the GCM precipitation seasonality does not match that of the historical? For instance, the BCSD approach used in Christensen and Lettenmaier (2007) and USBR (2011) does not preserve the magnitudes of precipitation change as predicted by the GCM, but rather captures the change relative to historical precipitation in each season. This subtlety has little effect when future and historical simulations have similar seasonal cycles, but when future seasonality differs, it can affect the projected precipitation magnitudes.

Values of ε and S can also be useful tools in evaluating model performance. As demonstrated in Vano et al. (2012), these measures can be used to compare hydrologic model performance to other models and observations. Spatial ε and S maps can help to identify locations where there is more uncertainty as well as areas more sensitive to future change, and imply locations that might be targeted for *in situ* observations. While a body of research has evolved that estimates ε from observed streamflows (e.g., Schaake 1990; Dooge et al. 1992; Dooge et al. 1999; Sankarasubramanian et al. 2001; among others), methods for calculating S values from observations are less clear and arguably more challenging as they depends more on current conditions (which depend on prior weather conditions, e.g., snowpack). A better understanding of observed S would be valuable in model evaluation, as it is a common input variable to land surface hydrology models in climate studies. This ultimately requires a better understanding of evaporative demand, which is the key driver for which temperature is just an index (see Dooge et al. 1992; Dooge et al. 1999). Further research into how best to express these evaporative changes would be beneficial and could be done within this sensitivity framework.

3.5. Conclusions

We have described a sensitivity-based approach that generates estimates of annual average future streamflow change and the dominant causal factors, without detailed simulations. The method is especially appropriate for producing initial estimates of future streamflow to accompany alternative global model future projections of precipitation and temperature, the key drivers of land surface hydrology. Our work shows that:

• The sensitivity-based approach produces plausible estimates of future streamflow change, which are mostly within about ±15% of those estimated from a full-simulation approach. Performance of the sensitivity-based approach was improved by three adjustments: (1) accounting for varying precipitation elasticity (ε) and temperature sensitivity (S) as a function of precipitation and temperature change, (2) incorporating monthly variations in S, and (3) adjusting monthly precipitation change to be a percentage of historical P (instead of from raw GCM output), which is more consistent with downscaling methods of the full-simulation approach. In test applications to predict future mean annual flows at Lees Ferry, the sensitivity-based approach provides a conservative estimate; estimating larger streamflow declines (with an average bias of up to -3%).

• For purposes of assessing risk, the sensitivity-based approach produces viable initial estimates that can be used to bound future streamflow uncertainties for water

management purposes. The cumulative distribution functions of ensemble GCM scenarios match well for the relatively near future (first three decades of the next century), however values further into the future and for severe emissions scenarios mostly overestimate the magnitude of future streamflow changes (mostly reductions in the case of the Colorado River system).

• The sensitivity-based approach helps to focus attention on the causal factors driving future change, and their relative importance, as contrasted with the full-simulation approach which tends to lead to a focus on managing ever-larger quantities of model output. For example, the sensitivity-based approach facilitates evaluation of contributions from precipitation and temperature change separately.

The sensitivity-based approach should be appealing to water managers in that it is computationally efficient, and hence can be used to generate ensembles of hydrologic simulations, which can help in selecting a representative range of simulations for further analysis. For example, it can be easily applied to newly released climate scenarios (e.g., from the Coupled Model Intercomparison Project 5th Assessment), and help in providing context as to why results differ. In the comparisons we report here, we used the Variable Infiltration Capacity (VIC) hydrologic model, but these methods are applicable to any other hydrology/land surface models (LSMs), and can be used to better quantify uncertainty from hydrologic simulations of multiple LSMs.

The approach has limitations, and is best thought of as complimentary to other approaches. It is intended for evaluating long-term (e.g., 30-year) average annual

changes, and it does not provide information on daily values, extreme events, or land cover change. We have focused on annual responses, which are of greatest importance to management in the Colorado basin. For other systems, seasonal responses are critical, and understanding how to best capture these responses is currently being investigated.

Acknowledgements

The authors thank James Prairie (USBR) for his assistance in accessing USBR Colorado River Basin Water Supply and Demand Study data and Bart Nijssen (University of Washington) for his thoughtful feedback on the sensitivity-based approach development. Support for this work was provided by the Climate Impacts Research Consortium (CIRC) and the NOAA Regional Integrated Scientific Assessment (RISA) program.

References

Abatzoglou, J.T., and T.J. Brown, 2012: A comparison of statistical downscaling methods suited for wildfire applications. *Int. J. Climatol*., **32**: 772–780. doi: 10.1002/joc.2312.

Barnett, T., R. Malone, W. Pennell, D. Stammer, B. Semtner, and W. Washington, 2004: The effects of climate change on water resources in the West: Introduction and overview. *Climatic Change*, ***62***(1), 1-11.

Barnett, T. P., and D. W. Pierce, 2008: When will Lake Mead go dry?, Water Resour. Res., 44, W03201,doi:10.1029/2007WR006704.

Bates, B.C., Z.W. Kundzewicz, S. Wu and J.P. Palutikof, Eds., 2008: Climate Change and Water. Technical Paper of the Intergovernmental Panel on Climate Change, IPCC Secretariat, Geneva, 210 pp.

Brekke, L.D., J.E. Kiang, J.R. Olsen, R.S. Pulwart, D.A. Raff, D.P. Turnipseed, R.S.Webb, and K.D. White, 2009: Climate change and water resources management—A federal perspective: U.S. Geological Survey Circular 1331, 65 p. Available online at: http://pubs.usgs.gov/circ/1331.

Christensen, N.S., and D.P. Lettenmaier, 2007: A multimodel ensemble approach to assessment of climate change impacts on the hydrology and water resources of the Colorado River basin. *Hydrol. Earth Syst. Sci*., **3**, 1–44.

Das, T., D.W. Pierce, D.R. Cayan, J.A. Vano, and D.P. Lettenmaier, 2011: The Importance of warm season warming to western U.S. streamflow changes. *Geophysical Research Letters* **38**, L23403, doi:10.1029/2011GL049660.

Dooge, J. C. I., 1992: Sensitivity of runoff to climate change: A Hortonian approach.

Bull. Amer. Meteor. Soc., **73**, 2013–2024.

Dooge, J.C., M. Bruen, and B. Parmentier, 1999: A simple model for estimating the sensitivity of runoff to long-termchanges in precipitationwithout a change in vegetation. *Adv. Water Resour*.,**23**, 153–163, doi:10.1016/S0309-1708(99)00019-6.

Elsner, M.M., L. Cuo, N. Voisin, J.S. Deems, A.F. Hamlet, J.A. Vano, K.E.B. Mickelson, S.Y. Lee, and D.P. Lettenmaier, 2010: Implications of 21st century climate change for the hydrology of Washington State *Climatic Change* **102**, no. 1, 225-260.

Fulp, T., 2005: How low can it go. *Southwest Hydrology*, ***4***(2), 16-17.

Hamlet, A.F. 2010: Assessing water resources adaptive capacity to climate change impacts in the Pacific Northwest region of North America. *Hydrology and Earth System Sciences,* **7**(4): 4437-4471, doi:10.5194/hessd-7-4437-2010.

Harding, B. L., Wood, A. W., and J.R. Prairie, 2012: The implications of climate change scenario selection for future streamflow projection in the Upper Colorado River Basin, *Hydrol. Earth Syst. Sci. Discuss*., **9**, 847-894, doi:10.5194/hessd-9-847-2012.

Intergovernmental Panel on Climate Change (IPCC), 2007: Climate Change 2007: The Physical Science Basis. Contribution of Working Group I to the Fourth Assessment Report of the IPCC [Solomon, S., D. Qin, M. Manning, Z. Chen, M. Marquis, K.B. Averyt, M. Tignor and H.L. Miller (eds.)]. Cambridge University Press, Cambridge, United Kingdom and New York, NY, USA, 996 pp. Available online at *http://www.ipcc.ch/ipccreports/ar4-wg1.htm.*

Liang, X., D. P. Lettenmaier, E. F. Wood, and S. J. Burges, 1994: A simple hydrologically based model of land surface water and energy fluxes for General Circulation Models. J. Geophys. Res., 99, 14 415– 14 428.

Maurer, E. P., A. W. Wood, J. C. Adam, D. P. Lettenmaier, and B. Nijssen, 2002: A long-term hydrologically-based data set of land surface fluxes and states for the conterminous United States. *J. Clim.*, **15**, 3237–3251.

Nijssen, B., R. Schnur, and D. P. Lettenmaier, 2001: Global retrospective estimation of soil moisture using the Variable Infiltration Capacity land surface model, 1980–1993. J. Climate, **14**, 1790–1808.

Payne J.T., A.W. Wood, A.F. Hamlet, R.N. Palmer, and D.P. Lettenmaier, 2004: Mitigating the effects of climate change on the water resources of the Columbia River basin. *Clim Change* **62**:233–256.

Sankarasubramanian A., R.M. Vogel, and J.F. Limbrunner, 2001: Climate elasticity of streamflow in the United States, *Water Resour. Res*., **37**, 1771-1781.

Schaake, J. C., 1990: From climate to flow. Climate Change and U.S. Water Resources, P. E. Waggoner, Ed., John Wiley, 177–206.

USBR (United States Bureau of Reclamation), 2011: Colorado River Basin Water Supply and Demand Study, Interim Report No. 1. U.S. Department of the Interior, Boulder City, Nevada. http://www.usbr.gov/lc/region/programs/crbstudy.html, accessed October 18, 2011.

USBR (United States Bureau of Reclamation), cited 2012: CURRENT natural flow data 1906-2008, last updated January 16, 2011. [Available online at http://www.usbr.gov/lc/region/g4000/NaturalFlow/current.html.]

Vano, JA, T Das, and DP Lettenmaier, 2012: Hydrologic sensitivities of Colorado River runoff to changes in precipitation and temperature, *J. of Hydrometeorology*, **13**, 932-949, doi:10.1175/JHM-D-11-069.1.

Vano, J.A., B. Udall, D.R. Cayan, J.T. Overpeck, L.D. Brekke, T. Das, H.C. Hartmann, H.G. Hidalgo, M. Hoerling, G.J. McCabe, K. Morino, R.S. Webb, K. Werner, and D.P. Lettenmaier. 2013: Understanding Uncertainties in Future Colorado River Streamflow, *Bull. Amer. Meteor. Soc*., (in review).

Western Water Assessment (WWA), Colorado Climate Change: A Synthesis to Support Water Resource Management and Adaptation. Oct 2008 (available online at: http://cwcb.state.co.us/public-information/publications/Documents/ReportsStudies/ClimateChangeReportFull.pdf).

Wood A.W., L.R. Leung, V. Sridhar, and D.P. Lettenmaier, 2004: Hydrologic implications ofdynamical and statistical approaches to downscaling climate model outputs, *Climatic Change*, **62** (1-3): 189-216.

Wood, A.W., and D.P. Lettenmaier, 2006: A test bed for new seasonal hydrologic forecasting approaches in the western United States. *Bull. Amer. Meteor. Soc*., **87**, 1699–1712.

Woodhouse, C.A., S.T. Gray and D.M. Meko, 2006: Updated Streamflow Reconstructions for the Upper Colorado River Basin. *Water Resources Research*, **42**, W05415, doi:10.1029/2005WR004455.

IV. Mapping the diversity of seasonal hydrologic responses to climate change in the Pacific Northwest

This chapter will be submitted to the *Water Resources Research*: Vano, J.A. and D.P. Lettenmaier, 2013: Mapping the diversity of seasonal hydrologic responses to climate change in the Pacific Northwest, *Water Resources Research*

Abstract

Increased temperatures and precipitation change will lead to fundamental changes in the seasonal distribution of streamflow with serious implications for water resources management, especially in the western United States. Basin-specific implications of these changes are, however, complicated by the wide range of projections of future temperature and precipitation from global climate models, the spatial resolution of which is coarse from a hydrologic perspective, and therefore do not easily translate to local water management applications. To better understand local impacts of regional climate, we conducted experiments to determine basin-scale hydrologic sensitivities (to imposed annual and seasonal temperature and precipitation change) of seasonal and annual streamflow. We used the Variable Infiltration Capacity (VIC) land-surface hydrologic model applied at 1/16° latitude and longitude spatial resolution over the Pacific Northwest, a scale sufficient to support analyses at the hydrologic unit code eight (HUC-8) basin level. These experiments distinguish the spatial character of the sensitivity of future water supply to changing temperature and precipitation by identifying the seasons

and locations where climate change will have the biggest impact on streamflow. We also develop a methodology that uses these hydrologic sensitivities as basin-specific transfer functions to estimate future changes in long-term mean seasonal hydrographs. These can provide viable first-order estimates of the likely range of streamflow changes in seasonality from global climate models without performing detailed model simulations for each climate scenario.

4.1. Introduction

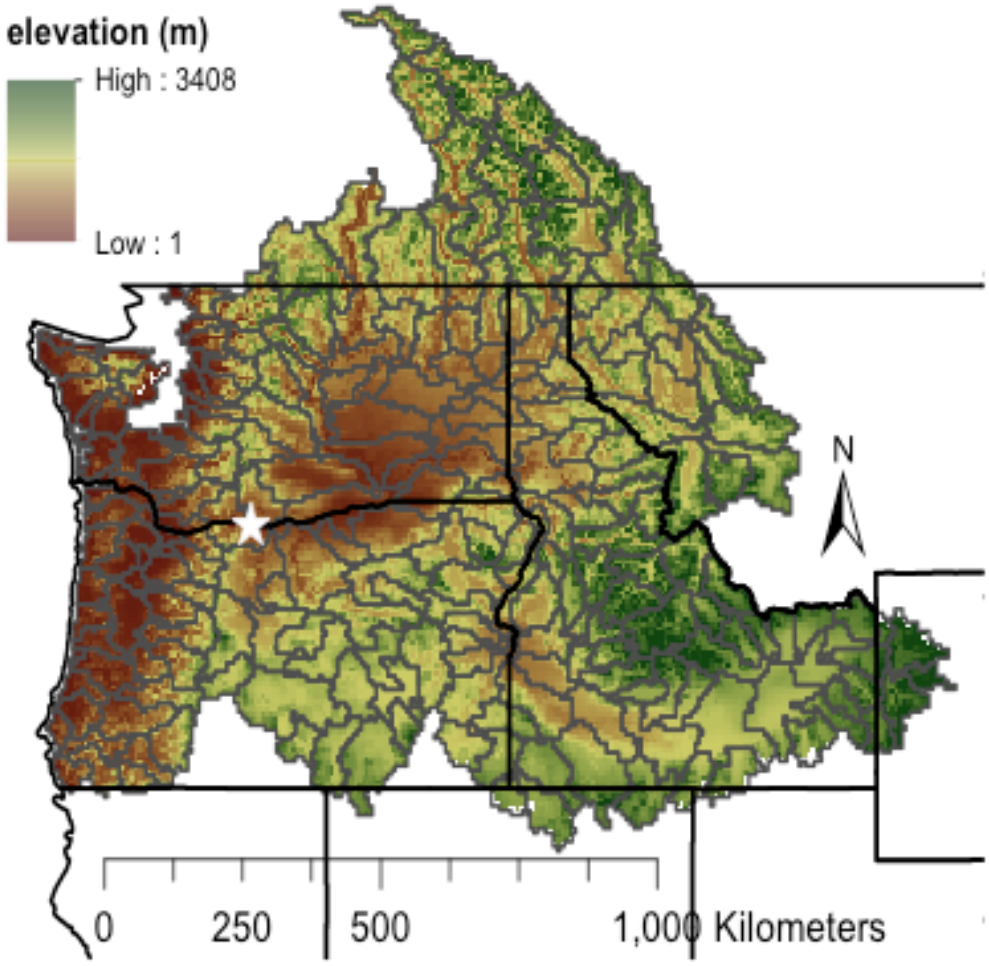

FIG 4.1 Pacific Northwest region including the Columbia River basin and coastal drainages, elevation shown at the 1/16° resolution. The Dalles, a major control point on the Columbia River, is indicated with a white star.

Healthy ecosystems and human communities in the Pacific Northwest (PNW), which we define as the Columbia River basin and its coastal drainages (Fig. 4.1), have a highly varying seasonal supply of water, with most precipitation occurring in the fall and winter, and water demands greatest in the summer. The region's snowpack serves as a natural reservoir that slowly releases water throughout the dry season providing sustained streamflow critical for agriculture, instream flows, and municipal and industrial use. Manmade reservoirs also serve this purpose, but can hold only ~30% of annual streamflow, and also depend on snowpack for in-season resupply.

There has been much interest in understanding climate impacts on streamflow in the PNW (Hamlet and Lettenmaier 1999; Payne et al. 2004; Lee et al. 2009; Elsner et al. 2010; and others). These interests stem from the region's vast hydropower resources (Lee et al. 2009), dangers of flooding (Payne et al. 2004), endangered species issues related to anadromous fish (Mantua et al. 2010), agricultural prosperity (Vano et al. 2010b), and the need to manage reservoir systems to balance these needs (Hamlet 2011). Past studies have used output from Global Climate Models (GCMs) which typically have spatial resolution order 200 km, and have difficulty simulating effects at the scale at which water is managed (arguably order ~10 km, as the GCM resolution does not capture fine-scale topographic barriers, e.g., the Cascade Mountain range) that control local climate. To overcome this, downscaling techniques, which also account for the bias inherent in GCM simulations, have been developed that apply coarse-scale (GCM) temperature (T) and precipitation (P) changes to local P and T observation-based datasets (Wood et al. 2004; Hamlet et al. 2010b). Via a two-step process that first downscales GCM output to the local scale, then uses the downscaled GCM output as input to a basin-

scale hydrologic model, information on global change can be translated into local streamflow projections that can be used to evaluate future changes to a river basin's hydrology (e.g. Hamlet and Lettenmaier, 1999; Payne et al., 2004; Hayhoe et al, 2007; Elsner et al. 2010; Vano et al. 2010a; 2010b; among many others).

While this approach provides important information about the possible direction of future hydrologic change, these studies are resource intense and results are highly dependent on which GCMs provide the basis for the regional downscaling (and what hydrologic models are used). In addition, it is difficult to know whether differences among results can be attributed to temperature (T) or precipitation (P) change and to distinguish the season in which these changes have the largest impact on hydrology. This complicates identification of regions that are more or less sensitive to future change and our overall understanding of the future hydrologic states (Vano and Lettenmaier 2013).

Elsner et al. (2010) divided the watersheds of the PNW into three categories: rain dominated, transitional, and snow dominated, based on the ratio of peak snow water equivalent (SWE) to October-March P. This classification has been useful to water managers in the region and has also been used in other reports and publications since (e.g., Tohver and Hamlet 2010; Hamlet 2011). We build on this approach to further identify drivers of hydrologic change. However, instead of using a hydrologic simulation approach that relies on downscaled GCM output and the use of a hydrologic model, we base our analysis on hydrologic sensitivities to temperature (T) and precipitation (P) changes. This is similar in concept to the approach used by Vano and Lettenmaier (2013) in the Colorado River basin. However, rather than evaluating sensitivities of annual runoff to annual P and T changes (arguably appropriate in the Colorado River basin

where water management is based on reservoirs with aggregate storage several times annual runoff), we utilize here an approach that assesses seasonal changes in runoff as affected by seasonal changes in P and T for watersheds much smaller than the entire region (Columbia River basin). This approach is more appropriate to water management in the Columbia River basin, which has aggregate storage much smaller than annual aggregate runoff, and reservoir storage more distributed among multiple facilities than in the Colorado basin.

This study also builds on the work of Das et al. (2011) who evaluated warm vs. cool season responses to temperature change in four major Western U.S. river basins – the Colorado, Sacramento (North Sierra), San Joaquin (South Sierra), and Columbia – using the Variable Infiltration capacity (VIC) model applied at 1/8° spatial resolution. Das et al. (2011) found that in these western U.S. river basins, three of the four are more sensitive to warming in the summer than in the winter, including the Columbia (at the Dalles, OR – essentially including all tributaries except those that head west of the Cascade Mountains, see Fig. 4.1). Das et al. (2011) did not, however, evaluate changes in seasonality of runoff, rather focusing on the sensitivity of annual runoff changes to summer and winter warming. A focus on the seasonal distribution of runoff is particularly valuable in the PNW, however, because despite abundant annual precipitation, reservoirs are relatively small and most runoff occurs in winter while water demands peak in summer. Hence, modest changes in the seasonal distribution of runoff taken together with relatively small reservoir volumes, can substantially affect reservoir system performance. We base our analysis therefore on sub-basins that can be

represented at the 1/16° spatial resolution (typically having drainage areas of 10^2 to 10^3 or so km^2) and monthly temporal resolution.

Our work is intended to provide a context for better understanding local-scale hydrologic change across the PNW by applying hydrologic sensitivity concepts to map spatial variations in precipitation elasticity (ε) and temperature sensitivities (S) across the entire region (section 4.4.1). We categorize hydrologic sensitivities at the Hydrologic Unit Code (HUC) 8-digit unit scale (section 4.4.2), and evaluate monthly response to seasonal changes in P and T (section 4.4.3). Finally, we evaluate the applicability of our monthly sensitivity construct to estimate future runoff changes (section 4.4.4) and provide examples for several tributaries (order $10^4 – 10^5$ km^2), specifically the Willamette River at Portland (WILPO), Yakima River near Parker (YAPAR), Columbia River at Keenleyside Dam (ARROW), the Snake River at Ice Harbor Dam (ICEHA), and the Columbia River at the Dalles (DALLE), although the method can be applied to any watershed.

Throughout our comparisons, we consider the nature of hydrologic sensitivities with an emphasis on two key features: (1) linearity, the extent to which a small change (e.g., 0.1 ºC), which provides a reasonable approximation of the tangent of the change, is similar per ºC to a larger change (e.g., 3 ºC) which captures the secant; larger divergence of these values indicates hydrologic sensitivity functions with greater nonlinearities, and (2) superposition, the extent to which hydrologic sensitivities identified through independent simulations can be added together to equal the same value as changes applied within the same simulation.

4.2. Site description

The Pacific Northwest (PNW) (Fig. 4.1) is defined to include the Columbia River basin and its adjacent coastal drainages. It is a diverse hydroclimatic region with varied vegetation, soil, and topography (sea level to 3400 m). Although hydrologic observations are somewhat sparse in the headwaters region, in general climatic and streamflow data are sufficient to evaluate model predictions across most of the hydroclimatic conditions experienced in the region (Elsner and Hamlet 2010).

Management of the region's water resources occurs at multiple levels including local municipalities, county, state, federal, and even international government agencies, making spatial information that spans political boundaries particularly valuable. For example, the river's headwaters are in Canada, and the Canadian portion (15% of the basin's drainage area) accounts for over 1/3 of the river's flow on average (USACE and BPA 2012). Furthermore, the basin's two largest reservoirs are in Canada. Joint management of the system for flood control and hydropower is controlled by the Columbia River Treaty of 1964, which currently is undergoing review with potential for renegotiations after 2024. As this paper is being written, the 2014/2024 Columbia River Treaty Review process is underway with discussion of how the system should be operated in the future (USACE and BPA 2012). Among the concerns is how and where runoff patterns might change in the future in response to a warming climate.

4.3. Methods

4.3.1. Models and forcing dataset

We performed a set of control experiments using the Variable Infiltration Capacity (VIC) macro-scale land-surface hydrology model (Liang et al. 1994) implemented as in Nijssen et al. (1997). We use version 4.0.7 of the model calibrated as in Hamlet et al. (2010), which has generally improved performance relative to earlier implementations (e.g. Hamlet and Lettenmaier 1999; Payne et al. 2004; Elsner et al. 2010) and higher spatial resolution (1/16° vs. 1/8°). The increased spatial resolution improves the ability of the model to represent topographic effects and resolve smaller watersheds, and hence to provide information that is relevant to local water management concerns (Elsner and Hamlet 2010).

We force the VIC model using the same 1/16° latitude and longitude historical driving dataset developed in previous efforts (Elsner et al. 2010; Hamlet et al. 2010). This data set contains daily values of precipitation, maximum and minimum air temperature, and wind speed; which are used in a preprocessing step within VIC that uses MTCLIM algorithms (Thornton and Running 1999) to calculate other forcing variables such as long and short wave radiation and relative humidity (see Bohn et al. (2013) for details). We perform simulations for the period 1915-2006, and calculate sensitivities over the period 1975-2006. Our choice of a relatively recent three decade period reflects a desire to a baseline period that is consistent with recent climate, however past work has shown that hydrologic model sensitivities do not change much when calculated over different time periods (Vano et al. 2013).

4.3.2. Hydrologic sensitivities

We estimated hydrologic sensitivities defined as in Vano et al. (2012), specifically precipitation elasticity (ε), the (percent) change in streamflow per (percent) change in precipitation (P), and temperature sensitivity (S), the percent change in streamflow per degree increase in temperature (T). We calculated ε and S using control experiments where a baseline simulation is compared with a simulation where either T or P is perturbed. We used the VIC model, although other hydrologic and land-surface models could also be used. For the computation of both ε and S, changes were applied: year-round (every day of the year), in the warm (every day in April-September) season, in the cool (every day in October-March) season, and in four three-month increments (JFM, AMJ, JAS, OND) depending on the particular analysis. All results were averaged over the reference 32-year time period. We implemented the change in using 1% P increases and 3 ºC and 0.1 ºC T increases. The 3 ºC increases provide results directly comparable with Das et al. (2011) whereas the 0.1 ºC increases, as applied in Vano et al. (2012) and Vano and Lettenmaier (2013), are more appropriate for constructing future seasonal streamflow estimations as discussed below.

We develop two watershed classifications to more clearly show differences in S values across the region. The first identifies changes in annual responses (total magnitudes) from warming applied in different seasons; we defined three categories, (1) locations were annual S is more negative when warming is applied in the cool season (October-March) vs. applied only in the warm season (April-September), (2) locations were the opposite is true, annual S is more negative when warming is applied in the warm

season than when it is applied in the cool season, and (3) locations were warming applied in the cool season results in positive annual S values, which is a special case of the 2nd category. The second classification defines the differences in seasonal responses to warming applied in the cool season. This identifies locations more sensitive to shifts in seasonality, where values were determined by subtracting the warm season S response from the cool season S response for simulations of warming applied in the cool season (i.e., the difference between the "warm seas" and "cold seas" bars in figure 3 of Das et al. 2011). Categories are six gradations of 10% per ºC increments of total difference between seasons.

4.3.3. Estimating future streamflow with seasonal-sensitivities

We use seasonal ε and S values to construct future hydrographs. Seasonal ε and S are generated by applying 0.1 ºC and 1% P increases in OND, JFM, AMJ, and JAS (eight total VIC simulations) and calculating the percent change from the historical simulation in each month from each of these perturbations. We then apply GCM changes of regional-averaged T and P outputs, averaged for the same four 3-month increments for the historical (1970-1999) and future periods (e.g., 2030-2059) to calculate dT (as a degree of increase) and dP (as a percent) change. These future differences (four dT and four dP values) are then applied to the seasonal ε and S values to create future hydrographs; our seasonal focus requires applying seasonal changes and their interactions. We do this by applying each of the four 3-month period sensitivities separately (in sequence), i.e., we calculate OND changes and subtract them from the historical values, then calculate JAS changes from the OND-revised values and subtract,

and so on. This captures the nature of seasonal changes for each GCM and translates these changes into monthly land-surface responses. Further details of this are in section 4.4.4.

We compare these future hydrographs with flows from Hamlet et al. (2010) generated with the full simulation approach for five management-relevant tributaries of the Columbia (WILPO, YAPAR, ARROW, ICEHA, and DALLE). Specifically, we used Hamlet et al. (2010) streamflow values that were generated using the hybrid-delta method to downscale temperature and precipitation output for ten GCMs to drive the VIC model, after which streamflow was routed and bias corrected (for all locations except WILPO, where bias corrected flows were not available), see Hamlet et al. (2010) and http://warm.atmos.washington.edu/2860/products/sites for details.

4.3.4. Spatial extents

We examined the spatial character of hydrologic sensitivities at three spatial scales: (1) grid-level (1/16°, or approximately 30 km^2 area); over the PNW domain there are 24,108 1/16° grid cells, (2) U.S. Geological Survey 8-digit Hydrologic Unit Code scale, or cataloging unit and similar sub-basin level (GeoBase's National Hydro Network Work Unit) in Canada. Within the PNW there are 226 such watershed units, with an average drainage area of 3000 km^2 (range 200 km^2 to 11,600 km^2). Herein we refer to these as watersheds. For these watersheds, we aggregated the runoff from all 1/16° grid cells that are at least 50% within the watershed boundary, and (3) the five major sub-basins of the Columbia noted in section 4.1.

4.4. Results and Discussion

4.4.1. Spatial variations in hydrological responses

4.4.1.1. Precipitation elasticities (ε)

Annual responses to warm and cool season wetting: To determine basin-wide sensitivities and the extent to which warm and cool season changes contribute to these sensitivities, we applied a 1% P increase year-round (Fig. 4.2, left column, top panel), in the warm season (middle panel), and in the cool season (bottom panel). As an example, an ε of 3 implies that a 3% increase in P would result in a 9% increase in runoff. For these 6-month changes, superposition holds; the lower two panels, which reflect the contribution of each season to annual sensitivities, sum to the top panel to within ±0.15 for all grid cells (i.e., to a first approximation, seasonal elasticities are additive). Seasonally applied precipitation changes reflect the time of year when precipitation is greatest. In other words, year-round ε is primarily determined by cool season changes (on average, more than 70% of the annual ε can be attributed to cool season changes), when the majority of precipitation occurs.

4.4.1.2. Temperature sensitivities (S)

Annual responses to warm and cool season warming: Fig. 4.2, right column shows annual responses plotted spatially, where the top panel is for warming applied throughout the year, the middle panel is for warming applied only in the warm season, and lower panel is for warming applied only in the cool season. Superposition applies in most grid

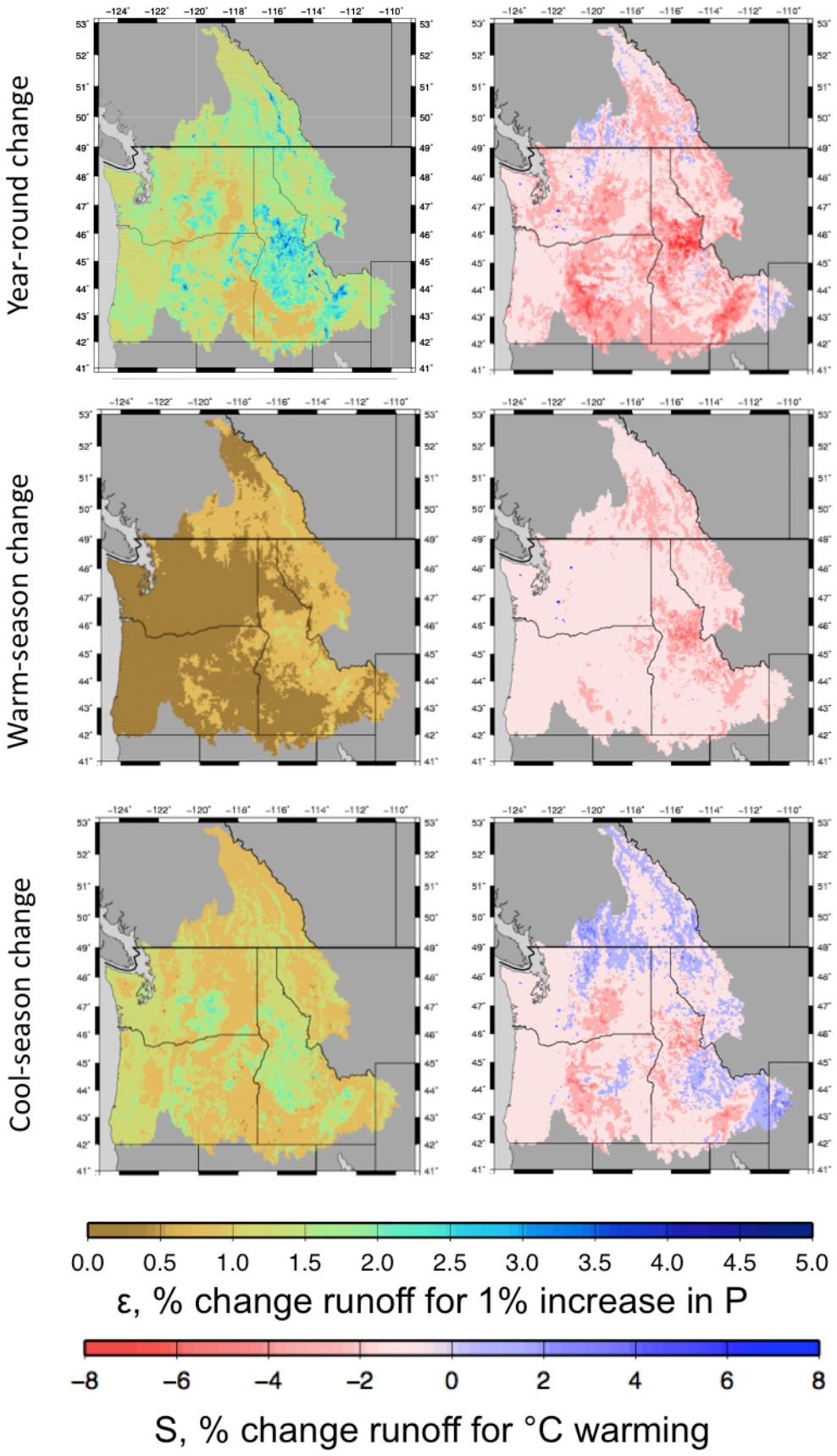

FIG 4.2 Annual responses to P (left panels) and T (right panels) change.

cells; warm and cool season responses are close to additive (e.g., the contribution of each season to annual sensitivities sum (to within ±0.5% for 80% of grid cells). Spatially, there is a range of responses including both areas of increases (blue) and decreases (red). If warming only occurs in the cool season, 80% of grid cells show decreases in annual runoff, whereas if warming occurs throughout the year 97% of grid cells show decreases in annual runoff (where the larger portion of grids having decreases is the result of declines from warm season warming being greater than increases from cool season warming). Note that these decreases were also the case for all four large river basins examined by Das et al. (2011), however they did not report the spatial distribution of these changes. The reason for flow increases (20% and 3%) is often referred to as the Dettinger hypothesis, details described in Jeton et al. (1996), where due to warming, water leaves the system earlier and is not available for evapotranspiration later in the year – hence it is possible for runoff to be higher in a warmer climate, even with precipitation unchanged.

In this analysis, we calculated S values using a perturbation of daily T of 3°C (Fig. 4.2, right column), a T increment that is directly comparable to values of Das et al. (2011) where variations in annual responses to warming applied annually, in the warm, and in the cool season where shown in bar graphs (see black bars on their figure 3) for four major western river basins. Specifically, they found that for the Columbia basin at The Dalles, the annual response was greater from warming applied in the warm season than warming applied in the cool season. The patterns of annual responses across the PNW with a 3°C T increment were similar to changes using a 0.1°C increment used to calculate sensitivities in Vano et al. (2012) (Fig. 4.3).

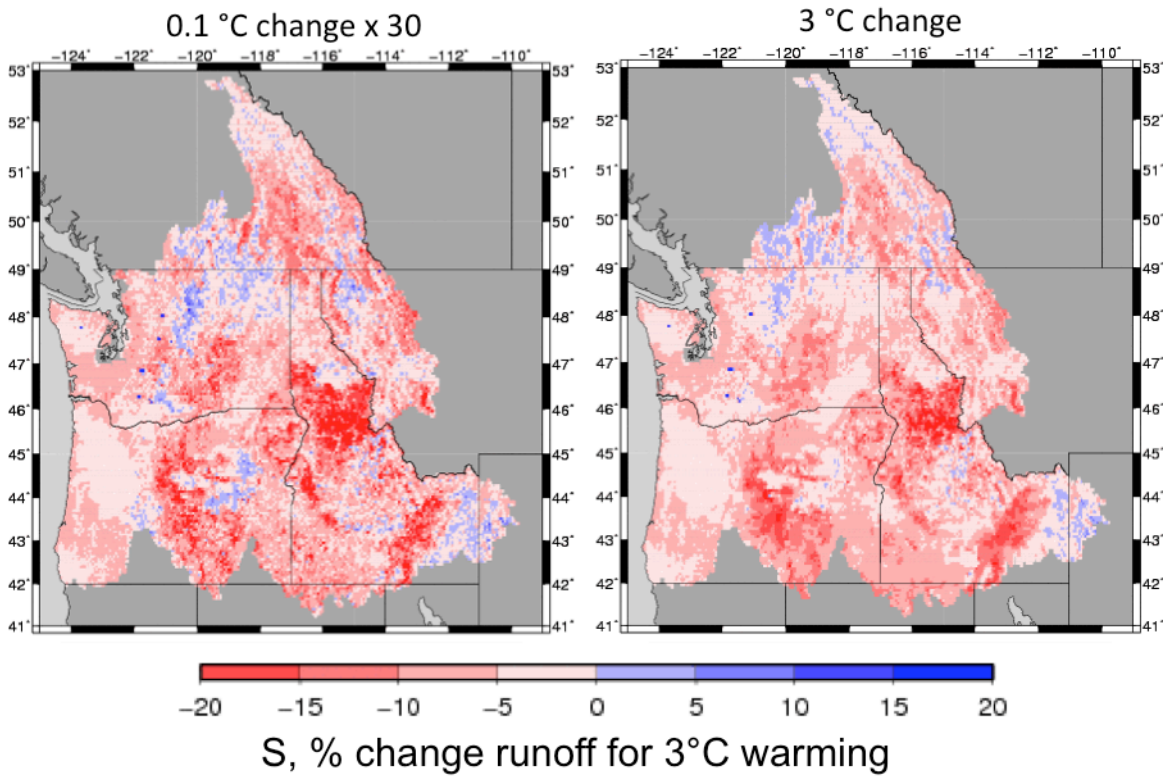

FIG 4.3 Effects of temperature increment on annual temperature sensitivities (S). S values from simulations using a 0.1 °C temperature increase (left panel) and a 3 °C temperature increase (right panel). Panels are on the same scale, i.e., the 0.1 °C change is multiplied by 30.

Seasonal response to warming: Fig. 4.4 shows the response of streamflow annually and in each season. By definition, the warm and cool season responses add to equal the annual response exactly. Fig. 4.4 contains the same three panels as in Fig. 4.2 on the left, in addition to the responses in each season (these values coincide to a spatial representation of the blue and orange bars in Das et al.'s (2011) figure 3). Note, however, that to capture the values of seasonal responses, the scale of Fig. 4.4 differs by a factor of 2.5 from Fig. 4.2. Warm season warming reduces streamflow throughout the year, whereas cool season warming increases streamflow in the cool season but reduces streamflow in the warm season. Therefore although the net streamflow change is less for cool season than warm season warming, the change in seasonality is much greater. The

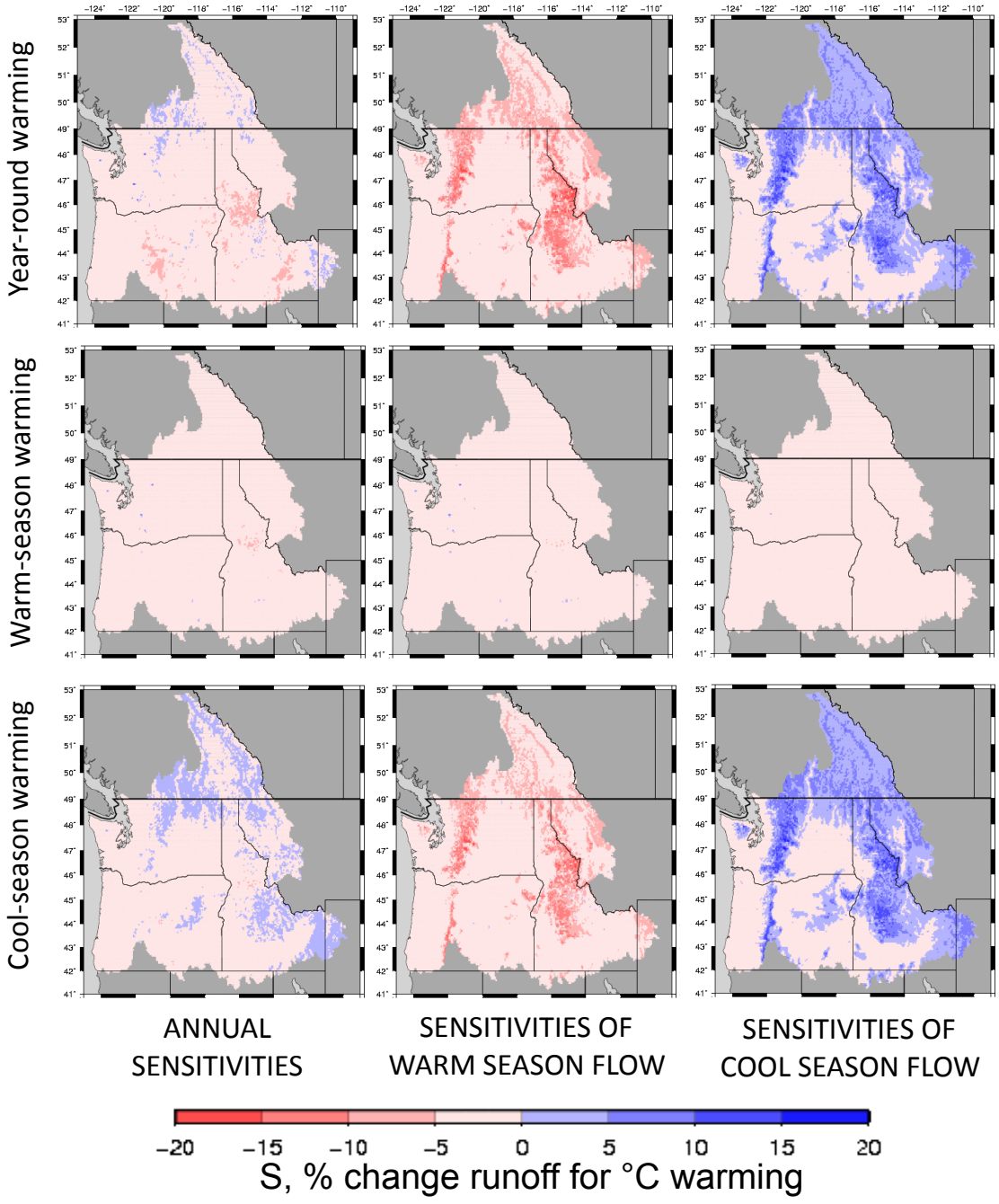

FIG 4.4 Seasonal responses to warming. Annual S responses (left panels, % change in annual runoff per °C warming), warm season S responses (center panels, % change in warm season flow per °C warming) and cool season S (right panels, % change in cool season flow per °C warming) for warming applied throughout the year (top), only in the warm season (middle) and only in the cool season (bottom). The annual S responses (left panels) contain the same information as annual S values in Fig. 4.2, but the scale has been increased by a factor of 2.5 to account for greater changes in seasonality.

differences in hydrologic responses in warm and cool seasons are controlled in substantial part by the relatively high elevation regions as shown in Fig. 4.1.

Precipitation elasticities (ε) also have seasonal responses that vary by location due to temperature (i.e., snow processes). These seasonal responses are straightforward (and therefore not shown): when the change is applied in the warm season, all change occurs in the warm season, whereas when change is applied in the cool season, change occurs in the cool season at low elevations and in the warm season at high elevations.

4.4.2. Categorizing hydrologic changes at the watershed scale

We complement the fine-scale spatial information in Figs. 4.2 and 4.4 with watershed-based categorizations. The categories facilitate the interpretation of spatial results by synthesizing responses in terms of both changes in total magnitude (annual response) and shifts in seasonality.

4.4.2.1. Annual watershed-level precipitation elasticities (ε) and temperature sensitivities (S)

Fig. 4.5 shows the watershed-scale response to annual P and T changes. This information is similar to the top panels in Fig. 4.2, but averaged for each of the 226 watershed units where S values are per °C and ranges of ε and S changes are smaller as they are watershed averages. Watershed averages accentuate watersheds that are more (or less) sensitive to future changes. Watershed ε values range from 0.9 to 2.5, with five watersheds having an ε of less than one. These annual values can be compared with results of Sankarasubramanian et al. (2001) who evaluated precipitation elasticities

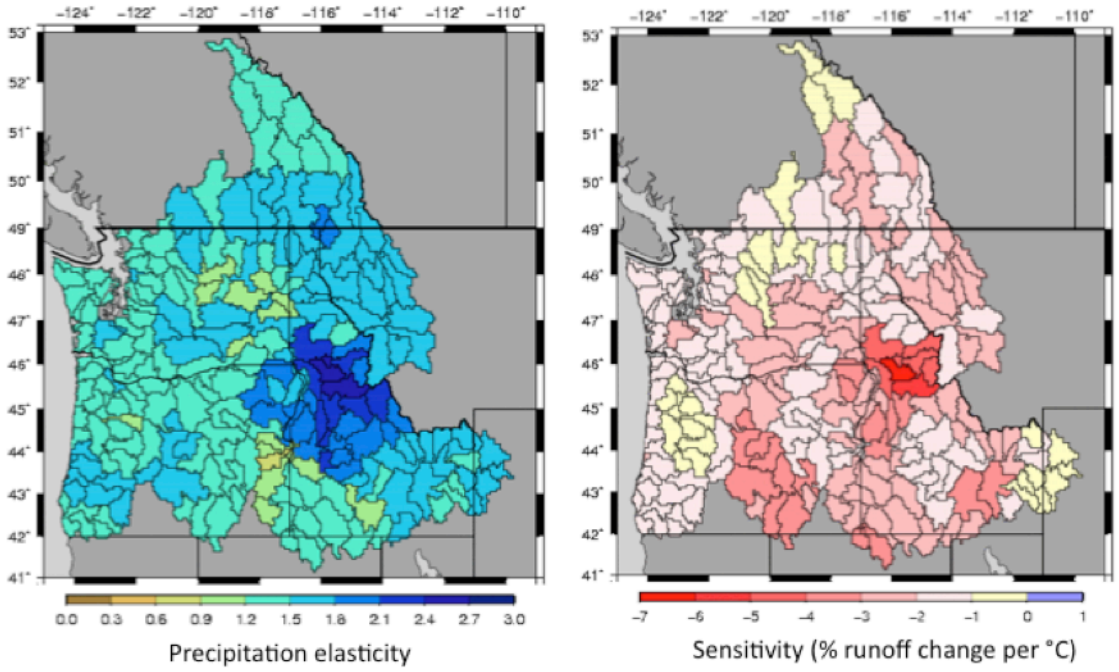

FIG 4.5 Watershed scale annual precipitation elasticities (ε) and temperature sensitivities (S). Annual responses (percent) to annually applied change (percent precipitation change or °C warming)

throughout the conterminous United States using a non-parametric measure. Within the PNW, the map provide in Sankarasubramanian et al. (2001) has contours with magnitudes ranging from 1.0 to 2.0, with a similar increase in elasticities from west to east, although Sankarasubramanian et al. (2001) report higher values in eastern Oregon, instead of west-central Idaho.

Regions with the greatest S values in annual response to annually applied temperature changes are also clustered in Idaho, in the upper Salmon River basin, while areas that are least sensitive to temperature change are at both extremes of the elevation spectrum -- low lying coastal areas and headwaters in Canada and Wyoming (both rain- and snow-dominated watersheds). When averaged across watersheds, all locations show decreases in discharge with increasing temperature (S values ranging from -0.2% to -8% per º C), i.e. blue grids in Fig. 4.4 top right, which are increases in discharge, when

averaged with the other grids in the watershed, are outweighed by decreases. These *annual responses* to *annually applied changes* capture one aspect of temperature sensitivities, in the next section we present characterizations that address seasonality as well.

4.4.2.2. Annual responses to warm and cool season warming (total magnitude)

Fig. 4.6a classifies the 226 watersheds into one of three categories with similar sensitivities according to how warming applied in warm and cool seasons affects annual streamflow magnitudes:

(1) *More sensitive to cool season warming* - Locations where annual streamflow magnitudes decline more with cool season warming than with warm season warming. 83

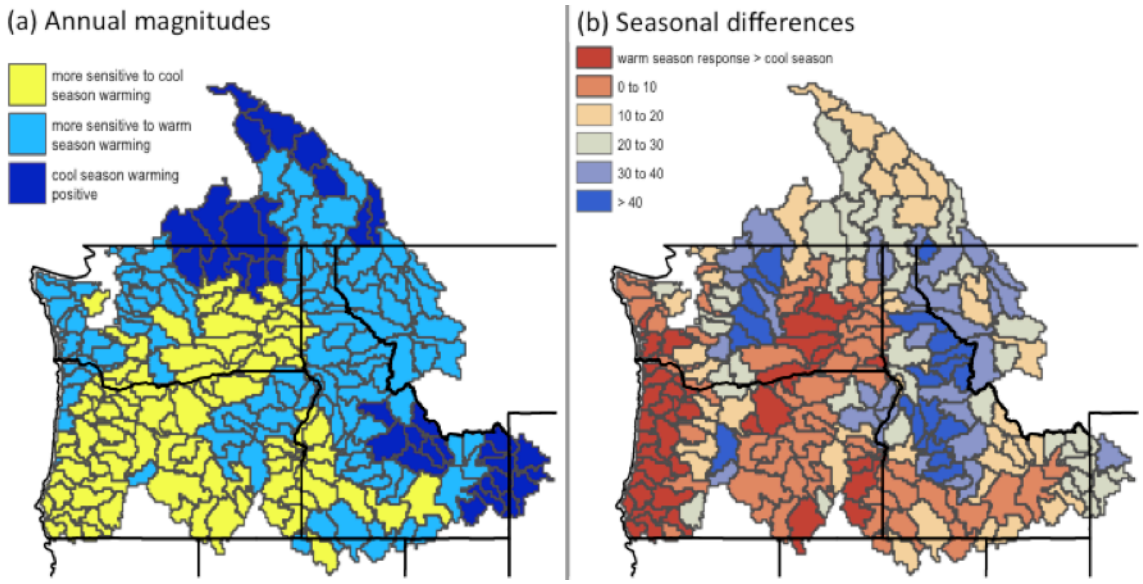

FIG 4.6 PNW watershed classifications. Watershed-level comparisons of how sensitivities responded to warm and cool season warming that reflect the time of year that has the greatest impact on annual flow magnitudes (a) and the difference between warm and cool season sensitivities when warming is applied in the cool season, reflecting locations (in blue) most likely to experience seasonal differences in their hydrograph with increased temperatures (b).

of the 226 sub-basins (36%), mostly low elevation watersheds, have this characteristic, which is similar to temperature effects in the South Sierra as shown in Das et al. (2011).

(2) *More sensitive to warm season warming* - Annual streamflow magnitudes decline more with warm season warming than with cool season warming. This characteristic is seen in basin-wide responses in the Colorado, Columbia, and North Sierra (Das et al. 2011). This response is most common (in 64% of all watersheds, including the special case below).

(3) *Cool season warming positive* – In this special case, increases in cool season flows are greater than decreases in warm season flow resulting in net increases in flows if warming occurs only in the cool season (i.e., warmer winter temperatures lead to increased annual flows). This occurs in 14% of watersheds in the PNW (Fig. 4.6a), and generally at high elevations (see Fig 4.1 for elevations).

In general, even though the Columbia River basin as a whole has substantially greater sensitivity in annual magnitude to warm as contrasted with cool season warming, 27% of the 151 watersheds upstream of The Dalles show the reverse behavior (dominant sensitivity to cool season warming). This pattern pertains to many of the coastal drainages downstream of The Dalles as well, especially in Oregon (Fig. 4.6a, yellow watersheds).

4.4.2.3. Seasonal responses to warming (shifts in seasonality)

To quantify the sensitivity of watersheds to shifts in seasonality, we define six categories that are gradations of the differences in seasonal sensitivities between warm season and cool season flows for all PNW watersheds (Fig. 4.6b). Watersheds that have the largest

difference in S values in their warm and cool season responses (darker blue) are for watersheds that are most sensitive to warming – essentially mixed snow/rain systems (or transition basins as defined by Elsner et al. (2010)). The highest elevations that are snow-dominated (with hydrographs that peak in the spring) and the lowest elevations that are rain-dominated (with hydrographs that peak in the fall-winter) do not undergo large changes in S when temperatures increase either because they are already rain-dominated or because temperatures are cold enough that a small amount of warming does not affect high-elevation snowmelt enough to shift it to another season. The darker blue basins coincide with the basins that are most vulnerable to change categories from snow to transition basins in future climate simulations as shown in Tohver and Hamlet (2010).

4.4.3. Monthly responses to seasonal precipitation and temperature changes

To quantify monthly responses, we evaluated streamflow sensitivities at more discrete time intervals. Instead of the six-month warm and cool season evaluation above, we applied changes in three-month increments (OND, JFM, AMJ, and JAS) and calculated monthly responses (Fig. 4.7, Table 4.1a,b). These "bubble" diagrams are similar in concept to those in Nijssen et al. (2001). We perform this evaluation for five major sub-basins that are important for management within the Columbia River basin, and that capture a diversity of responses and highlight both the influence of the time of year when changes are applied (y-axis) and the time of year of the streamflow response

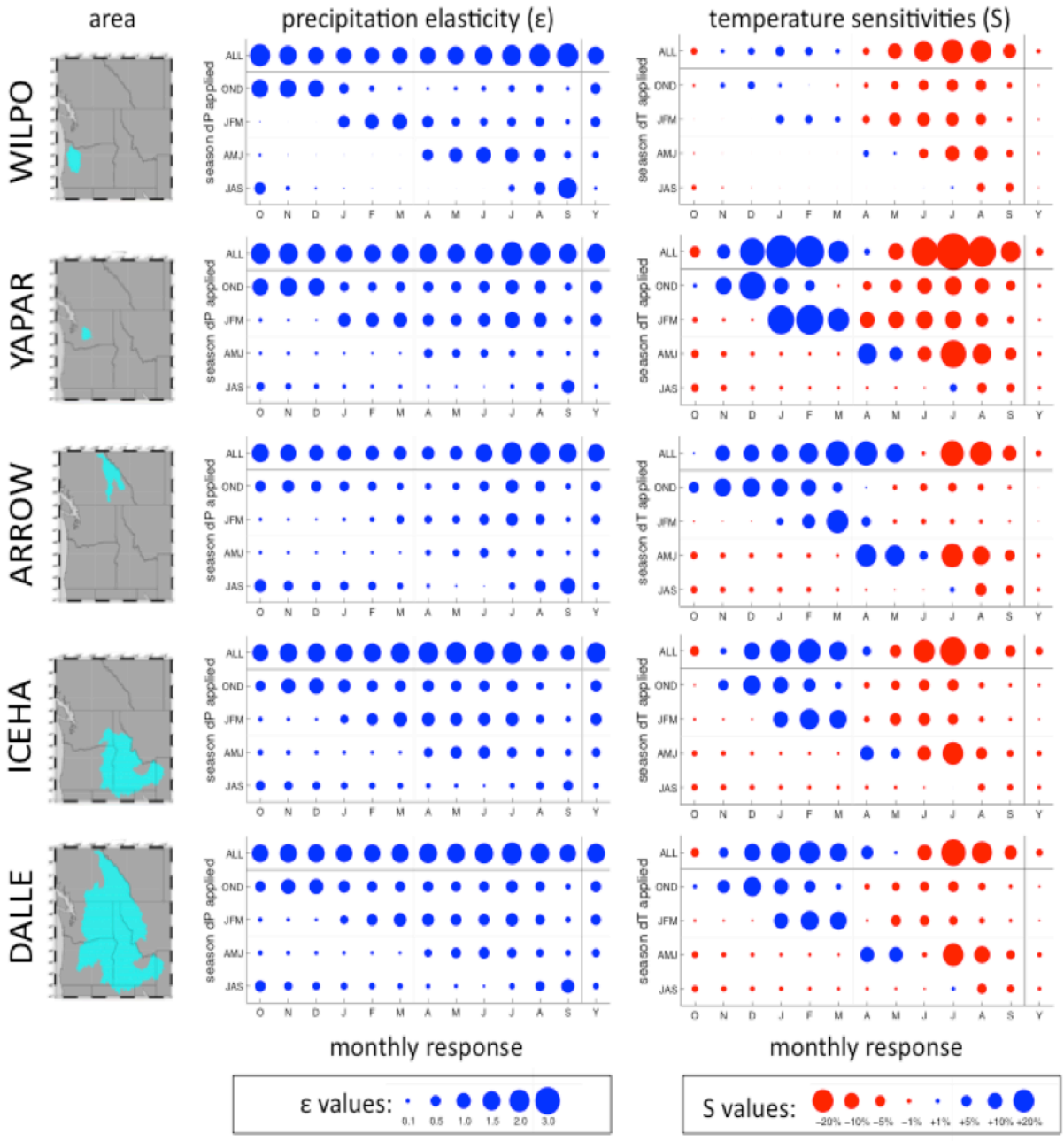

FIG 4.7 Monthly responses to seasonal precipitation (ε, % change streamflow per % change precipitation) and temperature changes (S, % change streamflow per °C). Warming is applied in 3-month increments (OND, JFM, AMJ, JAS) and throughout the year (ALL) and responses (ε or S) are shown for each individual month (O, N, D… S) and the annual response (Y). Maps on the left show the contributing area for each tributary.

TABLE 4.1a Seasonal precipitation elasticities (ε)

	period 1% P change applied	O	N	D	J	F	M	A	M	J	J	A	S
WILPO													
	ALL	2.0	1.5	1.2	1.1	1.1	1.1	1.2	1.3	1.5	1.7	2.0	2.2
	OND	1.3	1.4	1.2	0.5	0.2	0.1	0.1	0.1	0.1	0.2	0.3	0.1
	JFM	0.0	0.0	0.0	0.6	0.9	1.0	0.6	0.3	0.3	0.4	0.4	0.1
	AMJ	0.0	0.0	0.0	0.0	0.0	0.0	0.5	0.9	1.1	0.9	0.7	0.3
	JAS	0.6	0.1	0.0	0.0	0.0	0.0	0.0	0.0	0.0	0.2	0.6	1.7
	sum of 3-month	2.0	1.5	1.2	1.1	1.1	1.1	1.2	1.3	1.5	1.7	2.0	2.2
	% difference	-0.2%	0.0%	0.0%	0.0%	0.0%	0.0%	0.0%	0.0%	0.0%	-0.2%	0.3%	-0.1%
YAPAR													
	ALL	1.7	1.7	1.5	1.3	1.3	1.4	1.5	1.4	1.6	2.2	2.0	1.6
	OND	1.2	1.4	1.3	0.4	0.4	0.4	0.5	0.5	0.6	0.8	0.7	0.3
	JFM	0.1	0.0	0.0	0.8	0.8	0.9	0.6	0.6	0.7	1.1	0.8	0.3
	AMJ	0.1	0.1	0.1	0.0	0.0	0.0	0.4	0.3	0.3	0.2	0.2	0.1
	JAS	0.3	0.2	0.1	0.1	0.1	0.1	0.1	0.0	0.0	0.1	0.3	0.8
	sum of 3-month	1.7	1.7	1.5	1.3	1.3	1.4	1.5	1.4	1.6	2.2	2.0	1.5
	% difference	-0.5%	0.0%	0.1%	-0.3%	-0.1%	-0.1%	-0.2%	0.2%	-0.5%	-0.1%	-0.3%	-4.4%
ARROW													
	ALL	1.4	1.2	1.0	0.9	0.9	0.8	0.7	0.8	1.3	1.9	1.8	1.5
	OND	0.5	0.7	0.5	0.4	0.4	0.2	0.2	0.2	0.5	0.7	0.5	0.2
	JFM	0.1	0.0	0.0	0.1	0.1	0.3	0.3	0.3	0.5	0.7	0.4	0.1
	AMJ	0.1	0.1	0.0	0.1	0.1	0.0	0.2	0.2	0.4	0.3	0.2	0.1
	JAS	0.7	0.4	0.4	0.4	0.3	0.2	0.1	0.0	0.0	0.2	0.6	1.1
	sum of 3-month	1.4	1.2	1.0	0.9	0.9	0.8	0.7	0.8	1.3	1.9	1.8	1.5
	% difference	-0.3%	-0.1%	0.0%	0.0%	0.1%	0.0%	0.0%	0.1%	0.1%	-0.2%	0.0%	-0.3%
ICEHA													
	ALL	1.2	1.5	1.5	1.4	1.5	1.7	1.9	2.0	1.9	2.0	1.2	1.0
	OND	0.5	0.9	1.0	0.7	0.6	0.6	0.6	0.5	0.5	0.6	0.3	0.1
	JFM	0.1	0.1	0.1	0.3	0.6	0.9	0.8	0.7	0.7	0.8	0.3	0.2
	AMJ	0.2	0.1	0.1	0.1	0.1	0.1	0.4	0.6	0.7	0.5	0.3	0.2
	JAS	0.4	0.4	0.3	0.2	0.2	0.2	0.1	0.1	0.0	0.1	0.3	0.5
	sum of 3-month	1.2	1.5	1.5	1.4	1.5	1.7	1.9	2.0	1.9	1.9	1.2	1.0
	% difference	-0.2%	-0.2%	-0.2%	-0.2%	-0.3%	-0.4%	-0.2%	-0.2%	-0.1%	-0.1%	-0.6%	-0.1%
DALLE													
	ALL	1.3	1.4	1.4	1.3	1.3	1.4	1.6	1.6	1.7	2.0	1.6	1.3
	OND	0.5	0.9	1.0	0.6	0.5	0.5	0.5	0.5	0.5	0.7	0.5	0.2
	JFM	0.1	0.1	0.1	0.3	0.6	0.7	0.7	0.6	0.6	0.7	0.5	0.2
	AMJ	0.1	0.1	0.1	0.1	0.1	0.0	0.3	0.5	0.6	0.4	0.3	0.2
	JAS	0.6	0.3	0.3	0.2	0.2	0.1	0.1	0.1	0.0	0.2	0.4	0.8
	sum of 3-month	1.3	1.4	1.4	1.3	1.3	1.4	1.6	1.6	1.7	2.0	1.6	1.3
	% difference	-0.2%	-0.1%	-0.1%	-0.1%	-0.2%	-0.2%	-0.1%	-0.1%	-0.1%	-0.2%	-0.2%	0.0%

TABLE 4.1b Seasonal temperature sensitivities (S)

	period 0.1 ºC change applied	O	N	D	J	F	M	A	M	J	J	A	S
WILPO													
	ALL	-2.2%	0.8%	2.2%	3.8%	2.9%	1.2%	-2.3%	-9.3%	-15.8%	-21.6%	-19.3%	-7.7%
	OND	-0.4%	1.1%	2.3%	0.7%	0.0%	-0.4%	-1.1%	-2.9%	-4.6%	-6.1%	-5.3%	-1.3%
	JFM	0.0%	0.0%	0.0%	3.1%	3.0%	1.6%	-2.8%	-6.7%	-7.5%	-7.3%	-5.0%	-1.1%
	AMJ	-0.2%	0.0%	0.0%	0.0%	0.0%	0.0%	1.7%	0.4%	-3.9%	-9.2%	-8.4%	-2.2%
	JAS	-1.1%	-0.2%	-0.1%	0.0%	0.0%	0.0%	0.0%	0.0%	0.0%	0.4%	-3.0%	-3.1%
	sum of 3-month	-1.7%	0.8%	2.2%	3.8%	3.0%	1.2%	-2.2%	-9.2%	-16.1%	-22.1%	-21.8%	-7.8%
	% difference	-20.9%	1.1%	0.2%	0.9%	1.1%	1.4%	-5.9%	-1.2%	1.4%	2.6%	12.9%	1.5%
YAPAR													
	ALL	-5.0%	7.8%	28.2%	40.3%	36.8%	18.8%	1.9%	-10.9%	-31.7%	-51.3%	-35.2%	-17.3%
	OND	0.8%	11.6%	30.8%	10.4%	4.7%	-0.4%	-3.6%	-6.8%	-10.1%	-13.1%	-9.6%	-4.1%
	JFM	-1.5%	-0.7%	-0.5%	31.5%	33.3%	20.7%	-10.2%	-11.5%	-12.6%	-12.3%	-6.9%	-2.3%
	AMJ	-2.8%	-1.5%	-1.0%	-0.8%	-0.6%	-0.5%	16.8%	8.0%	-8.9%	-29.3%	-16.1%	-6.3%
	JAS	-2.8%	-1.6%	-1.1%	-0.8%	-0.6%	-0.6%	-0.6%	-0.4%	-0.2%	2.5%	-4.3%	-3.1%
	sum of 3-month	-6.2%	7.8%	28.2%	40.4%	36.7%	19.2%	2.4%	-10.7%	-31.8%	-52.2%	-36.8%	-15.8%
	% difference	22.9%	-0.1%	0.2%	0.0%	-0.3%	1.9%	25.4%	-2.1%	0.6%	1.7%	4.6%	-8.6%
ARROW													
	ALL	0.2%	9.6%	11.4%	12.2%	16.0%	24.3%	22.9%	14.3%	-0.8%	-24.7%	-21.8%	-9.0%
	OND	4.9%	12.6%	14.0%	12.2%	10.4%	4.2%	0.2%	-1.1%	-2.5%	-3.4%	-1.9%	-0.7%
	JFM	-0.2%	-0.1%	-0.1%	2.3%	7.7%	21.3%	4.1%	-0.9%	-1.3%	-1.3%	-0.8%	-0.3%
	AMJ	-2.4%	-1.4%	-1.2%	-1.1%	-0.9%	-0.5%	18.9%	16.5%	3.2%	-21.5%	-13.3%	-5.0%
	JAS	-2.2%	-1.5%	-1.4%	-1.3%	-1.2%	-0.7%	-0.3%	-0.1%	-0.2%	1.4%	-6.1%	-3.2%
	sum of 3-month	0.1%	9.5%	11.4%	12.1%	16.0%	24.3%	22.9%	14.4%	-0.7%	-24.8%	-22.1%	-9.2%
	% difference	-33.7%	-0.3%	-0.3%	-0.4%	-0.3%	0.3%	0.1%	0.6%	-6.4%	0.2%	1.1%	1.6%
ICEHA													
	ALL	-4.0%	1.9%	11.8%	19.2%	22.5%	14.6%	3.6%	-6.3%	-20.5%	-30.2%	-10.9%	-5.2%
	OND	-0.2%	4.8%	14.2%	10.7%	7.1%	2.3%	-1.9%	-3.8%	-5.4%	-5.8%	-1.6%	-0.6%
	JFM	-0.5%	-0.3%	-0.3%	10.1%	16.7%	13.7%	-1.8%	-6.0%	-6.4%	-5.0%	-1.5%	-0.7%
	AMJ	-1.5%	-1.1%	-0.8%	-0.6%	-0.5%	-0.4%	8.3%	4.3%	-8.5%	-20.0%	-5.7%	-2.2%
	JAS	-1.8%	-1.6%	-1.3%	-1.0%	-0.9%	-0.8%	-0.8%	-0.6%	-0.3%	0.0%	-2.3%	-1.7%
	sum of 3-month	-4.0%	1.9%	11.8%	19.2%	22.4%	14.7%	3.7%	-6.2%	-20.6%	-30.7%	-11.1%	-5.2%
	% difference	0.7%	-0.4%	0.0%	-0.2%	-0.3%	0.9%	4.3%	-1.3%	0.4%	1.9%	1.5%	0.7%
DALLE													
	ALL	-3.4%	4.0%	12.1%	17.6%	19.2%	13.3%	6.5%	0.6%	-9.6%	-26.9%	-18.9%	-7.3%
	OND	0.9%	6.9%	14.4%	9.7%	6.0%	1.5%	-1.6%	-3.0%	-3.9%	-4.8%	-2.4%	-0.8%
	JFM	-0.4%	-0.3%	-0.3%	9.6%	14.6%	12.9%	-0.4%	-4.8%	-4.3%	-3.4%	-1.6%	-0.6%
	AMJ	-1.9%	-1.1%	-0.9%	-0.7%	-0.6%	-0.4%	9.2%	9.0%	-1.2%	-19.7%	-11.1%	-3.5%
	JAS	-2.0%	-1.4%	-1.2%	-1.0%	-0.8%	-0.7%	-0.6%	-0.4%	-0.3%	0.9%	-4.1%	-2.5%
	sum of 3-month	-3.5%	4.0%	12.1%	17.6%	19.2%	13.3%	6.7%	0.7%	-9.6%	-27.1%	-19.2%	-7.4%
	% difference	2.2%	-0.4%	-0.1%	0.0%	0.2%	0.5%	2.6%	15.8%	0.3%	0.7%	2.0%	0.6%

TABLE 4.1c Seasonal temperature sensitivities (S) with a 3°C increment

	YAPAR, Seasonal temperature sensitivities (S)											
period 3ºC change applied	O	N	D	J	F	M	A	M	J	J	A	S
ALL	-3.1%	5.2%	25.6%	47.7%	35.2%	10.6%	-8.1%	-18.2%	-24.0%	-25.2%	-18.2%	-9.2%
OND	0.1%	8.0%	28.2%	8.9%	3.9%	0.1%	-2.5%	-5.6%	-9.2%	-12.2%	-8.2%	-3.5%
JFM	-1.3%	-0.7%	-0.5%	42.7%	38.1%	17.2%	-10.4%	-13.3%	-14.2%	-13.8%	-7.9%	-3.2%
AMJ	-2.0%	-1.1%	-0.8%	-0.6%	-0.5%	-0.4%	18.9%	3.8%	-12.0%	-19.3%	-11.7%	-5.4%
JAS	-2.1%	-1.4%	-1.0%	-0.7%	-0.5%	-0.5%	-0.5%	-0.4%	-0.2%	1.8%	-5.2%	-3.9%
sum of 3-month	-5.3%	4.7%	25.8%	50.2%	41.1%	16.4%	5.5%	-15.5%	-35.6%	-43.6%	-33.0%	-16.1%
% difference	70.6%	-10.2%	1.0%	5.3%	16.5%	54.3%	-168.2%	-14.8%	48.1%	72.8%	81.6%	74.8%

(x-axis). Both precipitation elasticity (ε) and temperature sensitivity (S) values are influenced by the timing of snow accumulation and melt and monthly streamflow magnitudes.

Fig. 4.7 shows seasonal ε and S values calculated as a percent difference relative to the VIC control flows in the month designated by the x-axis. For this reason, values sum vertically, but not horizontally. Values across the top row, "ALL", are calculated from simulations where the change is applied in each month of the year, where for instance OND indicates that the change is only applied in October-December, and so on. In general, we see that superposition holds, meaning changes should be additive, i.e., the four 3-month changes should equal the ALL column, however for reasons discussed below, this is not always the case. The Y column is the annual change, which is the total difference throughout the year divided by the annual streamflow (note: values do not add horizontally as they are percentages for individual months, i.e., denominators differ).

These bubble diagrams show how changes applied in one season are reflected in other seasons. Precipitation responses (Fig. 4.7, middle panels) for four of the basins (all except WILPO) are similar because precipitation changes applied in OND, JFM, and AMJ all affect streamflow response throughout the summer. This reflects the nature of large tributaries in the Columbia River basin - all are snowmelt dominant (see historical

hydrographs on Fig. 4.9), illustrating, as mentioned earlier, how seasonal precipitation responses are linked to seasonal temperature. It is only smaller basins, more on the west side of the Cascades, that are more rain-dominate, and for which seasonal ε values would have more phasing. WILPO, which has a greater peak from rain in the fall and winter than from snowmelt in the spring, is an example of responses that coincide more directly with the timing of precipitation changes.

The bubble diagrams for S (Fig. 4.7, right panels) show how streamflow responses to temperature warming vary by basin. The larger blue (increases) and red (decreases) bubbles highlight basins that are most sensitive to change (e.g., YAPAR) and the time of year when sensitivities transition from increases to decreases. These patterns provide insights as to how the basin will be affected by warming. For example, the greatest signature of temperature increases in WILPO will be decreases in summer streamflows (as contrasted with a relatively small effect on winter streamflow) as indicated by larger red bubbles. YAPAR, ARROW, and ICEHA are all currently snow dominated, but YAPAR is more vulnerable to temperature increases in JFM than the other basins and will experience a greater change in seasonality as temperatures increase. ARROW and ICEHA are more affected by AMJ warming (see AMJ row relative to others) as higher elevations (hence lower temperatures) provide a buffer such that these basins are relatively insensitive to winter warming. DALLE reflects the combined basin response, but effectively weighted by the areas that contribute the most runoff, hence it is most similar to the high-elevation headwater tributaries.

4.4.3.1. Linearity of seasonal responses

We test the linearity of seasonal responses by varying the increment of annually applied change used to calculate ε and S values in the YAPAR (Table 4.2, Fig. 4.8). If functions are linear, the ε and S values should be the same (all values are presented consistently as per % of P or per ºC). For ε values, we applied increments of -20%, -10%, 0.1%, 10%, and 20%. Across these increments, linearity is present in the winter and spring, but in the summer and fall seasonal responses are nonlinear (the largest range in seasonal ε values is in August). For S values, we applied increments of 0.1, 3, and 6 ºC. Again, there are times of year that respond similar regardless of the increment (e.g., October and November), but there are considerable changes, especially in the summer. The large differences in the summer correspond to the time of year when streamflow is historically low, and relatively small changes in magnitude from previous seasons can have a large effect on ε and S values.

TABLE 4.2 Seasonal linearity of ε and S

Seasonal precipitation elasticities (ε, % change streamflow per % change precipitation)

	O	N	D	J	F	M	A	M	J	J	A	S
-20%	1.54	1.58	1.43	1.25	1.28	1.36	1.47	1.46	1.62	1.96	1.68	1.38
-10%	1.62	1.65	1.47	1.26	1.31	1.38	1.50	1.47	1.62	2.08	1.73	1.39
1%	*1.72*	*1.73*	*1.49*	*1.29*	*1.30*	*1.42*	*1.52*	*1.44*	*1.61*	*2.22*	*2.00*	*1.56*
10%	1.81	1.79	1.52	1.31	1.31	1.44	1.53	1.44	1.61	2.25	2.21	1.68
20%	1.91	1.86	1.55	1.33	1.31	1.45	1.54	1.43	1.62	2.30	2.40	1.84
range	0.36	0.28	0.12	0.07	0.03	0.10	0.06	0.04	0.01	0.33	0.72	0.46

Seasonal temperature sensitivities (S)

increment of change (°C)	O	N	D	J	F	M	A	M	J	J	A	S
0.1	*-5%*	*8%*	*28%*	*40%*	*37%*	*19%*	*2%*	*-11%*	*-32%*	*-51%*	*-35%*	*-17%*
3	-3%	5%	26%	48%	35%	11%	-8%	-18%	-24%	-25%	-18%	-9%
6	-2%	3%	17%	35%	21%	3%	-9%	-13%	-14%	-14%	-10%	-6%
range	3%	5%	11%	13%	16%	16%	10%	7%	17%	37%	25%	12%

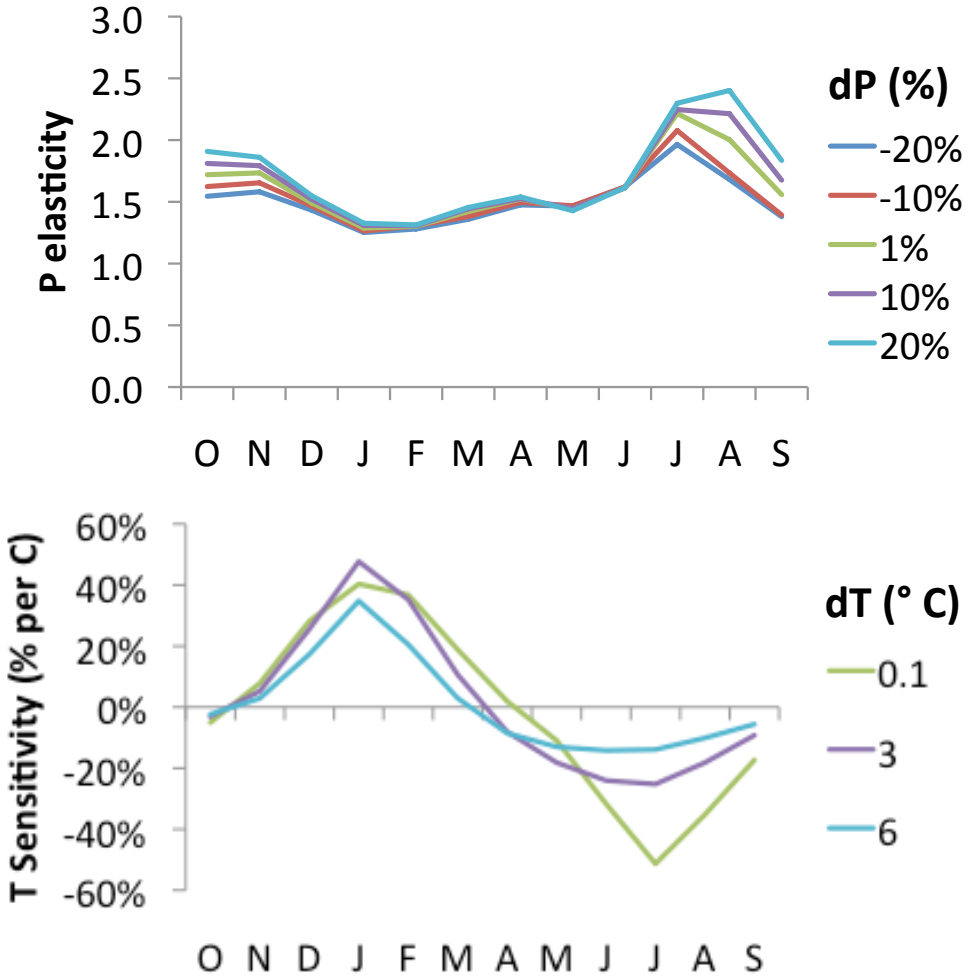

FIG 4.8 Seasonal response linearity for precipitation elasticities (top panel) and temperature sensitivities (bottom panel) in YAPAR for different change increments (colored lines). The largest differences (most non-linear responses) occur in the summer time. Values are also presented in Table 4.2.

4.4.3.2. Superposition of seasonal responses

For P changes, superposition generally applies; seasonal ε are close to additive (Table 4.1a). Values of ε for each of the four 3-month periods (OND, JFM, AMJ, JAS) calculated with a 1% P change in those seasons, when added together are close to ε values calculated from a 1% P change applied annually (ALL). This is the case for all five tributaries with sums that are less than ±0.5% for all but two months (YAPAR in September (-4.4%) and ICEHA in August (-0.6%), which correspond to low flow months

were small changes result in larger percentages). This indicates that if the precipitation changes are applied in each season and the responses are summed, the results are about the same as applying the changes uniformly throughout the year.

For T changes, superposition is less straightforward. Seasonal sensitivities generally are additive in their annual response, but are less additive in their monthly response (Table 4.1b), especially for large temperature increments. For example, in the YAPAR, when 0.1 ºC applied year round is compared with 0.1ºC applied in four seasons and added together, the annually applied 0.1ºC has a *annual response* in streamflow change that is nearly identical, only 0.006% per ºC (0.23%) higher than the four seasons added together (-2.575% vs. -2.581-% per ºC). The *monthly responses* range from being 1.6% per ºC higher in August and 1.5% per ºC lower in September. Generally, temperature changes at the tangent (0.1°C) adhere to principles of superposition. In contrast, we also tested these changes with a T increment of 3 ºC (a value that captures the secant of the function and is a change projected by many GCMs in the latter part of the 21st century) in YAPAR. With a 3 ºC increment, *annual response* in streamflow change is only 0.38% per ºC higher than the four seasons added together (-2.2% vs. -2.6%), but the *monthly responses* range from being 18.4% per ºC higher in July (-25.2% vs. -43.6%) and 13.6% per ºC lower in April (-8.1% vs. +5.5%) (Table 4.1c); and carryover effects become greater if changes are applied in individual months instead of 3-month intervals. These differences can be attributed to the influence of snowpack and that temperature increases, if applied in individual seasons and then added together, can essentially melt the snow faster (melting the same snow twice), resulting in higher springtime and lower summertime flows when sensitivities across simulations are added

together. This highlights the importance of selecting change increments that approximate the tangent of the change function when superposition will be applied (as in section 4.4.4). The YAPAR has the largest seasonal shift of the five locations evaluated, and thus is most sensitive to these temperature effects.

4.4.4. Application to climate change projections

An obvious application of the methods outlined above is to use the seasonal ε and S values as transfer functions to convert seasonal changes in precipitation (P) and temperature (T) from GCMs into future projections of seasonal hydrographs. Although the method is approximate, and only provides estimates of how mean seasonal discharge will change (and not, for instance, changes in variability) it has the advantage of being much less time consuming than full-simulation approaches. We illustrate here how the seasonal sensitivity-based approach compares with the full-simulation approach of Hamlet et al. 2010.

Seasonal-sensitivity based hydrographs were calculated by applying P and T changes for each 3-month period starting at the beginning of the water year, although any sequence of months will give the same result as long as interaction terms among the 3-month periods are captured. Specifically, we first incorporated P changes by multiplying the percent change in future P in OND (calculated from GCM P output) by the 12 OND monthly responses (the OND row in the bubble diagram) and applied this change to the historical streamflow values. Then, we incorporated T change in OND by similarly multiplying the future T change (from GCM T output) by the OND monthly responses and applied this change to the modified historical streamflow generated in the earlier step. These same

adjustments were then applied to the other 3-month periods of JFM, AMJ, and JAS using a similar sequencing with each additional change applied to the modified historical streamflow generated in the previous step. We tested the sensitivity of our results to the sequencing above in YAPAR (Table 4.3), as this basin has the greatest seasonal sensitivity to warming of the five basins. We find that sequencing is most important to T changes, if P is not sequenced, but applied either at the beginning or end, results change only slightly. If future seasonal T and P changes were applied to the matrix without sequencing, *annual responses* are closest to full-simulation results, but the seasonal-sensitivity based hydrographs significantly overestimate reductions in summertime flows compared to full-simulation hydrographs; flows become negative at YAPAR in July for some scenarios in 2040 and all scenarios in 2080 (Table 4.3). The sequencing reduces summertime declines by applying the change fractions to values that have already been reduced according to temperature impacts in previous seasons. It is, however, possible to project negative streamflow values nonetheless as these changes are being applied in a linear manner when, in reality, sensitivities are nonlinear (as demonstrated in section 4.4.3.1). For example, if there is a 4°C temperature increase in AMJ when July's sensitivity is -29% per °C, the percent decline will be over 100%. As such, this method works best for small changes (e.g. more typically ~30 years into the future rather than 100) and for basins were sensitivities are modest, hence nonlinearities in the sensitivities are small.

Fig. 4.9 and Table 4.3 show results for the YAPAR for three future time periods. The percent annual differences vary a fair amount between methods, but generally, the sensitivity-based method reproduces the change in seasonality quite well, providing

TABLE 4.3 YAPAR Future scenarios, differences from historical streamflow

	% difference in annual magnitudes		
	2020	2040	2080
Full-simulation (Hamlet et al)	*3% (-11 to 15%)*	*5% (-15 to 22%)*	*6% (-12 to 31%)*
P and T sequencing (Fig 8 & 9)	1% (-17 to 21%)	7% (-6 to 28%)	17% (-14 to 48%)
No sequencing	0% (-17 to 18%)	3% (-9 to 21%)	6% (-20 to 27%)
P applied then T sequencing	1% (-17 to 21%)	6% (-6 to 27%)	17% (-14 to 49%)
T sequencing then P applied	1% (-18 to 22%)	7% (-6 to 29%)	17% (-15 to 49%)
	% increases in winter (Nov-Apr)		
	2020	2040	2080
Full-simulation (Hamlet et al)	*30% (5 to 53%)*	*50% (28 to 87%)*	*72% (39 to 127%)*
P and T sequencing (Fig 8 & 9)	24% (-1 to 60%)	47% (27 to 87%)	88% (39 to 154%)
No sequencing	24% (-1 to 61%)	48% (27 to 90%)	92% (39 to 164%)
P applied then T sequencing	24% (-1 to 61%)	46% (26 to 88%)	88% (36 to 158%)
T sequencing then P applied	23% (1 to 54%)	44% (28 to 75%)	80% (44 to 125%)
	% decrease in peak flow (May)		
	2020	2040	2080
Full-simulation (Hamlet et al)	*-13% (-21 to 2%)*	*-25% (-55 to 1%)*	*-51% (-79 to -1%)*
P and T sequencing (Fig 8 & 9)	-10% (-22 to 0%)	-16% (-28 to 4%)	-36% (-69 to -1%)
No sequencing	-8% (-21 to 1%)	-13% (-22 to 5%)	-30% (-54 to 4%)
P applied then T sequencing	-9% (-21 to 0%)	-16% (-26 to 4%)	-36% (-65 to -0%)
T sequencing then P applied	-9% (-22 to 0%)	-14% (-27 to 5%)	-32% (-63 to 2%)
	% decrease in low flow (July)		
	2020	2040	2080
Full-simulation (Hamlet et al)	*-45% (-63 to -30%)*	*-63% (-86 to -43%)*	*-84% (-94 to -68%)*
P and T sequencing (Fig 8 & 9)	-50% (-74 to -29%)	-70% (-97 to -35%)	-98% (-119 to -72%)
No sequencing	-58% (-84 to -31%)	-98% (-148 to -46%)	-194% (-319 to -128%)
P applied then T sequencing	-49% (-69 to -28%)	-69% (-94 to -35%)	-96% (-113 to -75%)
T sequencing then P applied	-46% (-76 to -16%)	-59% (-102 to -17%)	-71% (-126 to -23%)

*Averages and ranges are from 10 GCMs for A1B emissions scenario as simulated by Hamlet et al. 2010.

similar information about both the average seasonal response (average of the 10 GCMs) and ensemble range, even as climate change becomes more pronounced in 2080, although notably this method captures the near term changes best and these are also what matter most to management. The ensembles (gray lines) of the seasonal-sensitivity approach are smoother, which would be expected as they are based on changes applied to long-term averages. For summertime streamflow, the seasonal-sensitivity approach captures the

nature of the changes, although one should interpret with caution the actual magnitudes for reasons mentioned earlier, especially when temperature increases are large.

We compare results between these two methods across five selected locations (Fig. 4.10), which represent a spectrum from rain-dominant and snow-dominant basins. We present results from 2040 as it tests the method more than 2020, but is not as extreme as 2080, which is of less interest to water managers. Results show that across the spectrum, the seasonal-sensitivity approach captures the nature of seasonal changes, both in the average and range of seasonal responses. The greatest difference between these

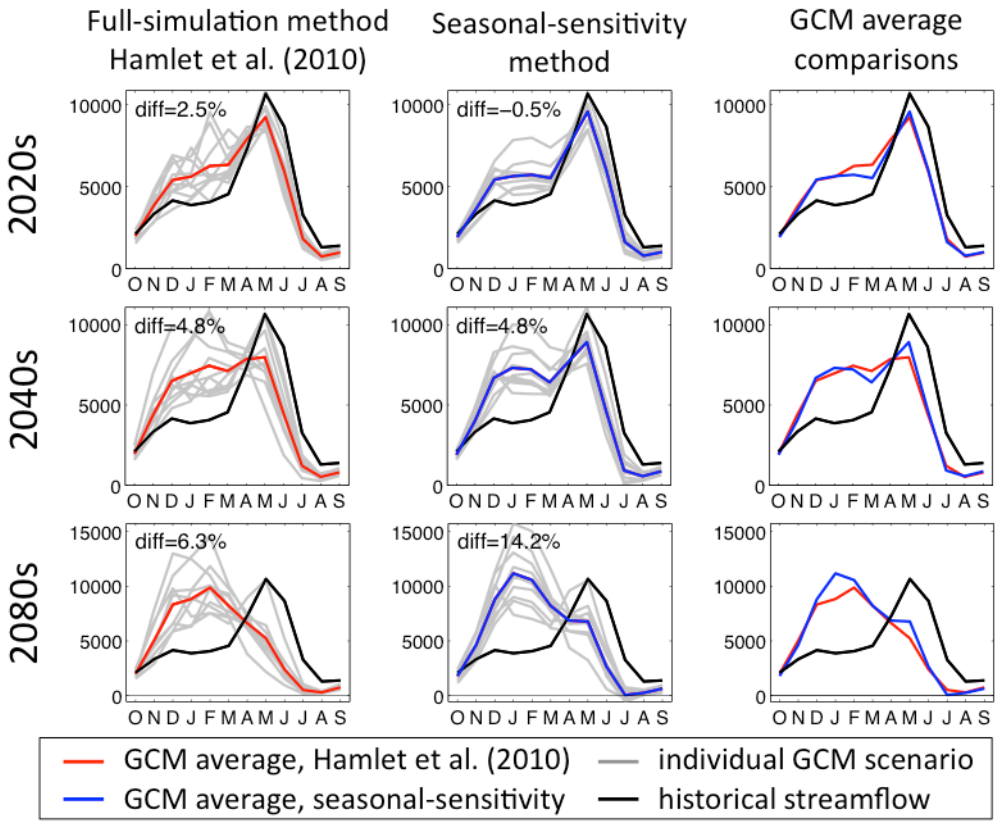

FIG 4.9 Yakima River basin at Parker (YAPAR) seasonal average streamflow projections for the 2020s, 2040s, and 2080s for the A1B emissions scenario. The left panels are results from Hamlet et al. (2010), which use the full simulation approach, whereas the middle panels are generated using the hydrologic-sensitivity method. The right panels compare averages of the 10 GCMs using both methods. "Diff" is the percent annual values differ from historical streamflow for both simulation methods.

two methods is the rate at which streamflow declines between June to September; this relates to the non-linearity in the seasonal response, which is greater in the summer (as highlighted in Table 4.2 and Fig. 4.8). Additionally, the sensitivity-based approach is most vulnerable to error when S values are large and negative, which also occurs in the summer (especially in July). In all cases, but especially in locations with the coldest temperatures (i.e., ARROW), the seasonal-sensitivity streamflow declines faster than that of the full-simulation approach. In the bubble figure for the ARROW, this is seen as the contrast between the positive S in June to the large negative S in July - with continuous change, as in the full-simulation, this transition is less abrupt. Overall, summertime flows with the seasonal sensitivity approach are lower (a more conservative estimate) than the full-simulation approach.

In general, these results support a straightforward approach to estimate how future changes in monthly P and T from GCMs translate to changes in seasonal streamflows. The approach uses only two matrixes (one for ε and one for S) of 48 values each as transfer functions to reproduce seasonal changes created from detailed model simulations. This simplified approach provides plausible seasonal hydrographs, but has important limitations. It focuses on seasonal shifts, not changes in total magnitude. For management concerns in the PNW, total magnitude is less critical; if, however, annual magnitude is more important, the alternate sensitivity-based technique that emphasizes adjustments designed to capture annual responses (Vano and Lettenmaier 2013) is more appropriate. These matrixes are specific to the baseline temperature and current land cover - if these change the sensitivities will likely also change. This is less a problem in the near-term, and would also not be reflected in most full simulation approaches as well.

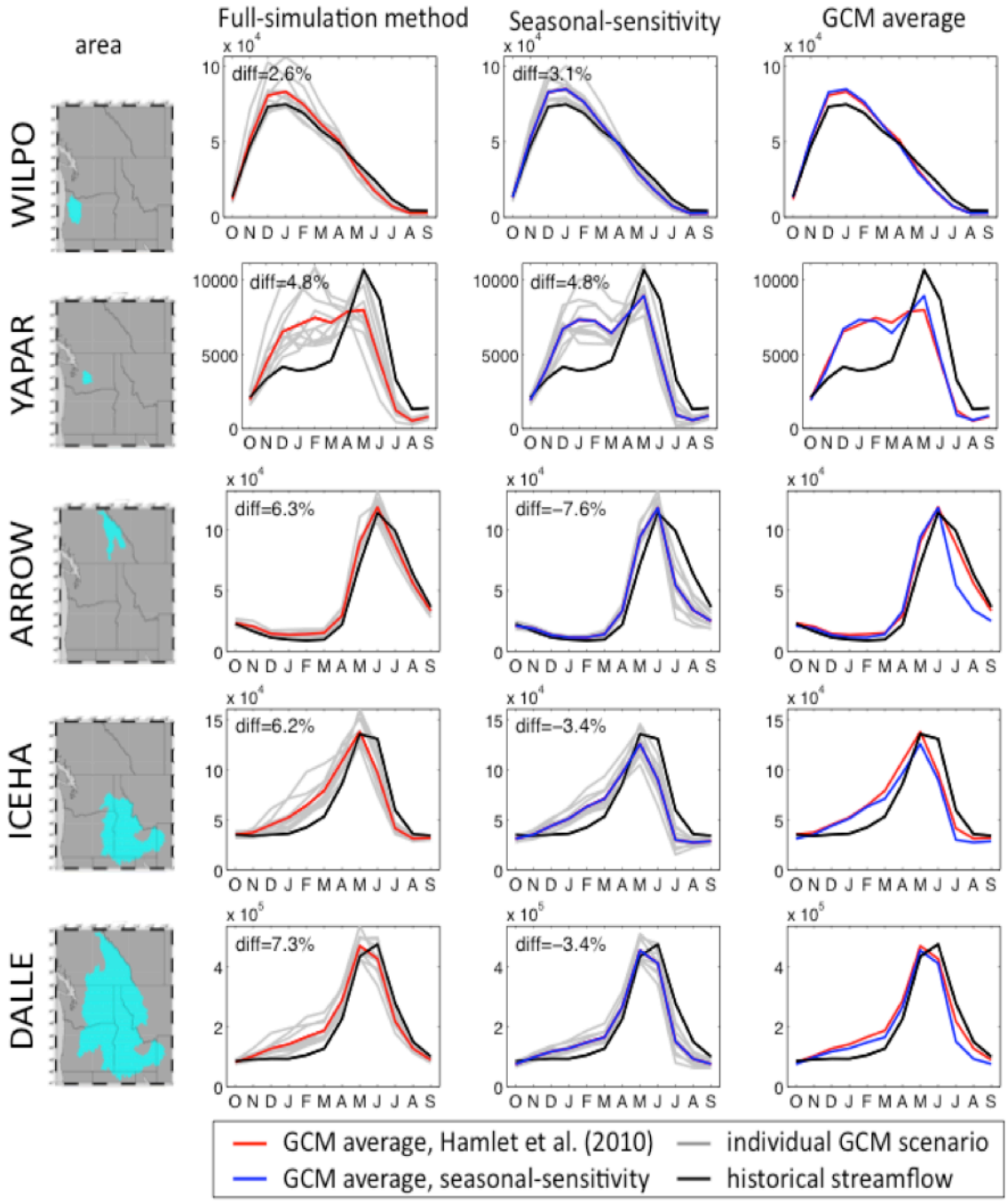

FIG 4.10 Seasonal average streamflow projections for the 2040s for A1B emissions scenario. "Diff" is the percent annual values differ from historical streamflow for both simulation methods.

An updated matrix requires five model runs, which is still considerably less computing than an update to the full-simulation estimations. The approach is based on a linear approximation to seasonal precipitation elasticities and temperature sensitivities, which in

fact are nonlinear. This results in general over-estimates of streamflow changes especially in summer, and exaggeration of the transition from cool to warm season.

4.5. Conclusions

The Pacific Northwest (PNW) will experience climate change in a variety of ways depending on the specific location, season, and magnitude of T and P change. To better define how the region - and its local watersheds - will respond to future change, we map the sensitivities of runoff to P and T changes both spatially and temporally. We use concepts of hydrologic sensitivities to (a) quantify watershed classifications that help define local hydrologic changes within a regional climate change context and (b) develop a methodology where sensitivities serve as a transfer function that can be used to quickly convert average seasonal T and P changes into an estimate of future hydrographs for local watersheds.

Through application of the hydrologic sensitivity approach to the PNW we found:

- For watersheds that receive some of their winter precipitation as snow (i.e., snow-dominate and transitional watersheds), warming applied in the warm season typically reduces streamflow throughout the year while warming in the cool season increases winter flows and decreases summer flows. Therefore cool season warming results in more change in the seasonality of flows, but generally reduces annual flows by a smaller magnitude than warming that occurs only in the warm season.
- The net change from cool season warming results in both increases (20% of the domain) and decreases (80% of the domain) in annual runoff depending on the

location, where increases occur in the high elevation regions in primarily snow-dominate watersheds, but runoff increases are easily overwhelmed by decreases when averaged over larger areas or temperature increases are applied throughout the year.

When applying hydrologic sensitivities to future change, we found:

- The ability to construct hydrographs from seasonal hydrologic sensitivities depends on how well hydrologic sensitivities adhere to principles of linearity and superposition. As such, the seasonal-sensitivity method works best for modest changes (e.g., ~30 years into the future rather than 100, which is also the time management agencies care most about) and for basins were sensitivities are modest, hence nonlinearities in the sensitivities are small.
- Seasonal precipitation changes (and their seasonal ε values calculated using a increment of 1%) are largely independent of each other (e.g., the runoff response from precipitation increases in JFM and AMJ generally have minimal interaction), adhering to principles of superposition.
- Seasonal temperature changes (and their seasonal S values calculated using a 0.1 °C) also appear to be additive, although less so than for precipitation. We found that three-month seasonal T changes and a 0.1°C increment resulted in largely independent responses. If the increment of change is larger (i.e., 3°C), it captures the secant instead of the tangent and results in values where superposition is not appropriate (melts snow that would be melted by temperature increases in other months, thus when the response from different seasons are added together, the same snow is melted twice).

- Future temperature changes should be added so interactions between months are accounted for (each three-month period should be added incrementally). For instance, first applying OND seasonal S values, then JFM, AMJ, and finally JAS results in an estimated future hydrograph that more closely replicates future hydrographs generated using the full-simulation approach. Conversely, the sequence in which precipitation changes are applied has little effect on the estimated future hydrograph.
- The sensitivity-based method compares well with the full-simulation approach for purposes of capturing the nature of changes in seasonality, even in the 2080s. There are, however, seasons and locations where change functions are more non-linear; and caution should still be exercised in interpreting the magnitude of flows, especially in the summer and when future temperature increases are large.

Acknowledgements

The authors thank Bart Nijssen, David Pierce, Tapash Das, and Daniel Cayan for their insights that led to this work and Marketa Elsner and Se-Yeun Lee for their assistance in model setup. Data from future simulations for this study was provided by the Columbia Basin Climate Change Scenarios Project, University of Washington, http://www.hydro.washington.edu/2860/. Support for this work was provided by the Climate Impacts Research Consortium (CIRC) and the NOAA Regional Integrated Scientific Assessment (RISA) program.

References

Bohn, T. J., B. Livneh, J. W. Oyler, S. W. Running, B. Nijssen, and D. P. Lettenmaier, 2013: Global evaluation of MTCLIM and related algorithms for forcing of ecological and hydrological models, Agr. Forest. Meteorol., **176**, 38-49, doi:10.1016/j.agrformet.2013.03.003.

Das, T., D.W. Pierce, D.R. Cayan, J.A. Vano, and D.P. Lettenmaier, 2011: The Importance of warm season warming to western U.S. streamflow changes. *Geophysical Research Letters* **38**, L23403, doi:10.1029/2011GL049660.

Elsner, M.M., L. Cuo, N. Voisin, J.S. Deems, A.F. Hamlet, J.A. Vano, K.E.B. Mickelson, S.Y. Lee, and D.P. Lettenmaier, 2010: Implications of 21st century climate change for the hydrology of Washington State *Climatic Change* **102**, no. 1, 225-260.

Elsner, M.M.. and Hamlet, A. F., 2010: Macro-scale Hydrologic Model Implementation, available at: http://warm.atmos.washington.edu/2860/r7climate/study_report/CBCCSP_chap5_vic_final.pdf

Hamlet, A. F., 2011: Assessing water resources adaptive capacity to climate change impacts in the Pacific Northwest Region of North America. *Hydrology and Earth System Sciences*, *15*(5), 1427-1443.

Hamlet, A.F., P. Carrasco, J. Deems, M.M. Elsner, T. Kamstra, C. Lee, S-Y Lee, G. Mauger, E. P. Salathe, I. Tohver, L. Whitely Binder, 2010: Final Project Report for the Columbia Basin Climate Change Scenarios Project, http://www.hydro.washington.edu/2860/report/".

Jeton, A.E., Dettinger, M.D., and J.L. Smith, 1996: Potential effects of climate change on streamflow, eastern and western slopes of the Sierra Nevada, California and

Nevada: U.S. Geological Survey Water Resources Investigations Report 95-4260, 44 p.

Lee, S.Y., A.F. Hamlet, C.J. Fitzgerald, and S.J. Burges, 2009: Optimized Flood Control in the Columbia River Basin for a Global Warming Scenario, Journal of Water Resources Planning and Management, DOI 10.1061/(ASCE)0733-9496(2009)135:6(440), 135(6) 440-450

Liang, X., D. P. Lettenmaier, E. F. Wood, and S. J. Burges, 1994: A simple hydrologically based model of land surface water and energy fluxes for General Circulation Models. J. Geophys. Res., 99, 14 415– 14 428.

Lohmann, D., R. Nolte-Holube, and E. Raschke, 1996: A large scale horizontal routing model to be coupled to land surface parameterization schemes. Tellus 48 A, pp. 708–72

Mantua, N., I. Tohver, and A.F. Hamlet, 2010: Climate change impacts on streamflow extremes and summertime stream temperature and their possible consequences for freshwater salmon habitat in Washington State, Climate Change, 102(1–2), 187–223, doi:10.1007/s10584-010-9845-2, 2010.

Nijssen, B., D. P. Lettenmaier, X. Liang, S. W. Wetzel, and E. F. Wood, 1997: Streamflow simulation for continental-scale river basins. *Water Resour. Res*, 33, 711-724.

Nijssen, B., G.M. O'Donnell, A.F. Hamlet, and D.P. Lettenmaier, 2001: Hydrologic sensitivity of global rivers to climate change. *Climatic Change*, *50*(1), 143-175

Payne J.T., A.W. Wood, A.F. Hamlet, R.N. Palmer, and D.P. Lettenmaier, 2004: Mitigating the effects of climate change on the water resources of the Columbia River basin. *Clim Change* **62**:233–256.

Sankarasubramanian A., R.M. Vogel, and J.F. Limbrunner, 2001: Climate elasticity of streamflow in the United States, *Water Resour. Res*., **37**, 1771-1781.

Schaake, J. C., 1990: From climate to flow. Climate Change and U.S. Water Resources, P. E. Waggoner, Ed., John Wiley, 177–206.

Tohver, I. and A.F. Hamlet, 2010: Impacts of 21st century climate change on hydrologic extremes in the Pacific Northwest region of North America, available at: http://www.hydro.washington.edu/2860/products/sites/ r7climate/study report/CBCCSP chap7 extremes final.pdf

Thornton, P.E. and S.W. Running, 1999: An improved algorithm for estimating incident daily solar radiation from measurements of temperature, humidity, and precipitation, Agr. Forest Meteorol., 93, 211–228.

U.S. Army Corps of Engineers (USACE) and Bonneville Power Administration (BPA), 2012: website for the Columbia River Treaty, Information accessed from: http://www.crt2014-2024review.gov/, information accessed June 15, 2012 and November 22, 2012.

Vano, J.A., M. Scott, N. Voisin, C.O. Stockle, A.F. Hamlet, K.E.B. Mickelson, M.M. Elsner and D.P. Lettenmaier, 2010: Climate change impacts on water management and irrigated agriculture in the Yakima River basin, Washington, USA, Climate Change, 102(1–2), 287–317, doi:10.1007/s10584-010-9856-z

Vano, J.A., T. Das, and D.P. Lettenmaier, 2012: Hydrologic sensitivities of Colorado

River runoff to changes in precipitation and temperature, *J. of Hydrometeorology*, **13**, 932-949, doi:10.1175/JHM-D-11-069.1.

Vano, J.A., B. Udall, D.R. Cayan, J.T. Overpeck, L.D. Brekke, T. Das, H.C. Hartmann, H.G. Hidalgo, M. Hoerling, G.J. McCabe, K. Morino, R.S. Webb, K. Werner, and D.P. Lettenmaier, 2013: Understanding Uncertainties in Future Colorado River Streamflow, *Bull. Amer. Meteor. Soc*., (in press).

Vano, J.A. and D.P. Lettenmaier, 2013, A sensitivity-based approach to evaluating future changes in Colorado River Discharge, *Climatic Change* (in review).

Wood, A.W., R.L. Leung, V. Sridhar, and, D.P. Lettenmaier, 2004: Hydrologic implications of dynamical and statistical approaches to downscaling climate model outputs. *Climatic Change*, 62(1), 189-216.

V. CONCLUSIONS

My research has aimed to better understand how climate and climate change influences hydrologic processes and has explored ways that this improved understanding can be useful to water management decision-making. I have done so by exploring the four questions introduced in Chapter I, specifically: (1) How sensitive is runoff to changes in precipitation, temperature, and to combined changes in both precipitation and temperature? (2) How do hydrologic sensitivities vary spatially across the western United States? (3) How can runoff sensitivities to precipitation and temperature changes be defined on a seasonal basis? (4) How can hydrologic sensitivities be used to construct future streamflow projections for use in water management applications?

To address these questions, I applied hydrologic models in both the Colorado River basin and the extended Columbia River basin (Pacific Northwest hydrologic region). These two regions provided diverse hydrologic conditions, where the coefficient of variation (standard deviation/mean) of annual streamflow volume is relatively high (0.37) in the Colorado River, and relatively low (0.18) in the Columbia River (McMahon 1982), and equally diverse management concerns, where the total storage relative to annual inflow ratio ranges from about 0.3 in the Columbia River to over four in the Colorado River. As such, these two regions served as useful test beds to examine the spectrum of hydrologic sensitivities and their applications in the western United States, as explored in the dissertation's three core chapters (Chapters II, III, and IV).

Chapter II provides a foundation for applying hydrologic sensitivities through model simulations in the Colorado River basin, a semi-arid system with relatively large

basin-average precipitation elasticities (ε) and temperature sensitivities (S). As such, model performance (the ability of the models to capture naturalized streamflow) was particularly challenging and comparisons between five commonly used land surface models [Catchment, Community Land Model (CLM), Noah, Sacramento Soil Moisture Accounting model (Sac), and the Variable Infiltration Capacity (VIC) model] revealed a range of responses. These investigations showed model-simulated annual ε at Lees Ferry ranged considerably from two to six and S ranged from declines of 2% to as much as 9% per °C. Spatially, ε and S were more consistent among models in the headwater regions that produce most of the Colorado basin's runoff, which tended to mask larger differences in locations within the basin that produced less runoff. Values of ε and S changed with reference conditions, indicating the nonlinearity of these sensitivities, with ε values being especially vulnerable to low flow biases. Superposition of precipitation and temperature changes largely held with respect to annual runoff; i.e., the combined effect of precipitation and temperature changes are essentially equivalent to the sum of the contributions computed separately.

Chapter III applied the results of Chapter II to develop a method that uses hydrologic sensitivities, in combination with global climate model projections of precipitation and temperature changes, to approximate cumulative distribution functions of future long-term (e.g., 30-year) average annual streamflow change in the Colorado River basin. In the development and testing of the method, I used the VIC hydrologic model, which has been widely used in other climate change studies that could be leveraged for comparison, although the method is also applicable to other models. Generally, the method produced plausible estimates of future annual average streamflow

change, mostly within about ±15% of those estimated from the more common, computationally intensive full-simulation approach, which forces the hydrologic model with downscaled future climate scenarios. It is, most effective in the near term, where assumptions of linearity and superposition are most appropriate. This is, advantageously, also the time periods that matter most to water managers.

Chapter IV applied concepts from Chapters II and III to the hydroclimatically diverse Pacific Northwest, which has watersheds with hydrology similar to the Colorado River basin, but also locations that receive considerably more precipitation and have much lower interannual variability. Again, I used the VIC model for this analysis to facilitate comparisons with previous studies (but other models could also be used). This provided the opportunity to investigate ε and S over a range of hydrologic behaviors and test how responses varied according to the season in which changes were applied. For example, I found that 64% of watersheds were more sensitive to warm season warming than cool season warming in terms of annual discharge. Concepts of sensitivities, mapped for watersheds throughout the PNW, could also be used to detect watersheds most sensitive to shifts in the seasonality of streamflow, which corroborated earlier studies that used the ratio of peak snow water equivalent (SWE) to October-March precipitation (Elsner et al. 2010; Hamlet et al. 2010; see Chapter IV for references). Within Chapter IV, I also used seasonal sensitivities to develop – with consideration for concepts of linearity and superposition – basin-specific transfer functions, essentially two 4x12 matrixes, to estimate future changes in long-term mean seasonal hydrographs. I showed that this approach captures the basin-specific hydrologic characteristics and provides viable first-order estimates of the likely range in long-term (e.g., 30-year)

annual streamflow changes without performing detailed model simulations. When compared to five major Columbia River tributaries (drainage areas order $10^4 – 10^5$ km^2), the sensitivity-based estimation approach compared well with the more computationally intensive full-simulation approach.

Both Chapters III and IV address the fourth question of applying hydrologic sensitivities to estimate future streamflow changes. While the two approaches outlined in these chapters are similar in concept, it is notable that they are not intended to be applied in a one-size-fits-all manner. The goal was to develop techniques that are straightforward (easy to understand and implement), location appropriate (account for basin-specific hydrology), and designed to address basin-specific management concerns (annual vs. seasonal streamflows). More specifically, in the Colorado River basin, understanding the *annual response* of streamflow change is most important to management concerns. Therefore, the sensitivity-based approach designed for the Colorado River basin estimated annual streamflow changes (the hydrologic sensitivities were only of annual responses, meaning a single value for each applied change, as opposed to twelve values for monthly responses). Also, because ε and S values were large, varying annual ε and S values as a function of temperature and precipitation change (i.e., accounting for nonlinearities) was important. This implies that annual changes require estimating seven additional model simulations (Table 3.2), which help capture nonlinear responses to temperature and precipitation changes. Alternatively, in the Columbia River basin, understanding how climate change will affect the *seasonal response* of streamflow change is of greatest interest to management, and generally annual ε and S are small relative to those in the Colorado River basin (thus the Columbia River basin is less

vulnerable to varying annual ε and S values as a function of temperature and precipitation change). Therefore, the seasonal-sensitivity approach estimated *monthly* streamflow change (the hydrologic sensitivities were of monthly responses, reported as a 4x12 matrix). For these monthly responses to be additive (i.e., adhere to superposition) the change increments should be small. In other words, in the seasonal-sensitivity approach in the Columbia River basin, the superposition of seasonal values was more important than capturing the nonlinearities of the larger temperature and precipitation changes.

Overall, hydrologic sensitivities in both the Colorado and extended Columbia River basin can provide valuable information to both researchers and water managers. They can be used to compare the performance of hydrologic models, particularly how models capture changes in temperature and precipitation relative to each other and, ideally, relative to observations. Maps of ε and S values can identify locations more (or less) sensitive to future change and where there is greater uncertainty, which can be used as a tool to help determine locations for future research or *in situ* observations. In the near term, which is also of greatest interest to water managers, sensitivity-based estimation methods work well and can be easily applied to newly released climate information to assess underlying drivers of change and to bound, at least approximately, the range of future streamflow uncertainties for water resource planners. These methods will be particularly useful as climate change simulations for the fifth Assessment Report of the IPCC are becoming available, generating interest in understanding how these new climate projections translate to future streamflow in the western United States.